NIST BUILDING SCIENCE SERIES 180

Database-Assisted Design for Wind: Concepts, Software, and Examples for Rigid and Flexible Buildings

Joseph A. Main and William P. Fritz

NIST BUILDING SCIENCE SERIES 180

Database-Assisted Design for Wind: Concepts, Software, and Examples for Rigid and Flexible Buildings

Joseph A. Main
William P. Fritz

Building and Fire Research Laboratory
National Institute of Standards and Technology
Gaithersburg, MD 20899-8611

March 2006

National Institute of Standards and Technology • Technology Administration • U.S. Department of Commerce

Disclaimer

Certain commercial entities, equipment, or materials may be identified in this document in order to describe an experimental procedure or concept adequately. Such identification is not intended to imply recommendation or endorsement by the National Institute of Standards and Technology, nor is it intended to imply that the entities, materials, or equipment are necessarily the best available for the purpose.

Abstract

Database-Assisted Design (DAD) represents a unified framework for analysis and design of buildings for wind loads that makes direct use of pressure time histories measured at a large number of pressure taps on one or more wind tunnel models. Local climatological information on extreme wind speeds and their direction-dependence can be used in conjunction with the measured pressures to obtain estimates of peak wind effects with specified return periods for use in structural design. Wind effects of interest may include internal forces and bending moments, demand/capacity ratios, or deflections and accelerations. Through direct use of measured pressures, rigorous accounting for wind directionality, and accurate modeling of structural dynamics for flexible buildings, DAD enables more accurate estimation of peak wind effects than is allowed by simplified procedures in current use, thus facilitating more risk-consistent designs. It is anticipated that in the not-too-distant future, pressure time series obtained by Computational Fluid Dynamics (CFD) may also be used in DAD.

This report provides an overview of DAD and presents details of its implementation for both rigid and flexible buildings, for which separate software packages have been developed. The report is intended as a companion to these software packages, which are being made publicly available at <http://www.nist.gov/wind>. The software for rigid buildings incorporates an interpolation scheme which allows for estimation of peak wind effects using wind tunnel models whose dimensions do not precisely match the dimensions of the structure of interest. To facilitate efficient implementation, the details of the DAD procedure are presented herein using matrix notation. However, no use of matrix algebra by design engineers is required, and the accompanying software packages incorporate graphical interfaces to make the procedure transparent and user-friendly. Example calculations are presented to illustrate the DAD approach.

Key words: building technology; aerodynamics; extreme winds; database-assisted design; structural dynamics; wind directionality; wind forces; wind tunnels.

Acknowledgements

Contents

List of Figures[1]

---

[1] Figures in the Appendices are not included in this list.

List of Tables

1. Introduction

Joseph A. Main and William P. Fritz

Advances in wind tunnel technology over the past several decades now enable simultaneous measurement of pressures at hundreds of pressure taps on the surface of building models, and parallel advances in computational and digital storage capabilities enable analysis of such large quantities of pressure data on standard desktop PCs. Database-Assisted Design (DAD) represents a unified framework for making direct use of such measured pressures in the analysis and design of structures. Local climatological information on extreme wind speeds and their direction-dependence is also used in conjunction with the measured pressures in order to obtain realistic estimates of peak internal forces with specified return periods for use in structural design. Currently, wind loads are typically represented fairly coarsely in design using standards such as the American Society of Civil Engineers (ASCE) 7-02 Standard (ASCE 2003). Such standards are based on the results of wind tunnel tests, but reducing these results into a simple and generally applicable tabular format necessitates considerable simplification and loss of information. For tall, flexible buildings, simplified approximate procedures such as the High-Frequency Force Balance (HFFB) methodology are in common use. Through direct use of measured pressures, rigorous accounting for wind directionality effects, and more accurate modeling of structural dynamics for flexible buildings, the DAD approach enables more accurate estimation of peak wind effects, with a view to achieving more risk-consistent building designs. It is anticipated that in the not-too-distant future, pressure time series obtained by Computational Fluid Dynamics (CFD) may also be used in DAD. Improvements in sensor technologies are also enabling measurement of pressures on buildings at full scale. Such full-scale measurements will play an important role in the validation of pressures obtained from wind tunnel tests and CFD simulations, and full-scale pressures may eventually be used in DAD as well.

The DAD approach was originally conceived for predicting the linear, static response of low-rise buildings (Whalen et al. 1998, Rigato et al. 2001, Simiu et al. 2003). Whalen et al. (2002) developed a user-friendly pilot software package known as WiLDE (Wind Load Design Environment), which implements the approach for low-rise metal frame structures. Subsequently, the DAD approach has been extended to consider nonlinear static response of low buildings (Jang et al. 2002) and linear dynamic response of high-rise buildings (Fritz et al. 2004). For high-rise buildings, wind tunnel tests are routinely conducted in the design stages, and the pressure measurements required for the DAD approach can be obtained from such tests. For low-rise buildings, however, constraints on project budgets and timelines generally do not permit specialized wind tunnel testing. To facilitate more widespread use of the DAD approach for low-rise buildings, an aerodynamic database is being assembled at the U.S. National Institute of Standards and Technology (NIST), containing measured pressure time series for a fairly large number of gable-roofed building models with various dimensions, as discussed in Ho et al. (2005).

To illustrate and facilitate implementation of the DAD approach, software has been developed using the MATLAB language (MathWorks 2005) and is being made available through the internet at <http://www.nist.gov/wind>, along with other information, software, and data

related to extreme winds and wind effects on buildings. At this website, separate software packages are available for rigid, gable-roofed buildings (developed by J.A. Main) and for tall, flexible buildings (developed by W.P. Fritz). These software packages, along with user instructions, can be obtained from the website by following the links for Database-Assisted Design software. The software for rigid, gable-roofed buildings is similar in concept to that previously developed by Whalen et al. (2002). However, the present software (a) eliminates the need for preprocessing of pressure data through automated handling of pressure databases in the standard HDF format developed by Ho et al. (2005) and (b) incorporates an interpolation scheme for cases in which the building dimensions do not precisely match those of an available wind tunnel model.

In this report, an overview of the DAD methodology is first presented in Section 2, which discusses the format and requisite scaling of the wind pressure time series and directional wind speed data used in DAD, describes the different stages of the analysis in general terms, and highlights some of the differences in implementation for rigid buildings and flexible buildings. Section 3 presents further details specific to the treatment of rigid buildings (i.e., buildings with negligible dynamics effects), for which a number of simplifications can be introduced. An interpolation scheme is also presented in Section 3, to enable treatment of cases in which the building dimensions do not precisely match those of an available wind tunnel model. Section 4 discusses the application of DAD to flexible buildings, for which dynamic effects cannot be neglected. Sections 3 and 4 also include brief descriptions of the corresponding software packages for rigid and flexible buildings – available through the website discussed above – and present example calculations illustrating the application of these software packages. Further details related to the setup and operation of the software packages for rigid and flexible buildings are presented in Appendices A and B, respectively.

2.   Overview of Database-Assisted Design

Joseph A. Main and William P. Fritz

A variety of wind effects must be considered in structural design. Wind effects of interest include internal forces and bending moments in structural members, from which demand/capacity ratios must be evaluated and interaction equations considered (e.g., for combined flexure and axial loading). Global wind effects such as overturning moment and base shear may also be of concern, and deflections and accelerations are commonly required for serviceability considerations. For design purposes, it is necessary to evaluate the values of such wind effects corresponding to a specified return period, where the return period (also known as the mean recurrence interval) is defined as the inverse of the annual probability of exceedance.

In computing wind effects corresponding to a specified return period, the DAD approach makes use of two distinct types of databases in conjunction. The first type of database, described in subsection 2.1, represents the building aerodynamics, containing pressure time series measured in the wind tunnel for various wind directions. These pressure time series are combined with structural analysis, as described in subsection 2.2, to compute peak wind effects corresponding to winds with various speeds and directions. In laying out the basic DAD procedure in this section, it is assumed for simplicity that pressure data are available for the exact structural dimensions of interest. This is generally the case for high-rise buildings, for which specialized wind tunnel tests are routinely conducted in the design stages. This is generally not the case when using the NIST aerodynamic database for low-rise buildings, however, and this assumption is relaxed in Section 3, which discusses the use of pressure time series from models with differing dimensions and presents an interpolation procedure. The second type of database, described in subsection 2.3, represents the extreme wind climate at the site of interest, containing directional wind speed data based on simulation or historical observation. These directional wind speed data are combined with the peak wind effects computed for various wind speeds and directions, as described in subsection 2.2, to obtain peak wind effects corresponding to specified return periods. Subsection 2.5 concludes this section with some brief comments on integration of the DAD approach within the structural design process.

2.1.   AERODYNAMIC DATABASES: PRESSURE TIME SERIES

Pressure time series used in representing the spatio-temporal distribution of wind pressures on a building surface are obtained using boundary layer wind tunnels, which enable simulation of the turbulent flow characteristics and the variation in mean flow velocity with elevation that are associated with specified terrain conditions. For a given building model, tests are conducted for different terrain conditions by varying the height of roughness elements on the upwind floor of the wind tunnel and/or reproducing to model scale the built environment upwind of the building being tested. For each terrain condition, tests are conducted for a range of different wind directions, and in each test, pressure time series are recorded simultaneously using a large number of pressure taps distributed over the surface of a building model. Letting p denote the

number of directions for which tests are conducted, it is convenient to introduce the symbol $\mathbf{\theta} = [\theta_1 \quad \theta_2 \quad \cdots \quad \theta_p]$ to denote the $1 \times p$ vector of wind directions for which pressure time series are available. The wind directions in $\mathbf{\theta}$ are measured relative to a reference axis on the building model, which typically coincides with one of the building's primary axes, as illustrated in Figure 1. While the present report is limited to the treatment of buildings with rectangular plan dimensions, as in Figure 1, it is noted that the approach described herein could be applied in a fairly straightforward manner to buildings with more complicated geometry. For symmetric building models (e.g., gable-roofed buildings), wind tunnel tests can be conducted over a range of less than 360°, and as discussed in Section 3.3.4, symmetry can be exploited to extend these results over a full 360° range. Symmetry seldom exists for tall buildings, for which the built environment is usually reproduced at model scale, and in such cases, wind tunnel tests are generally conducted over a full 360° range.
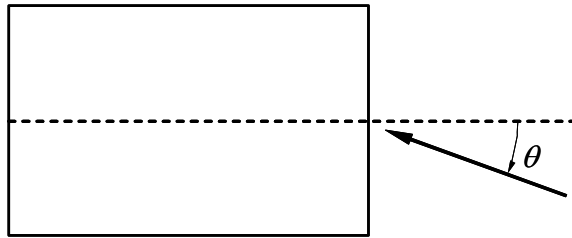
Figure 1. Plan view of example building showing definition of wind direction.

Measured pressures are typically stored in nondimensional form as pressure coefficients, from which pressures for any particular wind speed can be obtained by appropriate scaling. Letting l denote the number of pressure taps and s the number of samples in each time series, the measured pressure coefficients for specified terrain conditions and for a given wind direction θ_j can be expressed as an $l \times s$ matrix $\mathbf{C}_{\mathrm{P},\theta_j}$, where the ith row of $\mathbf{C}_{\mathrm{P},\theta_j}$ is the measured time series for the ith pressure tap. In scaling the pressure coefficients to obtain pressures for a given wind speed, it is important to ensure that the elevation, the averaging time, and the terrain conditions associated with the wind speed of interest are consistent with those of the wind speed used in referencing the pressure coefficients. While pressure coefficients in ASCE 7-02 (ASCE 2003) are referenced using 3 s gust wind speeds at 10 m (33 ft), pressure coefficients herein are referenced using the mean wind speed at roof or eave height, and the averaging time associated with the mean wind speed is taken to be 1 h, which is a typical approximate duration for a wind tunnel test (after conversion to prototype scale). Pressure coefficients referenced using a wind speed at a different height can be re-referenced to roof-height wind speed as discussed by Ho et al. (2005), and the influence of averaging time can be accounted for as discussed in Simiu and Scanlan (1996, Section 2.3.6). Letting V_H denote an hourly mean wind speed at roof (or eave) height H for the appropriate terrain conditions, an $l \times s$ matrix of pressure time series associated with winds of this speed from direction θ_j can then be obtained by scaling the measured pressure coefficients as follows:

$$\mathbf{P}_{\theta_j} = \tfrac{1}{2} \rho V_H^2 \mathbf{C}_{\mathrm{P},\theta_j} \tag{1}$$

4

where ρ = air density, and ρ = 1.225 kg/m³ (ρ = 0.002377 lbf·s²/ft⁴) for dry air at sea level under standard atmospheric conditions. In the treatment of dynamic response in Chapter 4, it is convenient to partition the pressure time series in Eq. (1) to separate the pressures producing forces along each of the building's primary axes.

The prototype-scale sampling frequency associated with the pressure time series follows from the requirement of equivalence between the reduced frequencies at model scale and at prototype scale, which can be expressed as follows:

$$\left(\frac{Df}{V}\right)_m = \left(\frac{Df}{V}\right)_p \tag{2}$$

where D denotes a characteristic dimension of the structure, f denotes the sampling frequency, V denotes the mean wind velocity at a consistent height (e.g., roof height), and the subscripts m and p denote "model" and "prototype" scales, respectively. Letting $\lambda_L = D_m / D_p$ denote the length scale of the wind tunnel model, the prototype sampling frequency can be expressed as follows by rearranging Eq. (2):

$$f_p = f_m \left(\frac{V_p}{V_m}\right) \lambda_L \tag{3}$$

The model-scale sampling frequency f_m, the model-scale wind speed V_m, and the length scale λ_L are constants determined by the wind tunnel testing conditions. In contrast, it is generally necessary to consider a range of values of the prototype-scale wind speed V_p, to reflect the statistical variability of the extreme wind speeds from each direction at the site of interest, as is discussed in the following subsection. Because the prototype-scale sampling frequency f_p is proportional to the prototype-scale wind speed V_p, as shown in Eq. (3), each wind speed V_p that is considered corresponds to a different sampling frequency f_p. As is further discussed in subsection 2.2.2, this dependence of the sampling frequency on the wind speed is particularly important for dynamically sensitive structures, for which responses can be strongly affected by the frequency content of the loading.

2.2.   EVALUATION OF PEAK WIND EFFECTS

This section describes the evaluation of peak wind effects of interest (e.g., internal forces and bending moments) from the pressure time series discussed in the previous section. This process can be divided into two main stages. The first stage, described in subsection 2.2.1, involves transforming the wind pressures, which are applied to the cladding of the building, to resultant wind forces, which are applied to the primary structural system at a number of discrete locations. The second stage, described in subsection 2.2.2, involves the use of structural analysis to evaluate time series of wind effects produced by these resultant wind forces. This second stage is conveniently accomplished using influence coefficients. Peak wind effects are of greatest interest in structural design, and subsection 2.2.3 discusses the estimation of expected peak values from time series of wind effects.

2.2.1. Transforming wind pressures to structural loads

While wind pressures are applied to the cladding of a building, numerical models used in the analysis and design of the building's primary structural system generally do not include cladding elements. Therefore, some approximate procedure is required to represent the transformation of wind pressures on the cladding to resultant loads on the primary structural system. The first step in such a procedure is to determine the tributary area associated with each pressure tap, which defines the area over which the measured pressure is assumed to act. Tributary areas can be determined from the coordinates of the pressure taps, and this process is further discussed in Section 3.2.1. The wind load associated with a particular pressure tap is then given by the product of the measured pressure with the corresponding tributary area. The wind load associated with each of the pressure taps must then be distributed to the primary structural system at a number of discrete locations. Sections 3.2.2 through 3.2.4, present an approach for rigid, gable-roofed buildings, based on that presented by Whalen et al. (2000), in which the wind loads are distributed to the structural frames at the attachment points of girts and purlins which support the cladding panels. This approach is based on structural analysis of a cladding panel simply supported along two edges by girts or purlins, which in turn are attached to the structural frames by hinges. Using this procedure, a "tributary matrix" is assembled, which represents the transfer of wind pressures to structural loads at the girt and purlin attachment points. A simpler approach is used for flexible buildings in Section 4, in which the load associated with each pressure tap is applied to the structure as a point load at or near the position of the pressure tap. In both cases, time series of structural loads are obtained from the measured time series of wind pressures for each wind direction.

2.2.2. Evaluating time series of wind effects

Once time series of resultant wind loads on the primary structural system have been obtained, time series of the wind effects of interest (e.g., bending moments, shear forces, and displacements) can be evaluated from these by structural analysis. This is conveniently accomplished using influence coefficients, which give the values of the wind effects of interest resulting from unit forces at each loading point. Influence coefficients can be obtained using standard structural analysis software by defining load cases corresponding to unit forces at each loading point and computing the resulting wind effects of interest. Static loads are used in computing the influence coefficients, even in the treatment of dynamic responses in Chapter 4. The influence of structural dynamics on the wind effects of interest is handled in Chapter 4 by defining "inertial" influence coefficients associated with unit translational and torsional loads at each floor of the building. Time series of inertial loads associated with translational and torsional accelerations of each floor of the building are computed using modal analysis, and the dynamic contributions to the wind effects of interest are then evaluated from the product of these inertial loads with the "inertial" influence coefficients.

An important distinction between the treatment of static and dynamic responses (i.e., rigid and flexible buildings) concerns the influence of the sampling frequency associated with the time series of wind loads. As shown previously in Eq. (3), the prototype-scale sampling frequency, which determines the time scale of the loading, depends on the wind speed for which responses are required. This dependence is relatively unimportant in evaluating linear, static responses for rigid buildings, because the responses at each instant are simply proportional to the loads at that

6

instant and are independent of the time scale. Consequently, for rigid buildings it is sufficient to simply compute time series of the wind effects of interest corresponding to a unit wind speed. Because wind pressures in Eq. (1) are assumed to be proportional to the square of the wind speed, wind effects corresponding to any wind speed of interest can then be obtained from the effects induced by a unit speed through multiplication by the square of the wind speed, as is further discussed in Chapter 3. In contrast, the dynamic response of flexible buildings can be very sensitive to the time scale of the loading. Because of the dependence of the time scale on wind speed, dynamic responses are not simply proportional to the square of the wind speed, but must be computed independently for each wind speed of interest using the appropriate prototype-scale sampling frequency from Eq. (3).

2.2.3. Estimating expected peaks of time series

Peak wind effects (i.e., maximum and minimum values) are of greatest interest in structural design, and therefore it is necessary to evaluate peaks from the time series of wind effects discussed in the previous section. While the maximum and minimum values of a time series are readily evaluated, these *observed peaks* can exhibit wide variability from one realization to another, due to the highly fluctuating nature of wind pressures (i.e., significant differences might be expected in the peak wind effects computed using several different sets of pressure time series obtained under nominally identical conditions in the same wind tunnel). Therefore it is generally preferable to use a more stable estimator for the expected peaks. Sadek and Simiu (2002) present a procedure for estimating peaks that involves evaluation of probability distributions for the peaks through extension of classical results for Gaussian processes. As part of the software development in this study, a modified version of this procedure has been implemented as a set of MATLAB functions. These MATLAB functions for peak estimation are included with the DAD software packages for rigid and flexible buildings and can also be downloaded independently from <http://www.nist.gov/wind> by following the link for "Estimation of peaks from time series." Further details on the peak estimation procedure are provided at this website. Using such an approach, expected values of the peaks can be estimated and used in place of observed peaks.

It should be noted that the expected maximum and minimum value of a time series depend on the duration of the record under consideration, with increasing record duration leading to higher expected maximum values and lower expected minimum values. It is also noted that the prototype-scale duration of a wind tunnel test varies depending on the wind speed of interest, because of the dependence of the sampling frequency on wind speed, according to Eq. (3). The wind tunnel tests of Ho et al. (2005), for example, had a sampling frequency of $f_m = 500$ Hz and a duration of 100 s. For a model with a length scale of $\lambda_L = 1/100$ and a wind speed of $V_m = 6.1 \, \text{m/s} \, (20 \, \text{mi/h})$ at model eave height, a prototype-scale test duration of 1 h then corresponds to a prototype-scale wind speed of $V_p = 25 \, \text{m/s} \, (56 \, \text{mi/h})$, while a duration of 0.5 h corresponds to a wind speed of $V_p = 50 \, \text{m/s} \, (112 \, \text{mi/h})$ and a duration of 2 h corresponds to a wind speed of $V_p = 12 \, \text{m/s} \, (28 \, \text{mi/h})$. Because of the dependence of expected peak values on record duration, the same prototype-scale duration should ideally be used in evaluating all peaks, with an appropriate duration being 1 h, for consistency with the averaging time associated with the directional extreme wind speed data discussed in Section 2.3. The peak estimation procedure of Sadek and Simiu (2002) can be used to accomplish this, as it allows for estimation of expected

peaks for a duration that differs from the actual duration of the time series under consideration. However, using this procedure for a number of computed time series of bending moments for a rigid, gabled-roofed building, it has been observed that as the duration used in estimating peaks is varied from one-half to twice the actual record duration, the expected peak values differ by less than 5 % from the expected peaks using the actual record duration. This range in duration corresponds to quite a wide range of wind speeds – from 12 m/s (28 mi/h) to 50 m/s (112 mi/h) for the example from Ho et al. (2005) above. It is therefore concluded that peaks estimated using the actual record duration are in most cases acceptably close to peaks for a 1 h duration.

This simplification, that is, neglecting variations in record duration with wind speed, is particularly useful in evaluating peak wind effects for rigid buildings. Peak wind effects for any wind speed of interest can then be evaluated by simply multiplying the peak wind effects for a unit wind speed by the square of the wind speed, without further adjustment to account for variations in record duration due to wind speed. The values of the peak wind effects corresponding to a unit wind speed from each direction are referred to as Directional Influence Factors (DIFs), as in Rigato et al. (2001), and they are further discussed in Section 3.3.3. As noted previously in Section 2.2.2, wind effects for flexible buildings are not simply proportional to the square of the wind speed, but must be computed independently for each wind speed and direction, accounting for dynamic effects. An interpolation procedure is used in Chapter 4 to facilitate evaluation of peak wind effects for any wind speed and direction of interest for flexible buildings. In this procedure, peak responses are evaluated for a number of different wind speeds over the range of interest, and this is repeated for each wind direction for which pressure measurements are available. A polar grid of wind speed and wind direction values is thus defined, with values of the peak wind effects available at each grid point, and peak wind effects for intermediate wind speeds and directions are then estimated from their values at these grid points by interpolation.

2.3.   CLIMATALOGICAL DATABASES: DIRECTIONAL EXTREME WIND SPEEDS

Directional wind speed data, based on simulation or historical observations, are used in representing the probability distribution of extreme winds from each direction at the location of interest. Because events with long return period are of interest in structural design, data representing a significant span of time are required. Available meteorological data cover a relatively short time span (typically about 100 years for hurricanes; even shorter time spans are covered for non-hurricane regions), and therefore, statistical extrapolation techniques are generally required to obtain peak wind speed estimates with long return periods. Hurricane-prone regions and non-hurricane-prone regions require different techniques for estimation of long-period extreme wind speeds, as discussed in Simiu and Scanlan (1996, Chapter 3).

Simulated hurricane wind speeds from Batts et al. (1980) represent estimates of the largest wind speeds from each of 16 directions for 999 hurricanes, generated by Monte Carlo simulation using analytical and empirical models of hurricane winds. The 999 extreme wind events are provided for a large number of locations (mileposts) along the Gulf of Mexico and North Atlantic coast. These simulated data are publicly available at <http://www.nist.gov/wind> by following the links for extreme wind data sets. The simulations are based on the assumption that the hurricane frequency of occurrence is governed by a Poisson process with a constant rate, and this occurrence rate is provided with the wind speed data for each location. The data are reported

8

as one-minute averaged wind speeds in nautical miles per hour at 10 m (33 ft) elevation over open terrain. Because peak wind speeds depend on averaging time and because pressure coefficients are referenced using hourly averaged wind speeds, these one-minute averaged wind speeds must be converted to hourly averages through division by a factor of approximately 1.25 (Simiu and Scanlan 1996, Figure 2.3.10). In this report, simulated hurricane wind speeds are used for illustration; Section 3 uses wind speeds for Miami (milepost 1450), while Section 4 uses wind speeds for New York City (milepost 2550).

In non-hurricane regions or in hurricane regions where significant non-hurricane winds can occur, directional non-hurricane wind speed data are needed. Non-hurricane directional wind speed data are also available at <http://www.nist.gov/wind> in the form of largest annual wind speeds from each of eight directions at 37 locations in the continental United States where hurricanes are not expected to occur. These data are reported as peak 3 s gust speeds in miles per hour at 10 m (33 ft) elevation over open terrain, which must be converted to hourly averages using the procedure described in Simiu and Scanlan (1996, Section 2.3.6). For each of these non-hurricane locations, data are available for about 30 years. Another source of directional wind speed data for the United States is the Automated Surface Observing System (ASOS), which provides climatological observations at most of the nation's airports. ASOS records, which can be obtained from the National Oceanic and Atmospheric Administration, contain hourly reports of peak gust wind speeds and corresponding wind directions, along with many other climatological observations. Software to extract directional wind speed data sets from ASOS records is currently in development at NIST.

After appropriate scaling to account for the averaging time (e.g., Simiu and Scanlan 1996, Figure 2.3.10), directional wind speed data for a given location can be represented as an $h \times q$ matrix $\mathbf{V}_Z$ of hourly averaged wind speeds at elevation Z over terrain with roughness length Z_0, where h denotes the number of hurricanes (or the number of years, in the case of non-hurricane wind speeds) and q denotes the number of wind directions. The simulated directional hurricane wind speed data cited above correspond to Z = 10 m (33 ft) and open terrain, for which Z_0 = 0.03 m (0.1 ft) is representative. In the case of hurricane wind speeds, each row of $\mathbf{V}_Z$ corresponds to a particular hurricane, while in the case of non-hurricane wind speeds, each row corresponds to a particular year. In the former case, the occurrence rate ν of hurricanes at the location of interest is also required. For both hurricane and non-hurricane wind speeds, each column of $\mathbf{V}_Z$ corresponds to a particular wind direction, and it is convenient to introduce the symbol $\boldsymbol{\alpha} = [\alpha_1 \quad \alpha_2 \quad \cdots \quad \alpha_q]$ to denote the $1 \times q$ vector of wind directions for which extreme wind speeds are available.

Since roof-height wind speeds are generally used in referencing the pressure coefficients (e.g., Ho et al. 2005), the matrix $\mathbf{V}_Z$ of wind speeds at elevation Z must be scaled to wind speeds at roof height H. The ratio of mean wind speeds at different elevations depends upon the terrain conditions, as characterized by a roughness length parameter, and a vector of roughness lengths $\mathbf{z}_0 = [z_{01} \quad z_{02} \quad \cdots \quad z_{0q}]$ can be defined for the site of interest, giving the roughness lengths associated with winds from each of the directions in the vector $\boldsymbol{\alpha}$. Assuming a similarity model for the mean velocity profile (e.g., Simiu and Scanlan 1996, Section 2.2.5), a mean wind speed at elevation Z over terrain with roughness length Z_0, denoted V_Z, can be converted to a

9

mean wind speed at height H over terrain with roughness length z_{0j}, denoted V_H, through scaling by the following factor:

$$\lambda_j = \frac{\ln(H/z_{0j})}{\ln(Z/Z_0)}\left(\frac{z_{0j}}{Z_0}\right)^{0.0706} \tag{4}$$

It is noted that some practitioners use the power law, rather than the similarity model, and the power law is used in the software for flexible buildings in open or suburban terrain. However, for buildings in large cities neither the similarity model nor the power law may be applicable, and the scale factors must be estimated for each direction from wind tunnel tests. An $h \times q$ matrix $\mathbf{V}_H$ of hourly averaged wind speeds at eave height can then be obtained by multiplying each column of $\mathbf{V}_Z$ by the corresponding scale factor. This operation can be expressed as follows:

$$\mathbf{V}_H = \mathbf{V}_Z \cdot \text{diag}(\boldsymbol{\lambda}) \tag{5}$$

where $\boldsymbol{\lambda} = [\lambda_1 \quad \lambda_2 \quad \cdots \quad \lambda_q]$ is a $1 \times q$ vector of scale factors for each direction, with its elements defined by Eq. (4), and $\text{diag}(\boldsymbol{\lambda})$ is a $q \times q$ diagonal matrix formed by placing the elements of $\boldsymbol{\lambda}$ along the main diagonal, with zeros elsewhere. The directional extreme wind speeds in $\mathbf{V}_H$ then represent hourly averages at roof height for appropriate terrain conditions and are thus consistent with the wind speeds used in referencing the pressure coefficients.

It is generally necessary to shift the wind directions in $\boldsymbol{\alpha}$ so that they are defined consistently with the wind directions in $\boldsymbol{\theta}$, introduced in subsection 2.1, for which pressure time series are available. As shown in Figure 2, the wind directions in $\boldsymbol{\alpha}$ are measured in degrees clockwise from the north, in contrast with the wind directions in $\boldsymbol{\theta}$, which are measured relative to a reference axis of the building model. Letting α_0 denote the orientation of this reference axis, measured in degrees clockwise from the north, the wind directions in $\boldsymbol{\alpha}$ can be shifted by the orientation angle α_0 as follows to obtain a $1 \times q$ vector $\hat{\boldsymbol{\theta}} = [\hat{\theta}_1 \quad \hat{\theta}_2 \quad \cdots \quad \hat{\theta}_q]$ of wind directions that are defined consistently with those in $\boldsymbol{\theta}$:

$$\hat{\theta}_j = [\![\alpha_j - \alpha_0]\!]_0^{360} \tag{6}$$

where the brackets and specified bounds indicate that the resulting values are shifted by 360°, as necessary, to ensure that $0 \le \hat{\theta}_j < 360$. While the shifted wind directions in $\hat{\boldsymbol{\theta}}$ are defined consistently with those in $\boldsymbol{\theta}$, the values in these two vectors generally will not coincide. The reason for this is that wind tunnel pressure measurements are typically recorded at smaller increments in wind direction than directional extreme wind speed data are available. Therefore interpolation or resampling is generally required to evaluate peak wind effects corresponding to the wind directions in $\hat{\boldsymbol{\theta}}$ from peaks computed using pressure time series corresponding to the wind directions in $\boldsymbol{\theta}$.
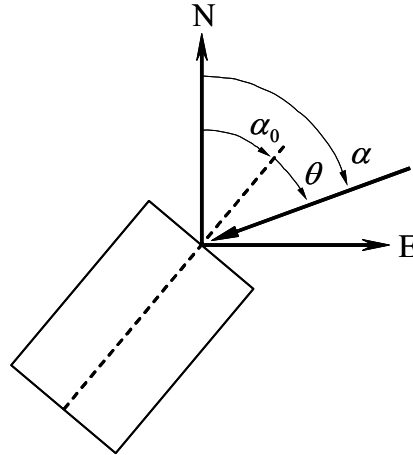
Figure 2. Plan view showing definition of building orientation and
relationship between alternative definitions of wind direction.

2.4. PEAK WIND EFFECTS WITH SPECIFIED RETURN PERIOD

The final stage of the analysis is to combine the site-specific climatalogical information with the building aerodynamics to evaluate peak wind effects with specified return period, rigorously accounting for building orientation and wind directionality. For each directional wind speed in the matrix $\mathbf{V}_H$ from Eq. (5), corresponding peak values of the wind effects of interest can be evaluated by interpolation from the peak values computed as described in Section 2.2. For rigid buildings, the influence of wind speed is represented by multiplying Directional Influence Factors by the square of the wind speed, and interpolation is performed only with respect to wind direction, as discussed in Section 3.5.1. For flexible buildings, interpolation of peak responses is performed with respect to both wind speed and direction. It is emphasized that because of the dependence of the wind directions in Eq. (6) on building orientation, the interpolation process to evaluate peak wind effects corresponding to each element of $\mathbf{V}_H$, as well as the subsequent procedure for evaluating return periods, must be repeated for each building orientation of interest. If the building orientation is unknown, then peak wind effects with a specified return period can be evaluated for a number of possible building orientations. Expected values of peak wind effects for the specified return period can then be estimated as a weighted combination of the results for each orientation, with weighting factors equal to the probability of occurrence of each orientation.

Each row of $\mathbf{V}_H$ corresponds to a particular hurricane (or year, for non-hurricane winds), and the highest peaks corresponding to each hurricane (or year) are of interest. For a given wind effect, the maximum (or minimum) value corresponding to each row of $\mathbf{V}_H$ is evaluated to obtain a time series of the maximum (or minimum) value of that wind effect in each hurricane (or year). Statistical analysis of these time series can then be used to estimate annual probabilities of exceedance associated with different values of the wind effect. These annual probabilities can be converted to return periods, where the return period is defined as the inverse of the annual probability of exceedance. Long return periods (e.g., 50 years or 500 years) are of interest in structural design, and because directional wind speed data are typically available for only a few

decades, extrapolation is generally required to estimate peak wind effects with long return periods. This can be accomplished by best-fitting an extreme value distribution to the time series of peak wind effects.

When using simulated directional hurricane wind speed data (Batts et al. 1980), time series of peak wind effects corresponding to 999 hurricanes are obtained, and because of the long duration of these time series, values with long return periods can be estimated fairly simply using order statistics, without the need to fit an assumed probability distribution. The time series of maximum values of a particular wind effect in each hurricane can be expressed as an $h \times 1$ vector $\mathbf{b}^{max} = [b_1^{max} \quad \cdots \quad b_h^{max}]$, where h is the number of hurricanes. Let the elements of this vector be sorted in descending order, so that $b_1^{max} = \max(\mathbf{b}^{max})$. The probability that the wind effect b will exceed the kth ranked value b_k^{max} in any given hurricane can then be estimated as follows:

$$P\left(b > b_k^{max} \mid 1 \text{ hurricane}\right) = \frac{k}{h+1} \tag{7}$$

The simulated hurricane wind speeds of Batts et al. (1980) were based on the assumption that the frequency of hurricane occurrence at a given site is governed by a Poisson process with constant occurrence rate. For hurricane winds, it is therefore consistent to make this same assumption in computing the annual probability of exceedance of b_k^{max} based on the probability of exceedance per hurricane given in Eq. (7), whereby the following result is obtained (see e.g., Simiu and Scanlan 1996, p. 115):

$$P\left(b > b_k^{max} \mid 1 \text{ year}\right) = 1 - \exp\left(-\frac{\nu k}{h+1}\right) \tag{8}$$

where ν denotes the hurricane occurrence rate, having units of year^{-1}. The return period associated with exceedance of b_k^{max} is then given by the inverse of this annual probability:

$$\bar{N}_k = \left[1 - \exp\left(-\frac{\nu k}{h+1}\right)\right]^{-1} \tag{9}$$

Responses of interest in structural design are generally associated with long return periods, for which $\nu k/(h+1) \ll 1$. Replacing the exponential in Eq. (8) with its Taylor series expansion and neglecting terms of second and higher order, the annual probability of exceedance of b_k^{max} can then be approximated as $\nu k/(h+1)$, which corresponds to a return period of $\bar{N}_k \simeq (h+1)/(\nu k)$. The return period given by this approximation is within 1 % of the exact value for return periods greater than 50 years. Using this approximation, or the original expression in Eq. (9), an $h \times 1$ vector $\bar{\mathbf{N}} = [\bar{N}_1 \quad \bar{N}_2 \quad \cdots \quad \bar{N}_h]^T$ can be assembled, giving the return period associated with each element of $\mathbf{b}^{max}$. The maximum value of the wind effect b corresponding to a specified return period $\bar{N}$ can then be computed from the vectors $\bar{\mathbf{N}}$ and $\mathbf{b}^{max}$ by interpolation. The minimum value of the wind effect b corresponding to a specified return period can be evaluated in an analogous manner, starting with a time series $\mathbf{b}^{min}$ of minimum values in each hurricane, sorted in *ascending* order.

2.5. IMPLEMENTATION IN STRUCTURAL DESIGN

It is noted that the DAD approach requires a preliminary structural design, so that influence coefficients corresponding to the wind effects of interest can be computed and used to evaluate peak wind effects as described in subsection 2.2. Preliminary member sizes for this purpose can be established using wind loads from standard provisions such as ASCE 7-02, and preliminary influence coefficients can be obtained by structural analysis using these member sizes. After peak wind effects with the specified return period have been evaluated using these preliminary influence coefficients, demand/capacity ratios can be evaluated and structural members can be resized. Updated influence coefficients can then be computed using the modified member sizes, and the DAD procedure can be repeated. This iterative process should be repeated as necessary until acceptable convergence is achieved in the wind effects of interest corresponding to the specified return period.

3. **Application to Rigid Buildings: Static Analysis and Interpolation Issues**

Joseph A. Main

This section describes an implementation of the DAD approach for predicting the linear, static response of rigid buildings to wind loading. The term "rigid" denotes a structure with negligible dynamic response to wind loads, and the defining criterion used in the ASCE 7-02 Standard is that the fundamental natural frequency is ≥ 1 Hz (ASCE 2003). The requisite computations in this section are presented using matrix notation to facilitate efficient implementation. While the basic approach described in this section is applicable to more general types of rigid buildings, the accompanying software is limited to the relatively simple type of gable-roofed building depicted in Figure 3, as are the example calculations presented in this section, which were performed using the accompanying software. The geometry of this relatively simple type of building can be represented by four independent length dimensions: the width W, length L, eave height H, and roof rise R. The software has also been developed specifically to handle aerodynamic databases in the standard HDF format developed by Ho et al. (2005). The use of this standard format allows the pressure time series to be loaded directly by the software and automatically applied to the structural model, eliminating the preprocessing of pressure data previously required by WiLDE-LRS (Whalen et al. 2002).
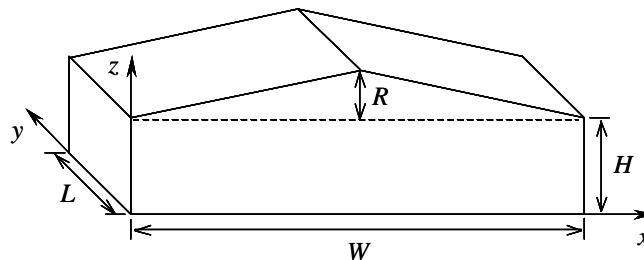
Figure 3. Simple gable-roofed building.

3.1. OVERVIEW

The outline of this section is as follows. Section 3.2 presents the approach used for transforming the wind pressures to structural loads, which was previously discussed in general terms in Section 2.2.1. A "tributary matrix" is introduced to represent the distribution of wind pressures from the cladding of the building to its primary structural system, and a procedure for assembling the tributary matrix is presented, which is implemented in the accompanying software. Section 3.3 presents the approach used to compute structural responses (i.e., wind effects such as internal forces and bending moments) from the resultant wind loads. The responses of interest are expressed using a matrix of influence coefficients associated with unit forces at the cladding attachment points, and a formal expression for the influence coefficient matrix is presented in

Section 3.3.1. Influence coefficients can be obtained using standard structural analysis software, and in the accompanying DAD software influence coefficients for the responses of interest are included in a building input file in spreadsheet format (comma-separated values). This building input file also contains additional information that defines the building, such as its dimensions, the frame locations, and the terrain conditions. As in Rigato et al. (2001) peak responses are expressed using Directional Influence Factors (DIFs), discussed in Section 3.3.3, which define peak responses corresponding to unit wind speeds from each direction and can be scaled to obtain peak responses for any wind speed of interest. Section 3.3.4 describes a formal procedure for exploiting model symmetry to extend the DIFs over a full 360° range of wind directions using measurements recorded over a smaller range.

Section 3.4 discusses the estimation of peak structural responses using pressure measurements from models with differing dimensions. Given the wide range of structural geometries encountered in design as well as practical limitations on the number of building model variations for which measured pressures can be obtained, it is unlikely in practice that measured pressures would be available for a model with dimensions that precisely match the dimensions of the structure of interest. Establishment of DAD as a broadly applicable methodology therefore requires some reliable means of interpolation to enable prediction of internal forces for structures with dimensions intermediate to those for which pressure measurements are available. Previous efforts to develop such means of interpolation have made use of artificial neural networks in attempting to account for the complexities in the spatio-temporal distribution of wind pressures and pressure dependence on model geometry and wind direction (Chen et al. 2003a; Chen et al. 2003b). While the predictions of these models were found to be fairly good, the complexity of these approaches could potentially be a hindrance to broader application in design.

In Section 3.4, a relatively simple method of interpolation is proposed, in which peak structural responses (e.g., bending moments and axial forces) are interpolated, rather than wind pressures, thus eliminating the necessity for the interpolation scheme to account explicitly for spatial and temporal distributions of the pressures. In the proposed approach, separate analyses are performed using measured wind pressures from a number of building models with dimensions that bound those of the structure of interest. In each of these bounding analyses, the coordinates of the pressure taps are scaled to match the dimensions of the structure of interest, as discussed in Section 3.4.1, and the measured pressures are then treated as if they had been measured on a model with the same dimensions as the structure of interest. The pressure tap coordinates and building dimensions are provided with the measured pressure time series in the standard HDF pressure database format. In the accompanying software, the procedures in Section 3.4.1 are implemented to automatically scale the tap coordinates, if necessary, before assembling the tributary matrix to transfer the pressures to the structural system.

This scaling procedure is clearly a simplification of the true building aerodynamics, resulting in inaccurate correlations between pressures at different locations due to the artificial adjustment of the separation distance between pressure taps, as well as failing to represent changes in the physics of the wind flow due to changing building geometry. However, the errors are considerably reduced when the peak responses for the structure of interest are obtained by interpolation between the peak responses estimated from each of the bounding analyses. In Section 3.4.2 a fairly simple multi-dimensional interpolation scheme is presented for this purpose, in which greater weight is given to results from building models that more closely match the dimensions of the structure of interest. The proposed approach is illustrated using

pressure measurements from Ho et al. (2005) for models with the same plan dimensions and roof slope but with three different eave heights. Peak responses generated by interpolation from the models with the largest and the smallest eave height are compared with values obtained by applying the pressures actually measured on the model with intermediate eave height, and remarkably good agreement is observed. In contrast, it is found that the interpolation procedure is not as successful for different roof slopes. Pressure measurements from Ho et al. (2005) are also considered for models with the same plan dimensions and eave height but with three different roof slopes, and peak responses generated by interpolation from the models with the largest and the smallest roof slope are found in some cases to be about 50 % less that the values obtained by applying the pressures actually measured on the model with intermediate roof slope. This example corresponds to a difference of 22° between the larges and smallest roof inclination angles, and it is therefore concluded that pressure data are required from models with smaller increments in roof slope in order for the proposed interpolation scheme to give reliable results.

Finally, Section 3.5 discusses the estimation of peak responses with specified return period. The accompanying software allows the extreme wind speed climate to be represented using simulated hurricane wind speed data from Batts et al. (1980) and could be readily extended to make use of other databases that may become publicly available. Section 3.5.1 presents a procedure for resampling DIFs to coincide with wind directions for which directional extreme wind data are available. Section 3.5.2 presents a simple, approximate procedure for interpolating DIFs obtained from pressure measurements for different terrain conditions, to accommodate cases in which the terrain conditions at the location of interest differ from those of available pressure measurements and may vary with direction. Section 3.5.3 then discusses the evaluation of time series of peak responses from the directional extreme wind speeds, from which responses with specified return period can be estimated as discussed previously in Section 2.4.

3.2. TRANSFER OF WIND LOADING FROM CLADDING TO STRUCTURE

3.2.1. Determination of tributary areas for pressure taps

In making use of measured pressures to predict structural responses, it is necessary to evaluate the tributary area associated with each tap, where "tributary area" denotes the area over which the pressure measured at a particular tap is assumed to act. A procedure has been developed that automatically evaluates tributary areas using the tap coordinates, which may be either scaled coordinates or actual coordinates. The procedure for evaluating tributary areas is applied to each face of the building in turn, and the coordinates of the taps on each face are expressed using a local s-y coordinate system in the plane of that face, as depicted in Figure 4. The y-coordinate coincides with the global y-coordinate, while the s-coordinate is obtained from the global x- and z-coordinates by transformation. Taps on the end walls are not considered, as structural responses in the y-direction are not evaluated at present.
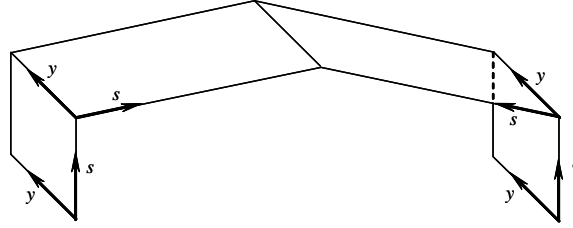
Figure 4. Definition of local coordinate system for each building face.

Figure 5(a) depicts a simple tap array plotted in the *s-y* plane (taps are indicated by the + signs). For this simple type of tap array, which has the same number of taps in each row and the same number of taps in each column, the bounds of the tributary areas are simply lines midway between the adjacent rows and columns of taps, while the exterior tributary bounds for the outermost taps are defined by the edges of the face. For taps located on the boundary between two faces, such as those shown along the top edge of Figure 5(a), the tributary areas are assumed to extend over both adjoining faces, and therefore, the taps must be included in both faces when evaluating tributary areas. More complicated tap arrays, such as that depicted in Figure 5(b), can in many cases be treated by dividing the array into a number of simple tap arrays, for which the tributary areas can be determined as described above. The portions of the tap array on each side of the vertical arrows in Figure 5(b) are simple arrays, having the same number of taps in each row and the same number of taps in each column.
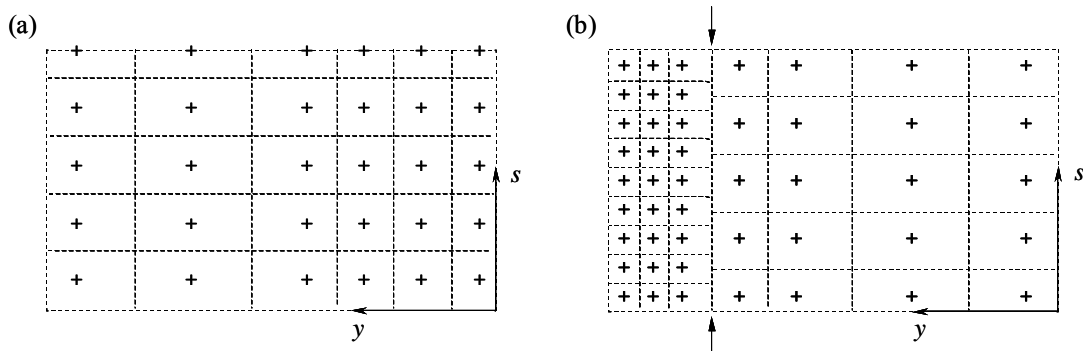
Figure 5. Identification of tributary areas for taps on a particular face.
(a) Simple tap array; (b) More complicated tap array with varying tap density.

3.2.2. Assumed form of structural system

The structural system of the building under consideration is assumed to be of the general form illustrated in Figure 6. The primary structural system consists of frames spanning the width of the building, in the *x-z* plane. These frames are plotted with heavy lines in Figure 6. The structural frames need not be equivalent, and some may have interior columns, like the end frames in shown Figure 6. The columns of the frames need not be pinned at the base. Girts and purlins, which are plotted with thin lines in Figure 6, span between the frames in the *y*-direction. The cross-members on the walls are called girts, while those on the roof are called purlins. Roof panels and wall panels, which form the exterior envelope of the building, are attached to the girts

and purlins, and the shaded area in Figure 6 indicates a roof panel. For conciseness, the term "purlin" is used in this paper to represent either a girt or a purlin, and the term "cladding panel" is used to represent either a roof panel or a wall panel.
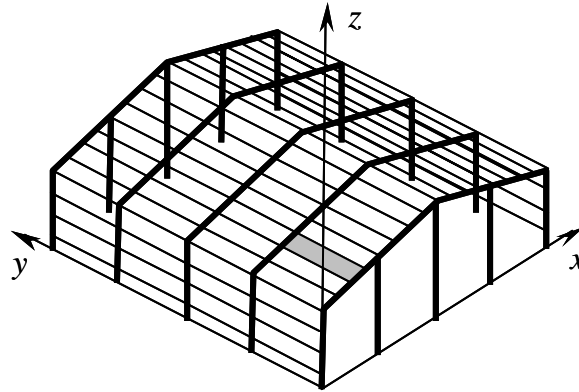
Figure 6. Typical form of structural system for low-rise building.

A number of simplifying approximations are introduced in analyzing the structural system of Figure 6. The major simplification is that the purlins and cladding panels are not included in the structural model, and only the structural frames are explicitly modeled. Further, responses to loads in the *y*-direction are not considered. The coupling between frames introduced by the cladding system is then neglected, and the response of each frame in the *x-z* plane is analyzed independently. Even though the purlins are not included in the structural model, it is noted that the out-of-plane restraint provided to the frames by the purlins can be important (e.g., for preventing lateral-torsional buckling) and should not be neglected in design. Because the purlins and cladding panels are not included in the structural model, it is necessary to determine how the wind pressures, which are applied to the cladding panels, are distributed as resultant wind loads to the structural frames at the girt and purlin attachment points.

In illustrating the DAD procedure in this section, a building is considered with dimensions given by $W = 36.6$ m (120 ft), $L = 57.2$ m (187.5 ft), $H = 5.5$ m (18 ft), and $R = 1.5$ m (5 ft). Pressure measurements for a 1:100 scale model with these dimensions are available from Ho et al. (2005), with tests performed over a range of 180° in 5° increments, for a total of 37 directions. A structural system consisting of 11 equally spaced frames is considered, as indicated by vertical lines in Figure 7, and the first interior frame, which is highlighted in Figure 7, is selected for analysis. A preliminary design for the selected frame was established using wind loads from ASCE 7-02 for open terrain, in combination with applicable dead and live loads.
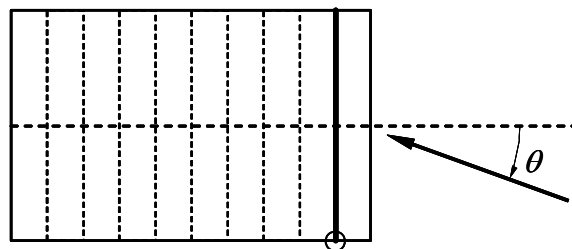
Figure 7. Plan view of example building showing wind direction and selected frame.

3.2.3. Resultant forces on structural frames

The procedure for predicting structural responses makes use of a discretized structural model (e.g., a finite element model). Let the number of unconstrained degrees of freedom in the structural model be denoted n. Assuming linear behavior and neglecting dynamic effects, the $n \times 1$ vector of generalized displacements $\mathbf{u}$ (which generally includes both nodal displacements and nodal rotations) can be related to the corresponding $n \times 1$ vector of generalized forces $\mathbf{f}$ through an $n \times n$ global stiffness matrix $\mathbf{K}$:

$$\mathbf{Ku} = \mathbf{f} \tag{10}$$

It is assumed that the wind pressures are applied to the cladding of the building, which is not included in the structural model, and that the cladding is attached to the primary structure at a number of discrete locations. For simplicity, it is assumed that the cladding is attached by hinges, so that no moments are transferred to the structure by the cladding. Since pressures by definition act normal to the surface of application, it is further assumed that the resultant forces are oriented normal to the cladding surface at each attachment point. For cases in which cladding surfaces with differing orientation are attached to the structure at a particular point, separate resultant forces are defined for each surface. The kth resultant force can then be represented as the product of a scalar coefficient φ_k with an $n \times 1$ vector $\mathbf{w}_k$ of unit magnitude that defines the orientation of the resultant force. The vector $\mathbf{w}_k$ has nonzero entries only for degrees of freedom associated with the relevant attachment point, and these nonzero entries correspond to the components of a unit vector normal to the relevant cladding surface at this attachment point, oriented in the direction of positive pressure. Figure 8 shows the unit force vectors $\mathbf{w}_k$ for the selected frame of the example building of Figure 7. The points of application of these unit loads correspond to the locations at which girts and purlins are attached to the structural frame, and these are spaced at intervals of approximately 1.2 m (4 ft).
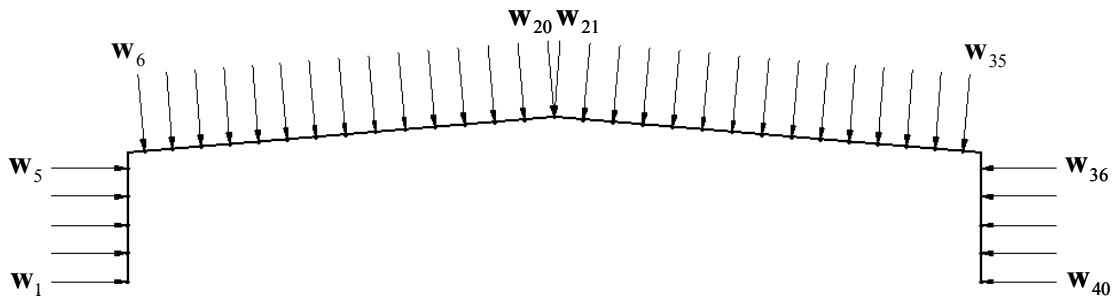
Figure 8. Elevation view of selected frame showing unit force vectors at cladding attachment points (girt and purlin locations).

Letting m denote the total number of resultant forces, the net global force vector $\mathbf{f}$ can then be expressed as a summation of all of the resultant forces, $\mathbf{f} = \varphi_1 \mathbf{w}_1 + \varphi_2 \mathbf{w}_2 + \cdots + \varphi_m \mathbf{w}_m$. In expressing this summation, it is convenient to define an $m \times 1$ vector $\mathbf{\varphi} = [\varphi_1 \quad \varphi_2 \quad \cdots \quad \varphi_m]^T$ of scalar coefficients (the superscript T denotes transposition) and an $n \times m$ matrix

$\mathbf{W} = \begin{bmatrix} \mathbf{w}_1 & \mathbf{w}_2 & \cdots & \mathbf{w}_m \end{bmatrix}$ whose columns are the unit vectors $\mathbf{w}_k$. The summation of resultant wind forces can then be expressed as follows:

$$\mathbf{f} = \mathbf{W}\boldsymbol{\varphi} \tag{11}$$

With the orientation of resultant forces having been assumed in the definition of the unit vectors $\mathbf{w}_k$, what remains to be done is to define the coefficient vector $\boldsymbol{\varphi}$ as a function of the applied pressures. In Eq. (1), an $l \times s$ matrix $\mathbf{P}_{\theta_j}$ of pressure time series was defined, with each row being the time series for a particular pressure tap. Let $\mathbf{p}$ denote an $l \times 1$ vector formed by taking one column from such a matrix, which thus defines the distribution of pressures at the various taps at a particular instant of time. The vector $\boldsymbol{\varphi}$ of resultant force coefficients at that instant can then be expressed as a linear transformation of the vector $\mathbf{p}$ in the following general form:

$$\boldsymbol{\varphi} = \mathbf{A}\mathbf{p} \tag{12}$$

The $m \times l$ "tributary matrix" $\mathbf{A}$ has units of area and can be expressed as $\mathbf{A} = \begin{bmatrix} \mathbf{a}_1 & \mathbf{a}_2 & \cdots & \mathbf{a}_l \end{bmatrix}$, where the kth column $\mathbf{a}_k$ specifies how the tributary area associated with the kth pressure tap is distributed to the various cladding attachment points. (The "tributary area" associated with a given tap is the area over which the measured pressure at that tap is assumed to act.) The validity of the general form of linear transformation in Eq. (12) can be verified conceptually by using a matrix condensation approach, presuming the existence of a detailed discretized model of the structure that includes the cladding. However, a detailed structural model that includes cladding elements is generally unavailable, and simpler approximate techniques are therefore generally required for assembling the matrix $\mathbf{A}$. An approximate procedure for this purpose is described in the following subsection. Combining Eqs. (11) and (12), the generalized force vector $\mathbf{f}$ corresponding to the pressure distribution $\mathbf{p}$ can then be expressed as $\mathbf{f} = \mathbf{W}\mathbf{A}\mathbf{p}$.

3.2.4. Assembly of "tributary matrix"

In this subsection, a relatively simple approximate procedure is introduced for assembling the tributary matrix $\mathbf{A}$ for gable-roofed buildings with the general form of structural system illustrated in Figure 6. The approximations used in this procedure are essentially equivalent to those used by Whalen et al. (2000) in WiLDE-LRS, while the present implementation using a tributary matrix introduces some significant efficiencies. Firstly, the automated assembly of the tributary matrix using information provided in standard UWO HDF files eliminates the manual preprocessing required in WiLDE-LRS, in which pressure time series corresponding to distinct rows of pressure taps must be extracted and saved as separate files. Secondly, since the pressure tap layout remains constant for a given wind tunnel model, the same tributary matrix can be used for pressure measurements from all wind directions, so that the load transfer calculations need to be performed only once at the outset of the analysis. In WiLDE-LRS, by contrast, the load transfer calculations are performed as part of the response analysis, and are thus repeated for each wind direction. The preprocessing of pressure time series described above must also be performed separately for each wind direction when using WiLDE-LRS.

The tributary matrix $\mathbf{A}$ is assembled by independently analyzing each rectangular cladding panel in turn. For each cladding panel, such as that indicated by shading in Figure 6, the pressure taps are identified whose tributary area overlaps the selected cladding panel. This procedure is

illustrated schematically in Figure 9, in which the boundary of the selected cladding panel is superimposed over the pressure tap layout for that face. Circles in Figure 9 indicate those taps whose tributary area overlaps the area of the selected panel. In general, only a portion of the tributary area associated with each of these taps will overlap the selected panel, and the remaining portions of tributary area are handled when considering neighboring cladding panels. Each portion of tributary area that overlaps the selected cladding panel is then distributed to the attachment points at the four corners of the selected panel according to the procedure illustrated in Figure 10.
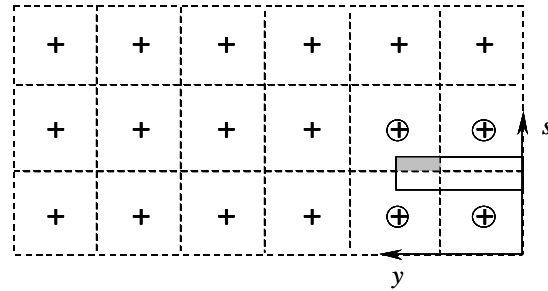
Figure 9. Identification of pressure taps that are tributary to a selected cladding panel.
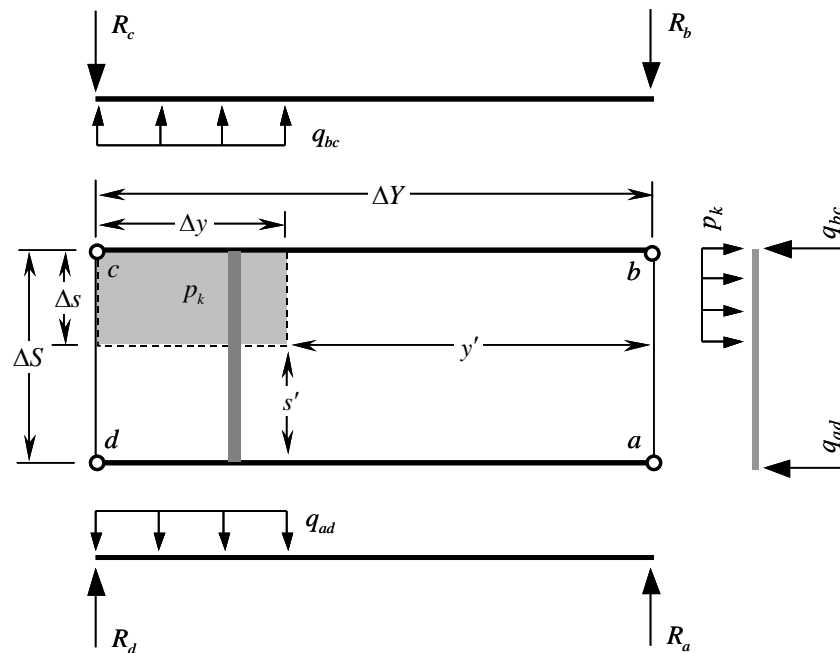
Figure 10. Distribution of pressure loading to resultant forces at the corners of a cladding panel.

The rectangular shaded area in Figure 10 corresponds to the shaded area in Figure 9, representing the portion of tributary associated with a particular tap, denoted tap k, that overlaps the selected cladding panel. The pressure acting over this area is then equal to the pressure measured at tap k, which is denoted p_k. The points labeled a through d in Figure 10 are the four corners of the selected panel, at which points the purlins are attached to the structural frames

and resultant forces are to be evaluated. The heavy lines at the upper and lower edges of the selected panel (i.e., segments bc and ad) represent purlins spanning in the y-direction between adjacent frames. The upper and lower edges of each cladding panel are assumed to be hinged to the purlins, while the left and right edges (i.e., segments ab and cd) are assumed to be free. The resultant forces at the four corners of the selected panel are evaluated by analyzing each purlin as a simply supported beam, as shown by the free-body diagrams at the upper and lower edges of Figure 10, and the resultant forces are equal to the reactions, denoted R_a, R_b, R_c, and R_d.

The loading intensity (force per unit length) on the purlins due to the distributed pressure p_k is evaluated by isolating a strip of cladding panel with unit width, spanning in the s-direction between adjacent purlins and passing through the region over which the pressure p_k is applied, as illustrated by the shaded vertical strip in Figure 10. Because a strip of unit width is considered, the loading intensity on loaded portion of the strip is equal to p_k. Neglecting shear forces on the left and right edges, the isolated strip is then analyzed as a simply supported beam, as shown in the free-body diagram at the right-hand edge of Figure 10. It is noted that cladding panels typically have ribs aligned perpendicularly to the purlins, making them much stiffer for bending in that direction. Therefore, plate action is not expected to dominate, and analyzing a strip of the cladding panel as a simply supported beam is considered a reasonable approximation. The reactions at the upper and lower ends of the strip give the loading intensities on the upper and lower purlins, denoted q_{bc} and q_{ad}, respectively. The values of these load intensities can be obtained by static equilibrium from the free-body diagram at the right-hand edge of Figure 10, and are given as follows:

$$q_{ad} = p_k \, \Delta s \left(1 - s'/\Delta S - \tfrac{1}{2}\Delta s / \Delta S\right); \quad q_{bc} = p_k \, \Delta s \left(s'/\Delta S + \tfrac{1}{2}\Delta s / \Delta S\right) \tag{13}$$

With the loading intensities q_{bc} and q_{ad} determined, the reactions at the ends of the upper and lower purlins can be similarly determined from the free-body diagrams at the upper and lower edges of Figure 10. Each of these reaction forces is proportional to the applied pressure p_k, and it is convenient to express them as follows:

$$R_a = p_k A_a; \; R_b = p_k A_b; \; R_c = p_k A_c; \; R_d = p_k A_d \tag{14}$$

where A_a, A_b, A_c, and A_d denote the portions of the tributary area $\Delta s \, \Delta y$ distributed to each of the four attachment points at the panel corners and are given as follows (it is noted that $A_a + A_b + A_c + A_d = \Delta s \, \Delta y$):

$$A_a = \Delta s \, \Delta y \left(1 - s'/\Delta S - \tfrac{1}{2}\Delta s / \Delta S\right)\left(1 - y'/\Delta Y - \tfrac{1}{2}\Delta y / \Delta Y\right) \tag{15}$$

$$A_b = \Delta s \, \Delta y \left(s'/\Delta S + \tfrac{1}{2}\Delta s / \Delta S\right)\left(1 - y'/\Delta Y - \tfrac{1}{2}\Delta y / \Delta Y\right) \tag{16}$$

$$A_c = \Delta s \, \Delta y \left(s'/\Delta S + \tfrac{1}{2}\Delta s / \Delta S\right)\left(y'/\Delta Y + \tfrac{1}{2}\Delta y / \Delta Y\right) \tag{17}$$

$$A_d = \Delta s \, \Delta y \left(1 - s'/\Delta S - \tfrac{1}{2}\Delta s / \Delta S\right)\left(y'/\Delta Y + \tfrac{1}{2}\Delta y / \Delta Y\right) \tag{18}$$

The areas A_a, A_b, A_c, and A_d can then be added to the appropriate entries in the kth column of the tributary matrix $\mathbf{A}$, and this can be repeated for each of the taps whose tributary area overlaps the selected cladding panel. By repeating this procedure for each cladding panel, the full tributary matrix can be assembled. It is noted that if only a subset of the structural frames are to

be analyzed, only the cladding panels that have an edge adjoining the selected frames need to be considered in assembling the tributary matrix.

3.3.   ANALYSIS OF STRUCTURAL RESPONSE

3.3.1. Expressing responses in terms of influence coefficients

The relationship in Eq. (10) can be solved for the displacements, which can be expressed as $\mathbf{u} = \mathbf{K}^{-1}\mathbf{f}$. The matrix inverse notation is used for convenience, while it is noted that Eq. (10) can generally be solved more efficiently without forming the explicit inverse $\mathbf{K}^{-1}$ (e.g., by Gaussian elimination). With all forces applied at element nodes, as ensured by the assumed form of $\mathbf{f}$ in Eq. (11), internal forces in structural elements, which are of interest in design, can be expressed as a linear combination of the generalized displacements in the following general form:

$$r_i = \mathbf{e}_i^T \mathbf{u} \tag{19}$$

where $\mathbf{e}_i$ is an $n \times 1$ vector, and the subscript i is simply an index to differentiate among the various internal force quantities of interest. The response quantity r_i can generally be expressed most directly in the local coordinate system of the element in which it occurs, as $r_i = \bar{\mathbf{e}}_i^T \bar{\mathbf{u}}$, where the overbar denotes quantities expressed in local coordinates. For a prismatic planar frame element, for example, the generalized displacements of the two ends can be expressed in the element's local coordinate system as $\bar{\mathbf{u}} = [\bar{u}_1 \ \bar{v}_1 \ \bar{\theta}_1 \ \bar{u}_2 \ \bar{v}_2 \ \bar{\theta}_2]^T$ where $\bar{u}$, $\bar{v}$, and $\bar{\theta}$ denote axial displacements, transverse displacements, and in-plane rotations, respectively. The axial force in the frame element (positive in tension) can then be expressed in terms of $\bar{\mathbf{u}}$ as $P = \bar{\mathbf{e}}^T \bar{\mathbf{u}}$, where $\bar{\mathbf{e}}^T = (EA/L)[-1 \ 0 \ 0 \ 1 \ 0 \ 0]$, L = element length, A = cross-sectional area, and E = modulus of elasticity. Similarly, the bending moment at end 1 of the frame element can be expressed as $M_1 = \bar{\mathbf{e}}^T \bar{\mathbf{u}}$, where in this case $\bar{\mathbf{e}}^T = (EI/L^2)[0 \ 6 \ 4L \ 0 \ -6 \ 2L]$ and I = moment of inertia for in-plane bending. Displacements $\bar{\mathbf{u}}$ in an element's local coordinate system can be expressed as a linear transformation of the global displacements in the form $\bar{\mathbf{u}} = \mathbf{C}\mathbf{u}$, where the nonzero entries of $\mathbf{C}$ are direction cosines. Substituting this transformation into the expression $r_i = \bar{\mathbf{e}}_i^T \bar{\mathbf{u}}$ allows the response quantity r_i to be expressed in the global form of Eq. (19) through the relationship $\mathbf{e}_i^T = \bar{\mathbf{e}}_i^T \mathbf{C}$. It is noted that when displacements or differential displacements are of concern (i.e., for serviceability considerations), these can also be readily expressed in the form of Eq. (19), so that r_i may represent either a displacement response or an internal force response.

Letting r (with no subscript) denote the number of response quantities of interest, it is convenient to define an $n \times r$ matrix $\mathbf{E}$, whose columns are the vectors $\mathbf{e}_i$:

$$\mathbf{E} = \begin{bmatrix} \mathbf{e}_1 & \mathbf{e}_2 & \cdots & \mathbf{e}_r \end{bmatrix} \tag{20}$$

Letting $\mathbf{r} = \begin{bmatrix} r_1 & r_2 & \cdots & r_r \end{bmatrix}^T$ denote the $r \times 1$ vector of response quantities of interest, it then follows from Eqs. (19) and (20) that $\mathbf{r}$ can be expressed as

$$\mathbf{r} = \mathbf{E}^T \mathbf{u} \tag{21}$$

Combining Eq. (11) with the inverse of Eq. (10), the displacements $\mathbf{u}$ can be expressed as $\mathbf{u} = \mathbf{K}^{-1}\mathbf{W}\boldsymbol{\varphi}$. Substituting this relationship into Eq. (21), the vector $\mathbf{r}$ of responses can then be expressed in terms of the vector $\boldsymbol{\varphi}$ of force coefficients as follows:

$$\mathbf{r} = \mathbf{N}^T \boldsymbol{\varphi} \tag{22}$$

where $\mathbf{N}$ is an $m \times r$ matrix of influence coefficients defined by its transpose as

$$\mathbf{N}^T = \mathbf{E}^T \mathbf{K}^{-1} \mathbf{W} \tag{23}$$

The matrix $\mathbf{N}$ can be expressed as $\mathbf{N} = \begin{bmatrix} \mathbf{n}_1 & \mathbf{n}_2 & \cdots & \mathbf{n}_r \end{bmatrix}$, where the ith column $\mathbf{n}_i$ is a vector of influence coefficients associated with the ith response quantity. The jth element of the vector $\mathbf{n}_i$ gives the value of the ith response quantity r_i resulting from a unit value of the jth force coefficient (i.e., $\varphi_j = 1$ and $\varphi_k = 0$ for $k \neq j$, so that $\mathbf{f} = \mathbf{w}_j$). While Eq. (23) represents a fairly general expression for the influence coefficients of interest, it is noted that in some cases, particularly for simple frames, the influence coefficients may be evaluated more efficiently through the use of the Müller-Breslau Principle (e.g., Sack 1984). The influence coefficients can also be evaluated using commercial structural analysis software by applying unit forces with appropriate orientation at the cladding attachment points and evaluating the resulting values of the response quantities of interest. For the selected frame of the example building in Figure 7, the moment at the left "knee" (circled in Figure 7 and in Figure 11) is taken as the response quantity of interest and is denoted r_1. Figure 11 shows a plot of the corresponding vector $\mathbf{n}_1$ of influence coefficients, with each element of $\mathbf{n}_1$ plotted in the direction of the corresponding unit vector $\mathbf{w}_k$ shown in Figure 8. While numerical values are not shown in Figure 11, the largest influence coefficient, associated with $\mathbf{w}_{21}$, has a value of $[\mathbf{n}_1]_{21} = -4.71\,\mathrm{N \cdot m/N}$ ($-15.5\,\mathrm{lbf \cdot ft/lbf}$). The influence coefficients shown in Figure 11 correspond to columns pinned at the base, but as noted previously, fixed column bases can also be considered, as well as more complicated frames with interior columns.
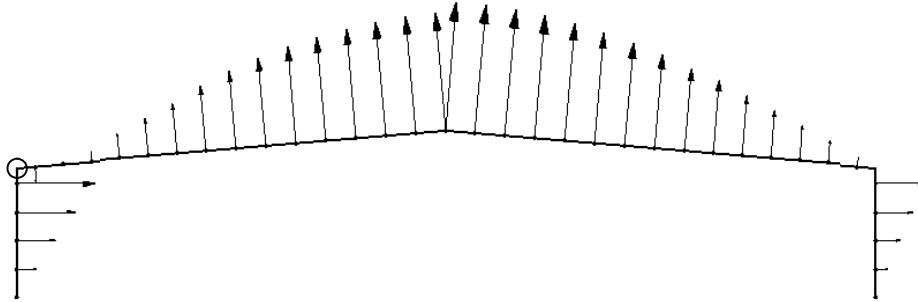
Figure 11. Influence coefficients associated with moment at left knee (circled)..

3.3.2. Time series of structural responses

While Eq. (22) defines the vector $\mathbf{r}$ of response quantities at a particular instant of time, it is necessary to evaluate *time series* of each response quantity from the measured pressure time series. In Eq. (1), an $l \times s$ matrix $\mathbf{P}_{\theta_j}$ of pressure time series associated with winds from direction θ_j was defined, and corresponding to this, an $r \times s$ matrix $\mathbf{R}_{\theta_j}$ of response time series

can be defined, where the ith row of $\mathbf{R}_{\theta_j}$ is a time series for the ith response quantity r_i. Each column of $\mathbf{R}_{\theta_j}$ then represents a vector $\mathbf{r}$ of response quantities at a particular instant, and an expression for $\mathbf{R}_{\theta_j}$ can be obtained using the results of the preceding sections, by replacing the vectors $\mathbf{p}$, $\boldsymbol{\varphi}$, and $\mathbf{r}$ with corresponding matrices. Replacing $\mathbf{p}$ with $\mathbf{P}_{\theta_j}$, Eq. (12) then becomes

$$\boldsymbol{\Phi}_{\theta_j} = \mathbf{AP}_{\theta_j} \tag{24}$$

where the $m \times s$ matrix $\boldsymbol{\Phi}_{\theta_j}$ represents time series of the force coefficients $\boldsymbol{\varphi}$. Replacing $\boldsymbol{\varphi}$ with $\boldsymbol{\Phi}_{\theta_j}$ in Eq. (22), the matrix $\mathbf{R}_{\theta_j}$ of response quantities can then be expressed as

$$\mathbf{R}_{\theta_j} = \mathbf{N}^T \boldsymbol{\Phi}_{\theta_j} \tag{25}$$

Combining Eqs. (1) and (24), the matrix $\boldsymbol{\Phi}_{\theta_j}$ of force coefficients can be expressed as $\boldsymbol{\Phi}_{\theta_j} = \frac{1}{2}\rho V_H^2 \mathbf{AC}_{\mathrm{P},\theta_j}$, and substituting this expression into Eq. (25), the matrix $\mathbf{R}_{\theta_j}$ of response quantities can be expressed directly in terms of the measured pressure coefficients as follows:

$$\mathbf{R}_{\theta_j} = \frac{1}{2}\rho V_H^2 \mathbf{N}^T \mathbf{AC}_{\mathrm{P},\theta_j} \tag{26}$$

The two stages in evaluating structural responses are clearly seen in Eq. (26), where the matrix $\mathbf{A}$ represents the transfer of pressure loading from the cladding to the primary structural system, and the influence coefficient matrix $\mathbf{N}$ expresses the response quantities of interest in terms of the forces applied to the primary structure.

3.3.3. Directional Influence Factors (DIFs)

Peak responses are of greatest interest in structural design, and therefore it is necessary to evaluate peaks from the response time series discussed in the previous section. Peak responses can be evaluated for a unit wind speed from each direction, which are called Directional Influence Factors (DIFs). Responses for a given wind speed from a particular direction can then be obtained simply by scaling the appropriate DIF by the square of the wind speed. It is often necessary to exploit model symmetry in order to obtain DIFs over a full 360° range.

An $r \times 1$ vector $\mathbf{r}_{\theta_j}^{\max}$ of the maximum value of each response quantity can be expressed in terms of the matrix $\mathbf{R}_{\theta_j}$ of response time series as follows:

$$\mathbf{r}_{\theta_j}^{\max} = \max_{rows}\left(\mathbf{R}_{\theta_j}\right) \tag{27}$$

where the notation $\max_{rows}(\ )$ denotes the row-wise maximum of its matrix argument, in which the maximum value in each row is evaluated and the resulting values are assembled to form a column vector. Eq. (27) represents *observed* peaks, which can exhibit wide variability from one realization to another, and it may therefore be preferable to use a more stable estimator for the expected peaks, as discussed in Section 2.2.3. The examples presented in this section use observed peaks, as indicated in Eq. (27). It is noted that the minimum values of the response quantities $\mathbf{r}_{\theta_j}^{\min}$ should generally be computed in addition to the maximum values, as either value may govern in design. For the sake of conciseness, only expressions for maxima are presented in

25

this section, but these expressions are readily extended to minima by simply replacing "max" with "min" in each expression.

Substituting Eq. (26) into Eq. (27) and dividing by V_H^2, the vector of maximum responses for a unit wind speed from direction θ_j, denoted $\mathbf{x}_{\theta_j}^{\max}$, can be expressed as

$$\mathbf{x}_{\theta_j}^{\max} = \mathbf{r}_{\theta_j}^{\max} / V_H^2 = \tfrac{1}{2}\rho \cdot \max_{rows}\left(\mathbf{N}^T \mathbf{A} \mathbf{C}_{\mathrm{P},\theta_j}\right) \tag{28}$$

The vectors of peak responses for unit wind speeds from each direction can then be assembled into an $r \times p$ matrix $\mathbf{X}^{\max}$ as follows:

$$\mathbf{X}^{\max} = \begin{bmatrix} \mathbf{x}_{\theta_1}^{\max} & \mathbf{x}_{\theta_2}^{\max} & \cdots & \mathbf{x}_{\theta_p}^{\max} \end{bmatrix} \tag{29}$$

It is convenient to introduce the symbol $\boldsymbol{\chi}_i^{\max}$ to denote the ith row of $\mathbf{X}^{\max}$, whereby $\mathbf{X}^{\max}$ can be alternatively expressed as

$$\mathbf{X}^{\max} = [\boldsymbol{\chi}_1^{\max} \quad \boldsymbol{\chi}_2^{\max} \quad \cdots \quad \boldsymbol{\chi}_r^{\max}]^T \tag{30}$$

The elements of the $1 \times p$ vector $\boldsymbol{\chi}_i^{\max}$ are then the Directional Influence Factors (DIFs) associated with the ith response quantity.

3.3.4. Exploiting model symmetry

If the wind tunnel model is symmetric about the axis corresponding to $\theta = 0$, then pressures measured for a wind direction of θ could also have been measured for a wind direction of $360° - \theta$ on an identical model with the pressure tap array reflected about the axis $\theta = 0$, as shown in Figure 12(b). The tap array itself need not be symmetric. Similarly, if the model is symmetric about the axis corresponding to $\theta = 90°$, then pressures measured for a wind direction of θ could have been measured for a wind direction of $180° - \theta$ on an identical model with the pressure tap array reflected about the axis $\theta = 90°$, as shown in Figure 12(c). If the model is symmetric about both $\theta = 0$ and $\theta = 90°$, then pressures measured for a wind direction of θ could also have been measured for a wind direction of $180° + \theta$ on an identical model with the pressure tap array reflected about both axes, $\theta = 0$ and $\theta = 90°$, as shown in Figure 12(d). For a doubly symmetric model, it is then possible to effectively obtain pressure measurements for four different wind directions from a single set of measurements, by exploiting model symmetry. It is convenient to introduce the symbols $\boldsymbol{\theta}^{\mathrm{b}}$, $\boldsymbol{\theta}^{\mathrm{c}}$, and $\boldsymbol{\theta}^{\mathrm{d}}$ to denote the $1 \times p$ vectors of symmetric wind directions depicted in Figure 12, where the elements of these vectors are defined as follows, in terms of the elements of $\boldsymbol{\theta}$:

$$\theta_j^{\mathrm{b}} = \left[\!\left[360° - \theta_j \right]\!\right]_0^{360}; \;\; \theta_j^{\mathrm{c}} = \left[\!\left[180° - \theta_j \right]\!\right]_0^{360}; \;\; \theta_j^{\mathrm{d}} = \left[\!\left[180° + \theta_j \right]\!\right]_0^{360} \tag{31}$$

where the brackets and specified bounds indicate that the resulting values are shifted by $360°$ degrees, as necessary, to ensure that they are $\geq 0°$ and $< 360°$.

To compute structural responses corresponding to these symmetric wind directions, it is necessary to assemble tributary matrices, corresponding to $\mathbf{A}$ in Eq. (12), that specify the manner in which pressures from each of the reflected tap layouts are distributed to the cladding attachment points on the primary structural system. The matrices corresponding to the symmetric wind directions defined in Eq. (31) are denoted $\mathbf{A}_{\mathrm{b}}$, $\mathbf{A}_{\mathrm{c}}$, and $\mathbf{A}_{\mathrm{d}}$, representing the reflected tap

layouts depicted schematically in Figure 12(b), (c), and (d), respectively. Responses for unit wind speeds from each of the symmetric wind directions can then be computed by replacing $\mathbf{A}$ in Eq. (28) with $\mathbf{A}_b$, $\mathbf{A}_c$, or $\mathbf{A}_d$, as appropriate. The $r \times 1$ vector of maximum responses for a unit wind speed from direction θ_j^b, for example, is denoted $\mathbf{x}_{b\theta_j}^{max}$ and is computed as $\mathbf{x}_{b\theta_j}^{max} = \frac{1}{2}\rho \cdot \max_{rows}(\mathbf{N}^T \mathbf{A}_b \mathbf{C}_{P,\theta_j})$. The maximum responses from each of the p wind directions can then be assembled as an $r \times p$ matrix $\mathbf{X}_b^{max} = [\mathbf{x}_{b\theta_1}^{max} \quad \mathbf{x}_{b\theta_2}^{max} \quad \cdots \quad \mathbf{x}_{b\theta_p}^{max}]$ of DIFs. Using $\mathbf{A}_c$ and $\mathbf{A}_d$, matrices $\mathbf{X}_c^{max}$ and $\mathbf{X}_d^{max}$ can be similarly assembled, giving DIFs for the wind directions in $\boldsymbol{\theta}^c$ and $\boldsymbol{\theta}^d$, respectively.
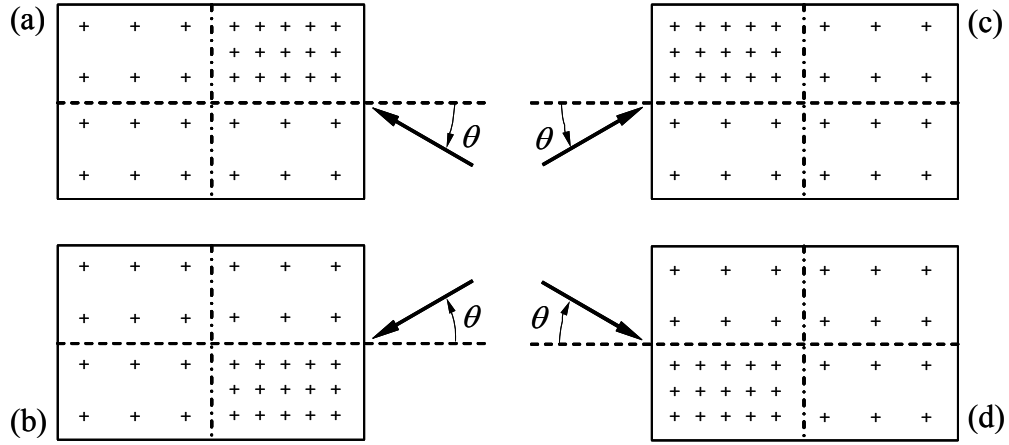
Figure 12. Schematic plan view of building model showing symmetric wind directions corresponding to reflection of pressure tap array about axes of symmetry.

A $1 \times \bar{p}$ vector $\bar{\boldsymbol{\theta}} = [\bar{\theta}_1 \quad \bar{\theta}_2 \quad \cdots \quad \bar{\theta}_{\bar{p}}]$ of wind directions can then be formed with its elements given by the union of the elements in $\boldsymbol{\theta}$, $\boldsymbol{\theta}^b$, $\boldsymbol{\theta}^c$, and $\boldsymbol{\theta}^d$ (with no repetitions), where $\bar{p}$ denotes the total number of unique elements in these vectors. In the case of a singly symmetric model, $\bar{\boldsymbol{\theta}}$ is formed from the union of $\boldsymbol{\theta}$ with $\boldsymbol{\theta}^b$ or $\boldsymbol{\theta}^c$, depending on the axis of symmetry. The resulting vector $\bar{\boldsymbol{\theta}}$ will span the full range of 360° if $\boldsymbol{\theta}$ spans a range of at least 90° for a doubly symmetric model or at least 180° for a singly symmetric model. If the range of $\boldsymbol{\theta}$ exceeds these specified values, then overlap will generally occur between the ranges of $\boldsymbol{\theta}$, $\boldsymbol{\theta}^b$, $\boldsymbol{\theta}^c$, and $\boldsymbol{\theta}^d$. Consequently, for a given wind direction $\bar{\theta}_j$ in the resulting vector $\bar{\boldsymbol{\theta}}$, multiple estimates of the corresponding DIFs may be available. Let the notation $\mathbf{X}^{max}|_{\boldsymbol{\theta} = \bar{\theta}_j}$ denote the column (if any) in the matrix $\mathbf{X}^{max}$ for which the corresponding element of $\boldsymbol{\theta}$ equals $\bar{\theta}_j$. Similarly, let $\mathbf{X}_b^{max}|_{\boldsymbol{\theta}^b = \bar{\theta}_j}$ denote the column (if any) in the matrix $\mathbf{X}_b^{max}$ for which the corresponding element of $\boldsymbol{\theta}^b$ equals $\bar{\theta}_j$, and let $\mathbf{X}_c^{max}|_{\boldsymbol{\theta}^c = \bar{\theta}_j}$ and $\mathbf{X}_d^{max}|_{\boldsymbol{\theta}^d = \bar{\theta}_j}$ be defined likewise for the matrices $\mathbf{X}_c^{max}$ and $\mathbf{X}_d^{max}$. These column vectors then provide as many as four estimates of the DIFs corresponding to $\bar{\theta}_j$, from which improved estimates of the expected peaks can be obtained by averaging. An $r \times 1$ vector

$\mathbf{x}_{\bar{\theta}_j}^{\max}$ of peak responses corresponding to a unit wind speed from direction $\bar{\theta}_j$ can then be evaluated by taking the average of all the available estimates:

$$\bar{\mathbf{x}}_{\bar{\theta}_j}^{\max} = \underset{rows}{\mathrm{mean}}\left(\left[\mathbf{X}^{\max}\Big|_{\boldsymbol{\theta}=\bar{\theta}_j} \quad \mathbf{X}_{\mathrm{b}}^{\max}\Big|_{\boldsymbol{\theta}^{\mathrm{b}}=\bar{\theta}_j} \quad \mathbf{X}_{\mathrm{c}}^{\max}\Big|_{\boldsymbol{\theta}^{\mathrm{c}}=\bar{\theta}_j} \quad \mathbf{X}_{\mathrm{d}}^{\max}\Big|_{\boldsymbol{\theta}^{\mathrm{d}}=\bar{\theta}_j}\right]\right) \tag{32}$$

where the notation $\mathrm{mean}_{rows}(\ )$ denotes the row-wise mean of its matrix argument. The peak responses for each direction in $\bar{\boldsymbol{\theta}}$ can then be assembled into an $r \times \bar{p}$ matrix $\bar{\mathbf{X}}^{\max}$ as follows:

$$\bar{\mathbf{X}}^{\max} = \left[\bar{\mathbf{x}}_{\bar{\theta}_1}^{\max} \quad \bar{\mathbf{x}}_{\bar{\theta}_2}^{\max} \quad \cdots \quad \bar{\mathbf{x}}_{\bar{\theta}_{\bar{p}}}^{\max}\right] \tag{33}$$

The matrix $\bar{\mathbf{X}}^{\max}$ gives averaged values of the DIFs for the maximum value of each response quantity for each of the wind directions in the vector $\bar{\boldsymbol{\theta}}$, which extends over the full 360° range. As in Eq. (30), $\bar{\mathbf{X}}^{\max}$ can be alternatively expressed in terms of its rows as $\bar{\mathbf{X}}^{\max} = [\bar{\boldsymbol{\chi}}_1^{\max} \quad \bar{\boldsymbol{\chi}}_2^{\max} \quad \cdots \quad \bar{\boldsymbol{\chi}}_r^{\max}]^T$.
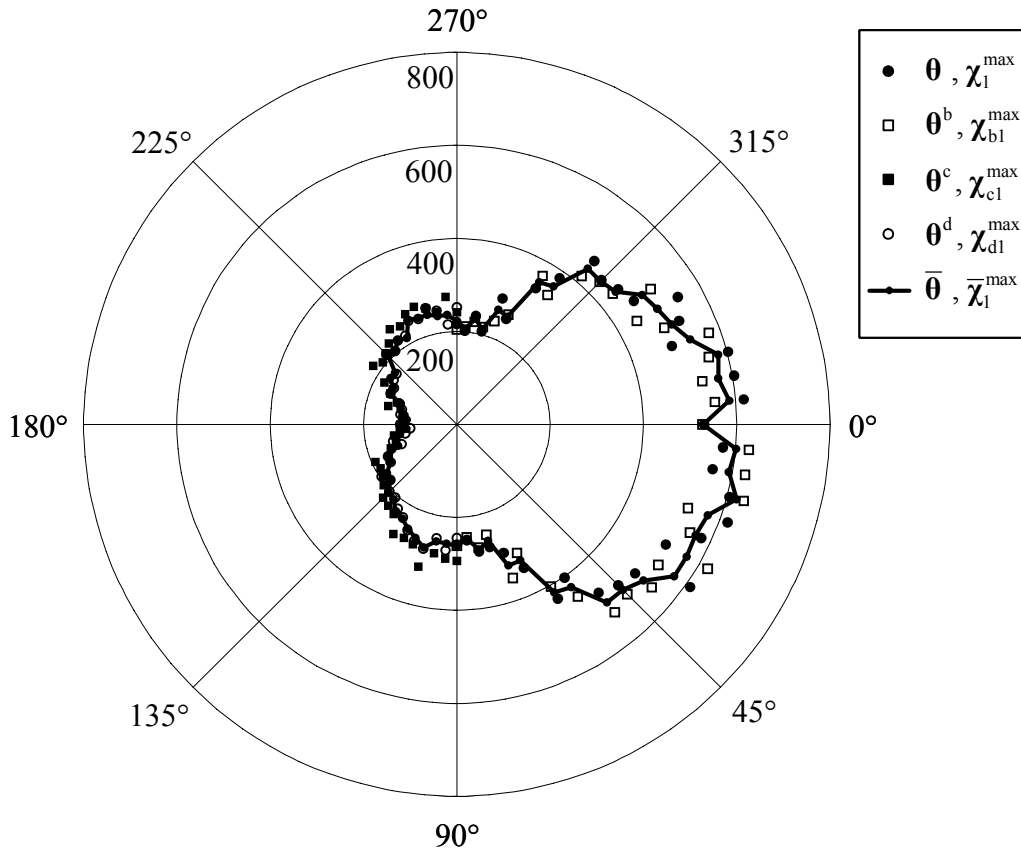
Figure 13. Directional Influence Factors (DIFs) giving maximum values of moment at left knee for a unit wind speed from each direction θ (units of $\mathrm{N \cdot m/(m/s)}^2$).

Figure 13 shows the DIFs associated with the maximum value of the moment at the left knee of the selected frame, plotted against the wind direction θ, as defined in Figure 7. The DIFs associated with $\boldsymbol{\theta}$ and $\boldsymbol{\theta}^{\mathrm{b}}$, denoted $\chi_{\mathrm{l}}^{\max}$ and $\chi_{\mathrm{bl}}^{\max}$, are plotted in the right-hand sector, between 270° and 90°, while the DIFs associated with $\boldsymbol{\theta}^{\mathrm{c}}$ and $\boldsymbol{\theta}^{\mathrm{d}}$, denoted $\chi_{\mathrm{cl}}^{\max}$ and $\chi_{\mathrm{dl}}^{\max}$, are plotted in the left-hand sector, between 90° and 270°. The averaged DIFs $\overline{\chi}_{\mathrm{l}}^{\max}$, associated with $\overline{\boldsymbol{\theta}}$, extend around the full circle, with the largest value being $621 \ \mathrm{N\cdot m/(m/s)^2}$ ($45.6 \ \mathrm{lbf\cdot ft/(ft/s)^2}$), corresponding to $\overline{\theta}_4 = 15°$.

3.4. ESTIMATION OF STRUCTURAL RESPONSES FROM MODELS WITH DIFFERENT DIMENSIONS

The procedure described in this paper is applicable to rigid buildings with the general form depicted in Figure 3. While Sections 3.2 and 3.3 treated cases in which a wind tunnel model is available whose full-scale dimensions exactly match the dimensions of the structure of interest, it is assumed in this section that a model with exactly matching dimensions is unavailable. Therefore, a number of models must be selected with dimensions that are reasonably close to the dimensions of the structure of interest. Preferably, the dimensions of these models should bound the dimensions of the structure of interest, so that improved estimates of the peak responses of interest can be obtained by interpolation. Letting b denote the number of building models selected, it is convenient in subsequent manipulations to use the subscript $i = 1, 2, \ldots, b$ as an index for each building model. The full-scale dimensions of the ith building model, as shown in Figure 3, are then denoted W_i, L_i, H_i, and R_i. The dimensions of the building of interest, for which no wind tunnel model is available, are denoted using the subscript $i = 0$, as W_0, L_0, H_0, and R_0.

3.4.1. Scaling of pressure tap coordinates

The basic approach proposed in this paper for making use of pressure measurements from a model with differing dimensions is simply to scale the coordinates of the pressure taps to match the dimensions of the structure of interest. Let $\mathbf{x}_i$, $\mathbf{y}_i$, and $\mathbf{z}_i$ be vectors specifying, respectively, the x-, y-, and z-coordinates of the pressure taps on the ith building model. With the origin of the coordinate system at a lower corner of the building, as depicted in Figure 3, vectors $\tilde{\mathbf{x}}_i$ and $\tilde{\mathbf{y}}_i$ of scaled x- and y-coordinates that match the dimensions of the structure of interest can be obtained as follows:

$$\tilde{\mathbf{x}}_i = \frac{W_0}{W_i}\mathbf{x}_i \ ; \ \tilde{\mathbf{y}}_i = \frac{L_0}{L_i}\mathbf{y}_i \qquad (34)$$

Scaling of the z-coordinates is somewhat more complicated because it depends on the two independent vertical dimensions H and R. It is convenient to partition the row vector $\mathbf{z}_i$ as $\mathbf{z}_i = [\mathbf{z}_i^H \ \mathbf{z}_i^R]$, where $\mathbf{z}_i^H$ contains the values of $\mathbf{z}_i$ that are $\leq H_i$ (i.e., the z-coordinates of taps on the walls below eave height) and $\mathbf{z}_i^R$ contains the values of $\mathbf{z}_i$ that are $> H_i$ (i.e., the z-

29

coordinates of taps on the roof and on the end walls above eave height). The *z*-coordinates of taps above and below eave height can then be scaled separately as follows:

$$\tilde{\mathbf{z}}_i^H = \frac{H_0}{H_i}\mathbf{z}_i^H \; ; \; \tilde{\mathbf{z}}_i^R = H_0\mathbf{1} + \frac{R_0}{R_i}(\mathbf{z}_i^R - H_i\mathbf{1}) \tag{35}$$

where $\mathbf{1}$ is a vector of ones with the same size as $\mathbf{z}_i^R$. The full vector $\tilde{\mathbf{z}}_i$ of scaled *z*-coordinates can then be formed as $\tilde{\mathbf{z}}_i = [\tilde{\mathbf{z}}_i^H \; \tilde{\mathbf{z}}_i^R]$. After partitioning and scaling, the elements of $\tilde{\mathbf{z}}_i$ should be reordered, as necessary, for consistency with $\tilde{\mathbf{x}}_i$ and $\tilde{\mathbf{y}}_i$, so that the scaled coordinates of the *k*th pressure tap are given by $([\tilde{\mathbf{x}}_i]_k, [\tilde{\mathbf{y}}_i]_k, [\tilde{\mathbf{z}}_i]_k)$. As noted previously, both the pressure tap coordinates and the building dimensions are stored in the standard UWO HDF pressure database files, and using this information, the scaling of tap coordinates represented by Eqs. (34) and (35) can be performed automatically for specified dimensions of the structure of interest.

This scaling of pressure tap coordinates is illustrated schematically in Figure 14, in which the tap coordinates from two models with eave heights H_1 and H_2 (shown in the left column) are scaled to match the dimensions of the model of interest, with eave height H_0 (shown in the right column). For clarity, scaling of the tap coordinates is illustrated only for the taps on the left face in Figure 14, and the other building dimensions (W, L, and R) are equivalent to those of the structure of interest. It is noted that the correlation between pressures measured at different taps depends on their separation distance, and because scaling of tap coordinates artificially adjusts their separation distance, some misrepresentation of the correlation in pressures should be expected. For the building with eave height H_1 in Figure 14, for example, scaling leads to increased separation distances between taps, and therefore, the measured pressures might be expected to be more highly correlated than would be expected for taps at the scaled locations. Conversely, for the building with eave height H_2, the separation distances between taps are reduced by scaling, so that the measured pressures might be expected to be less highly correlated than would be expected for taps at the scaled locations.
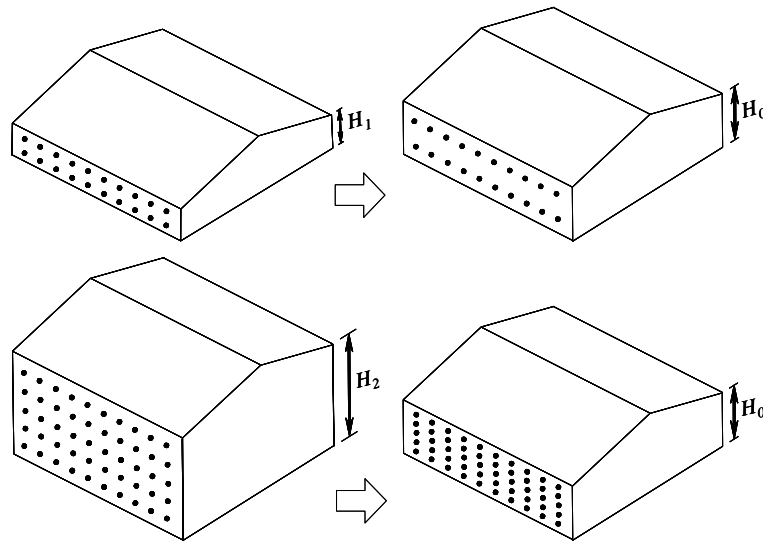

Figure 14. Scaling of pressure tap coordinates to match dimensions of structure of interest.

3.4.2. Interpolation between DIFs from different building models

Sections 3.2 and 3.3 treated cases in which the dimensions of the wind tunnel model exactly match the dimensions of the structure of interest. However, the approach outlined in these sections can be directly extended (in an approximate sense) to cases in which the dimensions differ, by assembling a tributary matrix using tap coordinates scaled to match the dimensions of the structure of interest. This allows influence coefficients for the structure of interest to be used in conjunction with pressure coefficients measured on a model with different dimensions, effectively treating the pressure measurements as if they had been recorded on a model with the same dimensions as the structure of interest. In this manner, peak responses can be estimated using pressure measurements from a number of models whose dimensions are close to the dimensions of the structure of interest, assembling a different tributary matrix for each model. The DIF matrix obtained using pressure measurements from the ith model (with dimensions W_i, L_i, H_i, and R_i) is then denoted $\bar{\mathbf{X}}_i^{\max}$, where the subscript $i = 1, 2, \ldots, b$ denotes the index of the building model. It is assumed for simplicity that the columns of the DIF matrix $\bar{\mathbf{X}}_i^{\max}$ for each model correspond to the same set of wind directions, given in the vector $\bar{\boldsymbol{\theta}}$. If necessary, interpolation can be performed to ensure that this is the case.

With DIF matrices $\bar{\mathbf{X}}_i^{\max}$ having been obtained using pressure measurements from a number of building models with differing dimensions, it is necessary to combine these estimates in some manner to obtain a "best" estimate of the DIF matrix for the structure of interest, which is denoted $\tilde{\mathbf{X}}^{\max}$. Consider first the simple example depicted in Figure 14, in which two models with heights H_1 and H_2 are available, and the response of a structure with height H_0 is of interest, where $H_1 < H_0 < H_2$. The other dimensions of the models are assumed to match those of the structure of interest. In this case, an appropriate means of estimating the DIF matrix $\tilde{\mathbf{X}}^{\max}$ for the structure of height H_0 is by linear interpolation between the DIF matrices $\bar{\mathbf{X}}_1^{\max}$ and $\bar{\mathbf{X}}_2^{\max}$, corresponding to the models with heights H_1 and H_2, respectively. This linear interpolation can be expressed as follows:

$$\tilde{\mathbf{X}}^{\max} = \frac{H_2 - H_0}{H_2 - H_1} \bar{\mathbf{X}}_1^{\max} + \frac{H_0 - H_1}{H_2 - H_1} \bar{\mathbf{X}}_2^{\max} \tag{36}$$

The simple form of linear interpolation in Eq. (36) is applicable only in restrictive cases in which all but one of the model dimensions match those of the structure of interest and in which results from only two building models are used. In general, as many as four of the model dimensions may differ from those of the structure of interest, and more than two building models may be required to adequately bound the dimensions of the structure of interest. A more general multi-dimensional interpolation method is thus required for realistic cases of practical interest.

While a number of different multi-dimensional interpolation approaches could be used to estimate the DIF matrix $\tilde{\mathbf{X}}^{\max}$, an approach is proposed in this paper that has the advantages of simplicity and ease of implementation. The approach can be viewed as a generalization of Eq. (36) to higher dimensions, and it is first noted that Eq. (36) can be written in the following alternative form, for $H_1 < H_0 < H_2$:

$$\tilde{\mathbf{X}}^{\max} = \frac{\gamma}{\Delta H_1} \overline{\mathbf{X}}_1^{\max} + \frac{\gamma}{\Delta H_2} \overline{\mathbf{X}}_2^{\max} \tag{37}$$

where ΔH_1, ΔH_2, and γ are defined as follows:

$$\Delta H_1 = |H_1 - H_0|; \ \Delta H_2 = |H_2 - H_0|; \ \gamma = \left(\frac{1}{\Delta H_1} + \frac{1}{\Delta H_2} \right)^{-1} = \frac{\Delta H_1 \Delta H_2}{H_2 - H_1} \tag{38}$$

It is thus noted that the linear interpolation of Eq. (36) can be viewed as a weighted average of $\overline{\mathbf{X}}_1^{\max}$ and $\overline{\mathbf{X}}_2^{\max}$, with the weighting factor for $\overline{\mathbf{X}}_i^{\max}$ being inversely proportional to the deviation ΔH_i of the building height from the height of the structure of interest. The sum of the weighting factors is unity (i.e., $\gamma / \Delta H_1 + \gamma / \Delta H_2 = 1$).

In generalizing the weighted average of Eq. (37) to accommodate deviations in more than one building dimension, it is helpful to introduce a vector to represent the dimensions of the simple type of gable-roofed building shown in Figure 3. The full-scale width of the building model W_i is selected to represent the absolute dimensions of the model, and the remaining dimensions are represented using three ratios: the aspect ratio L_i / W_i, the height-to-width ratio H_i / W_i, and the roof slope $2R_i / W_i$. Each of these four parameters is then normalized by its value for the building of interest to define the vector $\mathbf{d}_i$ of dimensions for the ith building model :

$$\mathbf{d}_i = \left[\frac{W_i}{W_0} \quad \frac{L_i / W_i}{L_0 / W_0} \quad \frac{H_i / W_i}{H_0 / W_0} \quad \frac{R_i / W_i}{R_0 / W_0} \right]^T \tag{39}$$

where the superscript T denotes transposition. The subscript $i = 0$ denotes the building of interest, and it is noted that $\mathbf{d}_0 = [1 \ 1 \ 1 \ 1]$ by definition. A vector of deviations in the normalized dimensions can then be defined as follows:

$$\Delta \mathbf{d}_i = \mathbf{d}_i - \mathbf{d}_0 \tag{40}$$

In generalizing Eq. (37), a scalar measure of this deviation in building dimensions is required in place of ΔH_i, as a measure of the overall "closeness" of the model dimensions to the dimensions of the structure of interest. Perhaps the simplest scalar measure would be the norm $\| \Delta \mathbf{d}_i \| = (\Delta \mathbf{d}_i^T \Delta \mathbf{d}_i)^{1/2}$, which represents the four-dimensional "length" of the vector $\Delta \mathbf{d}_i$. A disadvantage of this measure is that deviations in each of the model dimensions are given equal weight, while it is known that building aerodynamics are more sensitive to changes in some dimensions than others. For example, a deviation of 50 % in the roof slope of the model might be expected to have a more significant influence on the wind pressure distribution than an equivalent deviation in the aspect ratio of the model. To compensate for such disparities in aerodynamic sensitivity, each component of the deviation vector $\Delta \mathbf{d}_i$ can be scaled by a factor representing the sensitivity of peak responses to changes in that dimension, to obtain a scaled deviation vector $\Delta \tilde{\mathbf{d}}_i$:

$$\Delta \tilde{\mathbf{d}}_i = \mathbf{S} \Delta \mathbf{d}_i \tag{41}$$

where $\mathbf{S}$ is a 4×4 diagonal matrix containing scale factors for each of the building dimensions:

$$\mathbf{S} = \mathrm{diag}(S_W, S_{L/W}, S_{H/W}, S_{R/W}) \tag{42}$$

Larger scale factors in $\mathbf{S}$ correspond to dimensions on which peak responses depend more sensitively, and it might then be expected that $S_{R/W}$, the scale factor associated with the roof slope, would be greater than $S_{L/W}$, the scale factor associated with the aspect ratio, as discussed previously. Appropriate values of the scale factors in $\mathbf{S}$ can be determined empirically by using pressure measurements for available wind tunnel models to investigate the sensitivity of peak responses to changes in the various dimensions, and efforts along these lines are currently underway. Only the relative magnitude of the scale factors in $\mathbf{S}$ is of consequence, and it is convenient to scale the matrix $\mathbf{S}$ so that the largest scale factor equals unity. In the case of equal weighting, $\mathbf{S}$ then reduces to the identity matrix, and $\Delta\tilde{\mathbf{d}}_i = \Delta\mathbf{d}_i$. The norm of $\Delta\tilde{\mathbf{d}}_i$, given as follows, is then used to represent the "closeness" of the building model dimensions to those of the structure of interest:

$$\left\| \Delta\tilde{\mathbf{d}}_i \right\| = \sqrt{\Delta\tilde{\mathbf{d}}_i^T \Delta\tilde{\mathbf{d}}_i} \tag{43}$$

A generalized weighted average that accommodates deviations in more than one building dimension can then be obtained by substituting $\| \Delta\tilde{\mathbf{d}}_i \|$ in place of ΔH_i in Eq. (37). The summation in Eq. (37) can also be expanded to include an arbitrary number b of building models, whereby the following expression is obtained:

$$\tilde{\mathbf{X}}^{\max} = \sum_{i=1}^{b} \frac{\gamma}{\left\| \Delta\tilde{\mathbf{d}}_i \right\|} \bar{\mathbf{X}}_i^{\max} \tag{44}$$

The value of the constant factor γ follows from the condition that the sum of all the weighting coefficients equals unity (i.e., $\Sigma_{i=1}^{b} \gamma / \| \Delta\tilde{\mathbf{d}}_i \| = 1$), and is given as follows:

$$\gamma = \left(\sum_{i=1}^{b} \frac{1}{\left\| \Delta\tilde{\mathbf{d}}_i \right\|} \right)^{-1} \tag{45}$$

Eq. (44) represents a relatively simple multi-dimensional interpolation scheme that can be applied regardless of the number building models or the number of dimensions for each model that differ from those of the structure of interest. The scheme has the property that when the dimensions of the structure of interest $\mathbf{d}_0$ approach the dimensions of one of the models $\mathbf{d}_i$, the DIF matrix $\tilde{\mathbf{X}}^{\max}$ converges exactly to the corresponding DIF matrix $\bar{\mathbf{X}}_i^{\max}$. It should be noted that Eq. (44) does not extrapolate; rather, as the dimensions $\mathbf{d}_0$ pass beyond the range of the available models, the estimated DIF matrix $\tilde{\mathbf{X}}^{\max}$ tends to a uniformly weighted average of all the available DIF matrices. The accuracy of the interpolated DIFs depends on the availability of results from building models with dimensions that are reasonably close to the dimensions of the structure of interest. The scaled deviation vector $\Delta\tilde{\mathbf{d}}_i$ could potentially be used to select appropriate building models for use in interpolation from all the models available in the aerodynamic database, by forming the vector $\Delta\tilde{\mathbf{d}}_i$ for the dimensions of each model and selecting models for which the norm $\| \Delta\tilde{\mathbf{d}}_i \|$ is smallest.

Figure 15 presents interpolated DIFs for a case like that illustrated schematically in Figure 14, in which models are available with two different eave heights, H_1 and H_2, and peak responses are desired for a model with intermediate eave height H_0. Pressure measurements from Ho et al. (2005) are used, which correspond to 1:100 length scaling and "open" terrain. The larger eave height is H_2 = 7.3 m (24 ft), the smaller eave height is H_1 = 3.7 m (12 ft), and peak responses are desired for an intermediate height of H_0 = 5.5 m (18 ft). The other dimensions are the same in all cases, and are given by W = 36.6 m (120 ft), L = 57.2 m (187.5 ft), and R = 1.5 m (5 ft). As shown previously in Figure 7, a structural system consisting of 11 equally spaced frames is considered, and the selected response of interest is the moment at the left "knee" of the first interior frame, with corresponding influence coefficients shown previously in Figure 11. For the interpolation example shown in Figure 15, pressure measurements are actually available for the intermediate eave height as well, and DIFs computed using these measurements were shown previously in Figure 13. Figure 16 shows a comparison of the DIFs obtained by interpolation for H_0 = 5.5 m (18 ft) with those computed using the actual measured pressures. The agreement is remarkably good, and it is noted that the discrepancies are of comparable magnitude to the uncertainty in the computed DIFs themselves. This can be verified by comparison with the DIF plots in Figure 13, in which model symmetry was exploited to obtain two DIF estimates for each direction, with the difference between these estimates giving a measure of the uncertainty. It therefore could hardly be hoped that the interpolation scheme would perform much better.

Unfortunately, the interpolation is not nearly as successful when using models with differing roof rise R, as shown in Figure 17 and Figure 18. Figure 17 presents interpolated DIFs for a case in which two models are available with roof rise given by R_1 = 1.0 m (3.3 ft) (corresponding to an inclination angle of 4.8°) and R_2 = 6.1 m (20 ft) (inclination angle of 27°), and peak responses are desired for a model with intermediate roof rise of R_0 = 3.0 m (10 ft) (inclination angle of 14°). Pressure measurements from Ho et al. (2005) are used, corresponding to 1:100 length scaling and "open" terrain. The plan dimensions and eave height are the same in all cases, and are given by W = 24.4 m (80 ft), L = 38.1 m (125 ft), and H = 7.3 m (24 ft). In this case, a structural system consisting of 7 equally spaced frames is considered, giving a bay spacing of 7.6 m (25 ft). The selected response of interest is the moment at the left "knee" of the first interior frame, and the influence coefficients shown previously in Figure 11 are used in computing this response, with the girt and purlin locations scaled to match the building dimensions. In this example, pressure measurements are actually available for the intermediate roof rise as well, and Figure 16 shows a comparison of the DIFs obtained by interpolation with those computed using the actual measured pressures.

The agreement in this case is not very good, with the interpolated values about 50 % less than the computed values in some cases. It is noted that in this case, the DIFs computed from the intermediate model are actually larger than the DIFs from either of the bounding models for many wind directions. This example corresponds to a difference of 22° between the roof inclination angles of the bounding models, and it is therefore concluded that pressure data are required from models with a smaller difference in roof slope in order for the proposed interpolation scheme to give reliable results. It is noted, however, that most industrial metal buildings have quite shallow roof slopes. Because more pressure data are available in the NIST database for buildings with shallow roof slopes, it would not be necessary to interpolate between models with such a large difference in roof slope in many cases of practical interest. Further

research is required to establish bounds on the applicability of the proposed interpolation scheme given the current set of building models for which pressure data are available.

Figure 15. Interpolation for different eave height of DIFs for bending moment at left knee of first interior frame (units of $N \cdot m/(m/s)^2$, plotted against wind direction).

Figure 16. Comparison of interpolated (different eave height) and calculated DIFs for bending moment at left knee of first interior frame (units of $N \cdot m/(m/s)^2$, plotted against wind direction).
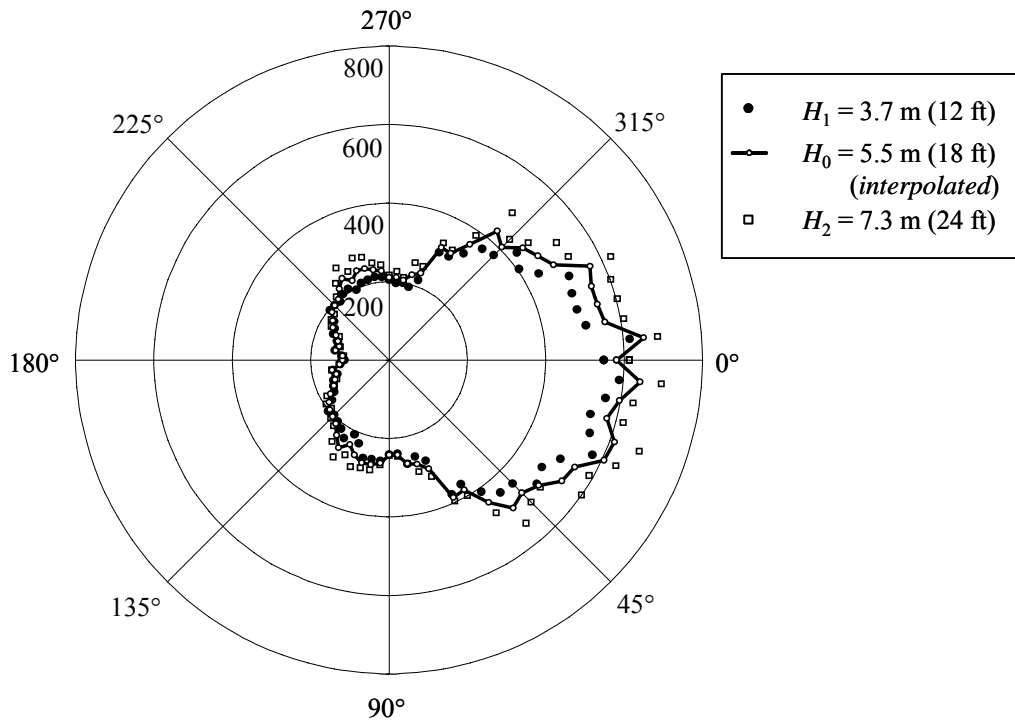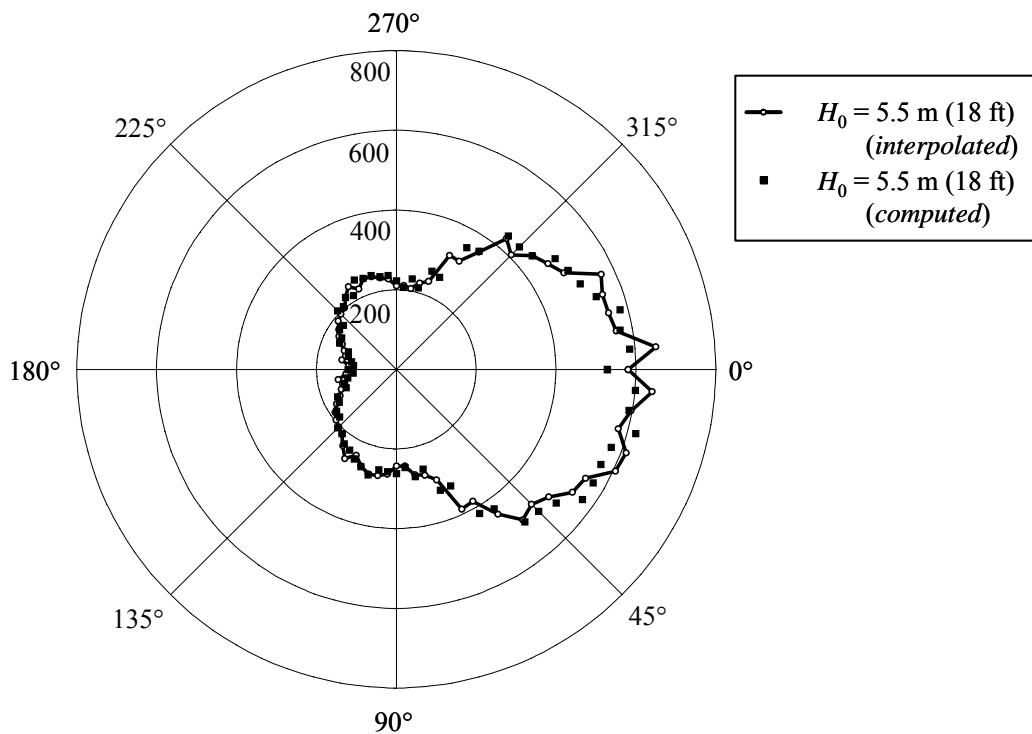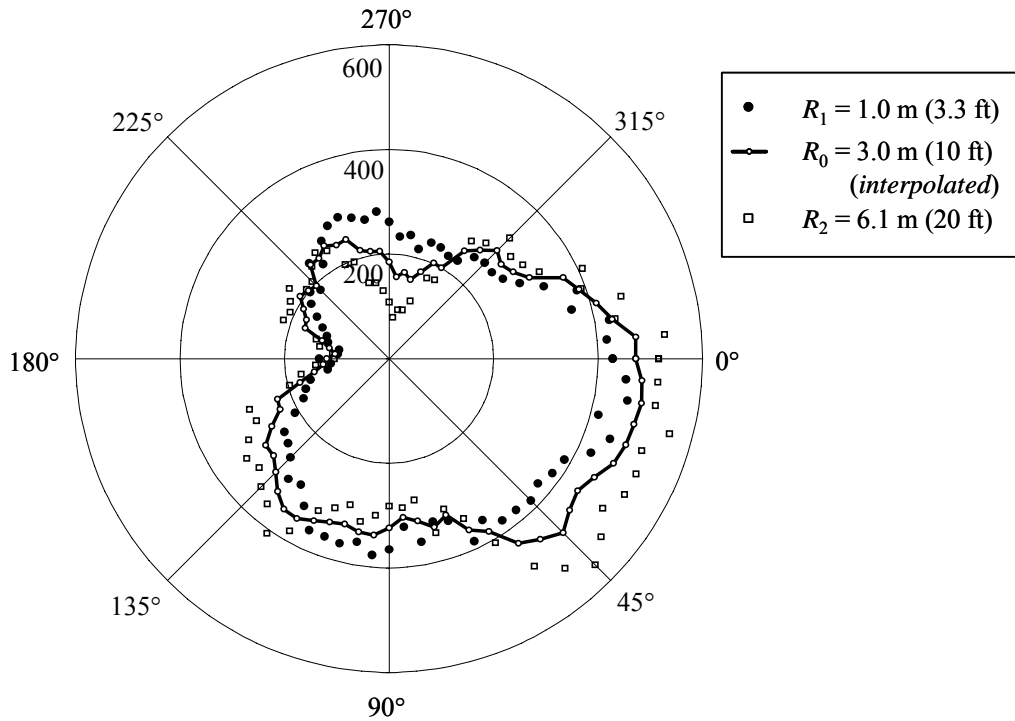

Figure 17. Interpolation for different roof rise of DIFs for bending moment at left knee of first interior frame (units of $N \cdot m/(m/s)^2$, plotted against wind direction).
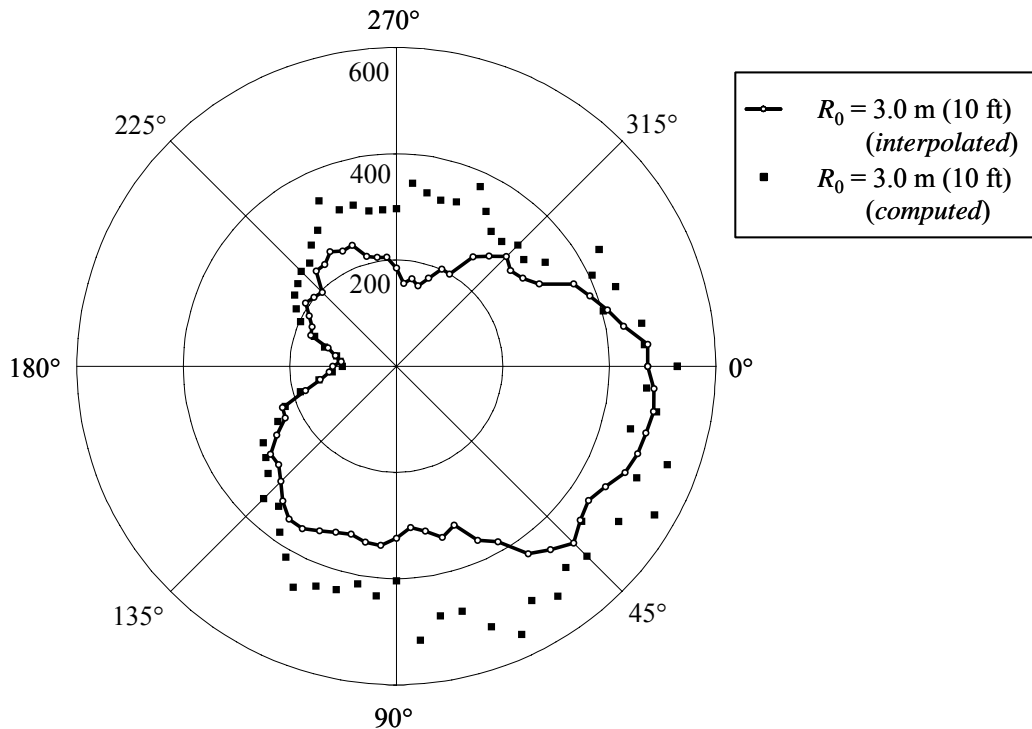
Figure 18. Comparison of interpolated (different roof rise) and calculated DIFs for bending moment at left knee of first interior frame (units of $\mathrm{N \cdot m/(m/s)^2}$, plotted against wind direction).

3.5. ESTIMATION OF PEAK RESPONSES WITH SPECIFIED RETURN PERIOD

DIFs evaluated as discussed previously, either by interpolation or by direct computation, can be used in conjunction with a matrix $\mathbf{V}_H$ of simulated wind speeds, as in Eq. (5), to compute peak values of the response quantities of interest over a significant time duration, from which responses with specified return period can be estimated. To enable this, it is generally necessary to resample the DIFs to coincide with the wind directions for which wind speeds are available in the matrix $\mathbf{V}_H$.

3.5.1. Resampling of DIFs

In Eq. (6), a $1 \times q$ vector $\hat{\mathbf{\theta}}$ of wind directions was defined that corresponds to the columns of the $h \times q$ matrix $\mathbf{V}_H$ of simulated wind speeds. The wind directions in $\hat{\mathbf{\theta}}$ generally do not coincide with those in $\overline{\mathbf{\theta}}$, the $1 \times \overline{p}$ vector of wind directions corresponding to the columns of the DIF matrix $\overline{\mathbf{X}}^{\max}$ (generally $q < \overline{p}$). Therefore resampling is generally required to make use of the DIFs in conjunction with the directional wind speeds.

A wind speed reported for direction $\hat{\theta}_j$ could potentially correspond to any wind direction within the sector bounded above by the midpoint between $\hat{\theta}_j$ and $\hat{\theta}_{j+1}$, and bounded below by the midpoint between $\hat{\theta}_j$ and $\hat{\theta}_{j-1}$. ("Wrapping" of wind directions about $360°$ must be accounted for in establishing these bounds.) It is convenient to introduce the symbol $\Delta\hat{\theta}_j$ to denote this sector associated with direction $\hat{\theta}_j$. In a similar manner, a sector $\Delta\overline{\theta}_k$ can be defined for each wind direction $\overline{\theta}_k$ in $\overline{\mathbf{\theta}}$. Because $\overline{\mathbf{\theta}}$ is sampled more finely than $\hat{\mathbf{\theta}}$, each sector $\Delta\hat{\theta}_j$ will generally overlap several sectors $\Delta\overline{\theta}_k$. With maximum responses for winds in each sector $\Delta\overline{\theta}_k$ given by $\overline{\mathbf{x}}_{\overline{\theta}_k}^{\max}$, the expected maximum responses for winds in sector $\Delta\hat{\theta}_j$, denoted $\hat{\mathbf{x}}_{\hat{\theta}_j}^{\max}$, can be expressed as follows:

$$\hat{\mathbf{x}}_{\hat{\theta}_j}^{\max} = \sum_{k=1}^{\overline{p}} P\left(\theta \in \Delta\overline{\theta}_k \middle| \theta \in \Delta\hat{\theta}_j\right) \cdot \overline{\mathbf{x}}_{\overline{\theta}_k}^{\max} \tag{46}$$

where $P(\theta \in \Delta\overline{\theta}_k | \theta \in \Delta\hat{\theta}_j)$ denotes the probability of winds in sector $\Delta\overline{\theta}_k$ given that winds are known to be in sector $\Delta\hat{\theta}_j$. This probability is nonzero only for sectors $\Delta\overline{\theta}_k$ that overlap $\Delta\hat{\theta}_j$, and it is convenient to let $\Delta\overline{\theta}_k \cap \Delta\hat{\theta}_j$ denote the sector defined by the intersection of $\Delta\overline{\theta}_k$ and $\Delta\hat{\theta}_j$. Assuming that winds from any direction within the sector $\Delta\hat{\theta}_j$ are equally likely, the

probability $P(\theta \in \Delta\bar{\theta}_k \mid \theta \in \Delta\hat{\theta}_j)$ is simply given by the fraction of $\Delta\hat{\theta}_j$ that is overlapped by $\Delta\bar{\theta}_k$, which can be expressed as follows:

$$P\left(\theta \in \Delta\bar{\theta}_k \mid \theta \in \Delta\hat{\theta}_j\right) = \frac{\angle(\Delta\bar{\theta}_k \cap \Delta\hat{\theta}_j)}{\angle(\Delta\hat{\theta}_j)} \tag{47}$$

where $\angle(\Delta\bar{\theta}_k \cap \Delta\hat{\theta}_j)$ and $\angle(\Delta\hat{\theta}_j)$ denote the interior angles associated with the sectors $\Delta\bar{\theta}_k \cap \Delta\hat{\theta}_j$ and $\Delta\hat{\theta}_j$, and $\angle(\Delta\bar{\theta}_k \cap \Delta\hat{\theta}_j)$ is nonzero only if $\Delta\bar{\theta}_k$ and $\Delta\hat{\theta}_j$ overlap. The estimates of $\hat{\mathbf{x}}_{\hat{\theta}_j}^{\max}$ resulting from Eqs. (46) and (47), giving expected maximum responses for unit wind speeds from each direction in $\hat{\boldsymbol{\theta}}$, can then be assembled into an $r \times q$ matrix $\hat{\mathbf{X}}^{\max}$ as follows:

$$\hat{\mathbf{X}}^{\max} = \begin{bmatrix} \hat{\mathbf{x}}_{\hat{\theta}_1}^{\max} & \hat{\mathbf{x}}_{\hat{\theta}_2}^{\max} & \cdots & \hat{\mathbf{x}}_{\hat{\theta}_q}^{\max} \end{bmatrix} \tag{48}$$

As in Eq. (30), the symbol $\hat{\boldsymbol{\chi}}_i^{\max}$ is introduced to denote the ith row of the matrix $\hat{\mathbf{X}}^{\max}$, which can be alternatively expressed as $\hat{\mathbf{X}}^{\max} = [\hat{\boldsymbol{\chi}}_1^{\max} \quad \hat{\boldsymbol{\chi}}_2^{\max} \quad \cdots \quad \hat{\boldsymbol{\chi}}_r^{\max}]^T$. The wind directions associated with the columns of $\hat{\mathbf{X}}^{\max}$ are then the same as those associated with the columns of $\mathbf{V}_H$.

3.5.2. Interpolation between DIFs for different terrain conditions

While terrain conditions were not mentioned in the previous discussion of DIFs, it is important to note that DIFs are computed using pressure coefficients corresponding to specific terrain conditions, and therefore, the DIFs themselves are specific to these terrain conditions. For building models in the NIST aerodynamic database, pressure measurements are generally available for two different terrain conditions, described as "open" and "suburban" (Ho et al. 2005). Let the two terrain conditions be denoted C and B, with corresponding roughness lengths denoted z_{0C} and z_{0B}, where $z_{0C} < z_{0B}$. Typical values are $z_{0C} = 0.03\,\text{m}$ ("open" terrain) and $z_{0B} = 0.3\,\text{m}$ ("suburban" terrain). Using the distinct sets of pressure measurements for terrain conditions C and B, two DIF matrices can be obtained for the ith building model, which are denoted $\bar{\mathbf{X}}_{C,i}^{\max}$ and $\bar{\mathbf{X}}_{B,i}^{\max}$. The interpolation scheme in Eq. (44) can then be applied separately to the results from all building models for each of the two terrain conditions to obtain two DIF matrices, $\tilde{\mathbf{X}}_C^{\max}$ and $\tilde{\mathbf{X}}_B^{\max}$, corresponding to roughness lengths z_{0C} and z_{0B}. These DIF matrices can then be resampled, as described in Section 3.5.1, to obtain DIF matrices $\hat{\mathbf{X}}_C^{\max}$ and $\hat{\mathbf{X}}_B^{\max}$, whose columns correspond to the wind directions in $\boldsymbol{\alpha}$.

The roughness lengths associated with each wind direction in $\boldsymbol{\alpha}$ are given in the vector $\mathbf{z}_0 = [z_{01} \quad z_{02} \quad \cdots \quad z_{0q}]$, which was used previously for scaling directional extreme wind speeds in Eq. (4). A matrix of DIFs corresponding to appropriate terrain conditions from each direction, denoted $\hat{\mathbf{X}}^{\max}$, can then be obtained by interpolating each column of $\hat{\mathbf{X}}^{\max}$ between the corresponding columns of $\hat{\mathbf{X}}_C^{\max}$ and $\hat{\mathbf{X}}_B^{\max}$, using the specified roughness length for that wind direction. This column-wise interpolation can be expressed as follows:

$$\hat{\mathbf{X}}^{\max} = \hat{\mathbf{X}}_C^{\max} \cdot \mathrm{diag}(\boldsymbol{\mu}_C) + \hat{\mathbf{X}}_B^{\max} \cdot \mathrm{diag}(\boldsymbol{\mu}_B) \tag{49}$$

where $\mathrm{diag}(\boldsymbol{\mu}_C)$ and $\mathrm{diag}(\boldsymbol{\mu}_B)$ denote the $q \times q$ diagonal matrices obtained by placing the elements of the $1 \times q$ vectors $\boldsymbol{\mu}_C$ and $\boldsymbol{\mu}_B$ along the main diagonals with zeros elsewhere, and the jth elements of the vectors $\boldsymbol{\mu}_C$ and $\boldsymbol{\mu}_B$ are defined as follows, in terms of the roughness length z_{0j} associated with direction α_j:

$$\mu_{Cj} = \frac{z_{0B} - z_{0j}}{z_{0B} - z_{0C}}; \quad \mu_{Bj} = \frac{z_{0j} - z_{0C}}{z_{0B} - z_{0C}} \tag{50}$$

It is noted that for cases in which $z_{0j} > z_{0B}$ or $z_{0j} < z_{0C}$, the weighting factors in Eq. (50) lead to linear extrapolation. If extrapolation is undesirable, the interpolation can be truncated at the limits z_{0C} and z_{0B} by setting $\mu_{Cj} = 0$ and $\mu_{Bj} = 1$ when $z_{0j} > z_{0B}$ and by setting $\mu_{Cj} = 1$ and $\mu_{Bj} = 0$ when $z_{0j} < z_{0C}$.

3.5.3. Computing peak responses from directional wind speeds

The notation $\mathbf{V}_H^2$ is introduced to denote the $h \times q$ matrix formed by squaring each element of the matrix $\mathbf{V}_H$:

$$[\mathbf{V}_H^2]_{kj} \equiv ([\mathbf{V}_H]_{kj})^2 \tag{51}$$

The maximum value of the ith response quantity corresponding to each of the directional wind speeds in the matrix $\mathbf{V}_H$ can then be evaluated by multiplying each column of $\mathbf{V}_H^2$ by the corresponding entry of the $1 \times q$ vector $\hat{\boldsymbol{\chi}}_i^{\max}$ of DIFs. The resulting matrix of directional maximum responses has the same dimensions as $\mathbf{V}_H^2$, and it can be expressed as $\mathbf{V}_H^2 \cdot \mathrm{diag}(\hat{\boldsymbol{\chi}}_i^{\max})$, where $\mathrm{diag}(\hat{\boldsymbol{\chi}}_i^{\max})$ denotes the $q \times q$ matrix formed by placing the elements of $\hat{\boldsymbol{\chi}}_i^{\max}$ along the main diagonal, with zeros elsewhere. Of interest is the maximum value of the ith response quantity in each hurricane, regardless of direction (or the maximum in each year, for non-hurricane winds). This can be expressed in the form of an $h \times 1$ vector $\hat{\mathbf{r}}_i^{\max}$, obtained by evaluating the maximum element in each row of the matrix of directional responses:

$$\hat{\mathbf{r}}_i^{\max} = \max_{rows}\left(\mathbf{V}_H^2 \cdot \mathrm{diag}(\hat{\boldsymbol{\chi}}_i^{\max})\right) \tag{52}$$

The vector $\hat{\mathbf{r}}_i^{\max}$ is then sorted in descending order, so that $[\hat{\mathbf{r}}_i^{\max}]_1 = \max(\hat{\mathbf{r}}_i^{\max})$ and $[\hat{\mathbf{r}}_i^{\max}]_h = \min(\hat{\mathbf{r}}_i^{\max})$, where $[\hat{\mathbf{r}}_i^{\max}]_k$ denotes the kth element of $\hat{\mathbf{r}}_i^{\max}$. In this manner, an $h \times 1$ vector $\hat{\mathbf{r}}_i^{\max}$ of ranked responses can be determined for each of the r response quantities of interest, from which responses with specified return periods can be evaluated as described previously in subsection 2.4.

Figure 19 shows maximum values of the bending moment at the left knee of the selected frame corresponding to return periods of 50 years and 500 years, plotted against building orientation α_0, as defined in Figure 2. These results correspond to simulated directional hurricane wind speeds from Batts et al. (1980) for Miami, for which the estimated hurricane

occurrence rate is $\nu = 0.560 \text{ year}^{-1}$. Responses corresponding to different building orientations were obtained by using Eq. (6) to define a new vector $\hat{\boldsymbol{\theta}}$ of wind directions for each value of α_0 and repeating the procedure described above from Eq. (46) onwards for each orientation. The largest value of the 500-year maximum response is $886 \text{ kN} \cdot \text{m}$ ($654 \text{ kip} \cdot \text{ft}$), corresponding to an orientation of $\alpha_0 = 202.5°$ (SSW).
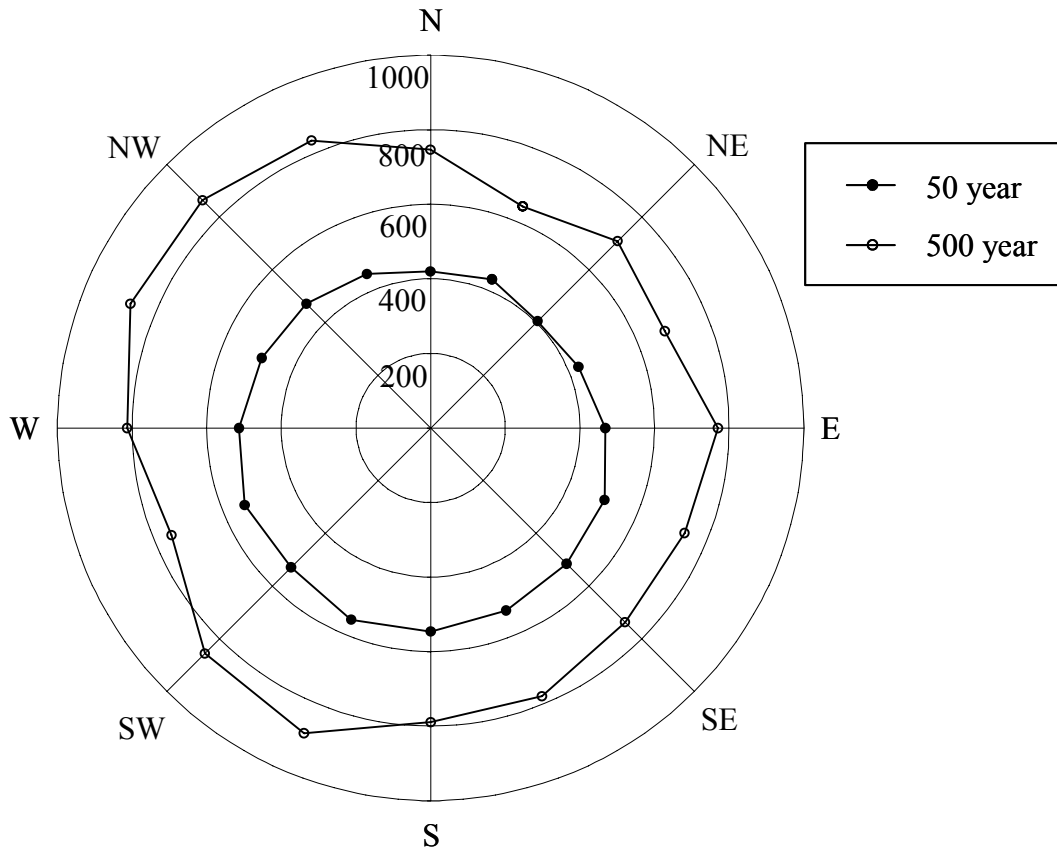
Figure 19. Maximum value of moment at left knee (units of $\text{kN} \cdot \text{m}$) having 50-year and 500-year return periods, for varying building orientation.

4. Application to Flexible Buildings: Dynamic Analysis

William P. Fritz

4.1. INTRODUCTION

Flexible buildings are defined as buildings that have significant dynamic effects when subjected to extreme loads. The application of DAD to flexible buildings is straightforward owing to the systematic conversion of wind tunnel pressures into wind effects. The wind effect of interest accounts for the applied loads due to wind and to the inertial forces they induce.

4.2. DYNAMIC MODELING

The combination of the pressure time series from wind tunnel measurements for winds blowing from direction θ, $\mathbf{C}_{\mathrm{P},\theta_j}$, and directional extreme wind speeds that represent hourly averages at roof height, V_H, yield external pressures at each of the pressure taps in the wind tunnel model as given in Eq. (1). These pressures are separated into their directional components: those normal to a rectangular building's principal axis y induce pressures in the x direction and those normal to the building's principal axis x induce pressures in the y direction. At a tap location denoted by l, the components of the wind-induced pressures are summarized as follows:

$$p_{lx\theta}(t) = \tfrac{1}{2}\rho V_H^2 C_{plx\theta} \qquad \text{acting in the } x \text{ direction} \qquad (53)$$

$$p_{ly\theta}(t) = \tfrac{1}{2}\rho V_H^2 C_{ply\theta} \qquad \text{acting in the } y \text{ direction} \qquad (54)$$

The function of time is expressed explicitly in these equations as will be the wind effects they induce. Positive and negative pressures correspond to pressure acting towards and away from the building face, respectively. Wind forces in the x and y directions, $F_{lx\theta}(t)$ and $F_{ly\theta}(t)$, can be obtained from the pressures $p_{lx\theta}(t)$ and $p_{ly\theta}(t)$ through multiplication by the respective tributary areas, A_{lx} and A_{ly}, of each pressure tap l. The static effects of these forces on the structure are determined by using influence coefficients described in Section 4.3, for which the sign convention (positive toward the building face) is the same as for the pressures. For the calculation of dynamic effects, positive forces are forces whose direction is the same as the direction of the building's principal axis x or y.

The structure is assumed to be linearly elastic and to have coincident elastic and mass centers. The case of non-coincident centers is considered in Venanzi et. al (2005). The dynamic model of the building consists of a lumped mass at each floor with applied forces $F_{lx\theta}(t)$ and $F_{ly\theta}(t)$ accumulated at each floor using tributary areas. Moments about the elastic center, $M_{l\theta}$, are produced by the wind forces $F_{lx\theta}$ multiplied by their distance from the elastic center, y_l, and by

the wind forces $F_{ly\theta}$ multiplied by their distance from the elastic center, x_l. These forces and moments at each floor act as forcing functions in the equations of motion for the lateral deflections in the x and y directions and for the angular rotation about the z direction, φ. This approach can be easily adapted for non-rectangular buildings.

The lateral deflections at elevation z in the x and y directions and the angular rotation about the z direction, φ, induced by a speed V_H blowing from direction θ can be written in terms of generalized coordinates and modal shapes of vibration as

$$x_\theta(z,t) = \sum_{i=1}^{n} x_i(z)\xi_{xi}(t) \tag{55}$$

$$y_\theta(z,t) = \sum_{i=1}^{n} y_i(z)\xi_{yi}(t) \tag{56}$$

$$\varphi_\theta(z,t) = \sum_{i=1}^{n} \varphi_i(z)\xi_{\varphi i}(t) \tag{57}$$

where $\xi_{xi}(t)$, $\xi_{yi}(t)$ and $\xi_{\varphi i}(t)$ are the generalized coordinates in the ith mode corresponding to motions in the x, y and φ directions, respectively, induced by wind from direction θ; $x_i(z)$, $y_i(z)$ and $\varphi_i(z)$ are the ith modal shapes; and n is the number of modes of vibration being considered. The equations of motion, fundamental modal mass and generalized force are summarized in Table 1 for each direction.

Table 1. Equations of motion for x, y and φ directions

Dir.	Equation of motion	Modal mass $M_{xi}, M_{yi}, M_{\varphi i}$	Generalized force $Q_{xi\theta}, Q_{yi\theta}, Q_{\varphi i\theta}$	Eq. No.
x	$\ddot{\xi}_{xi\theta}(t) + 2\varsigma_{ix}\omega_{ix}\dot{\xi}_{xi\theta}(t) + \omega_{ix}^2\xi_{ix\theta}(t) = M_{xi}^{-1}Q_{xi\theta}(t)$	$\sum_{k=1}^{n_f} x_i^2(z_k)m_k$	$\sum_{l=1}^{n_l} x_i(z_l)F_{lx\theta}(t)$	(58)
y	$\ddot{\xi}_{yi\theta}(t) + 2\varsigma_{iy}\omega_{iy}\dot{\xi}_{yi\theta}(t) + \omega_{iy}^2\xi_{iy\theta}(t) = M_{yi}^{-1}Q_{yi\theta}(t)$	$\sum_{k=1}^{n_f} y_i^2(z_k)m_k$	$\sum_{l=1}^{n_l} y_i(z_l)F_{ly\theta}(t)$	(59)
φ	$\ddot{\xi}_{\varphi i\theta}(t) + 2\varsigma_{i\varphi}\omega_{i\varphi}\dot{\xi}_{\varphi i\theta}(t) + \omega_{i\varphi}^2\xi_{i\varphi\theta}(t) = M_{\varphi i}^{-1}Q_{\varphi i\theta}(t)$	$\sum_{k=1}^{n_f} \varphi_i^2(z_k)I_k$	$\sum_{l=1}^{n_l} \varphi_i(z_l)M_{l\theta}(t)$	(60)

The variables n_f and n_l are the total number of floors and taps, respectively; ω_i and ζ_i are the circular frequency and damping ratio in the ith mode; m_k is the mass of floor k; and I_k is the mass moment of inertia of floor k. Solutions of the equations of motion combined with the modal shapes yield the lateral deflections and angular rotation in Eqs. (55), (56) and (57). Differentiating these equations twice yields the respective accelerations.

4.2.1. Transforming wind pressures to structural loads

The pressures in Eqs. (53) and (54) are measured at taps located on the building model in the wind tunnel. The pressure tap locations and their tributary areas are scaled to the prototype building to generate wind loads. The calculated forces at their specified locations induce wind effects within the structure, and are referred to as applied wind loads. They also induce vibrations about the mass center. Inertial loads result from multiplication of the accelerations,

found through solution of the equations of motion in Table 1 at each floor, by the floor mass or mass moment of inertia, and are referred to as inertial wind loads. A flexible building and its elements are designed for the combined effect of the applied and inertial wind loads.

4.3.   MODELING OF WIND EFFECTS

We assume that the structural system consists of beams, columns, and trusses, but the procedure can be easily adapted to other systems. The structure is subjected to known, time dependent aerodynamic forces at the pressure tap locations and inertial forces at each floor's center of mass. The wind effects at any cross-section of any member j, roof accelerations, and interstory drift, can therefore be calculated at each time t by summing up the products of the aerodynamic and inertial forces by the respective influence coefficients that convert the forces into the wind effect being sought.

For this report, the model utilizes the following influence coefficients characterizing the system and obtainable by using standard structural analysis programs: m_{jXWl} and m_{jYWl}, representing the bending moments induced about the local X and Y axis of member j by a unit load perpendicular to the building face at tap l (the subscript W indicates that the influence coefficients are associated with the calculation of effects due to wind forces); P_{jWl}, the axial force in member j due to a unit load perpendicular to the building face at tap l; m_{jXIxk} and m_{jYIxk}, the bending moments about the axes X and Y in member j due to a unit horizontal force acting through the center of mass in the x- direction at floor k (the subscript I indicates that the influence coefficients are associated with the calculation of effects due to inertial forces); m_{jXIyk} and m_{jIyk}, similar moments due to a unit horizontal force acting through the center of mass in direction y at floor k; P_{jIxk} and P_{jIyk}, the axial forces due to a unit horizontal force acting through the center of mass in the x- and y- directions at floor k; m_{jXTk} and m_{jYTk}, the moments induced about axes X and Y by a unit horizontal torque about the elastic center at floor k; P_{jTk}, the axial force induced by a unit horizontal torque about the elastic center at floor k. Other wind effects can be considered using similarly defined influence coefficients.

These sets of influence coefficients are combined with the wind forces based on the recorded pressures at the pressure taps and the calculated inertial forces to obtain the wind-induced internal forces. (In the expressions that follow we omit the subscripts x and y where they are not necessary.) The wind speed V_H therefore induces in member j and at time t a total axial load and total moments about local axes X and Y

$$P_{j\theta}(t)=\sum_{l=1}^{n_l}P_{jWl}\,p_{l\theta}(t)A_l - \sum_{k=1}^{n_f}\left[P_{jIxk}m_k\ddot{x}_{k\theta}(t)+P_{jIyk}m_k\ddot{y}_{k\theta}(t)+P_{jTk}I_k\ddot{\varphi}_{k\theta}(t)\right]$$ (61)

$$M_{jX\theta}(t)=\sum_{l=1}^{n_l}m_{jXWl}\,P_{l\theta}(t)A_l - \sum_{k=1}^{n_f}\left[m_{jXIxk}m_k\ddot{x}_{k\theta}(t)+m_{jXIyk}m_k\ddot{y}_{k\theta}(t)+m_{jXTk}I_k\ddot{\varphi}_{k\theta}(t)\right]$$ (62)

$$M_{jY\theta}(t)=\sum_{l=1}^{n_l}m_{jYWl}\,P_{l\theta}(t)A_l - \sum_{k=1}^{n_f}\left[m_{jYIxk}m_k\ddot{x}_{xk\theta}(t)+m_{jYIyk}m_k\ddot{y}_{k\theta}(t)+m_{jYTk}I_k\ddot{\varphi}_{k\theta}(t)\right]$$ (63)

where m_k is the mass of the kth floor, $\ddot{x}_{kq}(t)$ and $\ddot{y}_{kq}(t)$ are the accelerations in the x- and y-direction at floor k, and I_k and $\ddot{\varphi}_{kq}(t)$ are the mass moment of inertia and the rotational acceleration of floor k, assumed to be infinitely rigid, about the elastic center.

For design purposes it is not the individual internal forces that need to be considered, but rather combinations of internal forces governed by interaction equations and by load combinations. For example, for steel structures, the following design interaction equations (AISC, 2001, **16.1**-38) – or variants thereof – could be used for member j:

$$\text{For } \frac{P_{jf\theta}(t)}{\phi P_j} \geq 0.2: \quad W_{jf\theta}^e(t) = \frac{P_{jf\theta}(t)}{\phi P_{nj}} + \frac{8}{9}\left(\frac{M_{jXf\theta}(t)}{\phi_b M_{njx}} + \frac{M_{jYf\theta}(t)}{\phi_b M_{njy}}\right) \leq 1 \tag{64}$$

$$\text{For } \frac{P_{jf\theta}(t)}{\phi P_{nj}} < 0.2: \quad W_{jf\theta}^e(t) = \frac{P_{jf\theta}(t)}{2\phi P_j} + \left(\frac{M_{jXf\theta}(t)}{\phi_b M_{njx}} + \frac{M_{jYf\theta}(t)}{\phi_b M_{njy}}\right) \leq 1 \tag{65}$$

where $W_{jf\theta}^e$ is the wind effect of interest for wind direction θ, P_{nj}, M_{njx}, and M_{njy} are the nominal axial and flexural strengths of member j; ϕ and ϕ_b are axial and flexural resistance factors, and the quantities in the numerators are the total axial load and moments due to the specified factored combinations (hence the subscript f). For example, applicable load combinations specified by the ASCE 7-02 Standard, are:

$$1.2D + 1.6L \tag{66}$$

$$1.2D + 1.0L + 1.6W \tag{67}$$

$$0.9D + 1.6W \tag{68}$$

where D=dead load, L=live load, and W=wind load.

Some wind engineering consultants use methodologies requiring designers to consider as many as 20 separate combinations of axial loads and/or moments. These are affected by guessed-at combination factors or such methods for adding peak effects as the so-called "point-in-time" method, and are specified in accordance with a variety of in-house criteria. The difficulty experienced by the design engineer is to relate meaningfully those combinations to the interaction equations for the members being designed. The methodology just described covers simply and exhaustively all cases of interest as reflected clearly and unambiguously in interaction equations and load combinations specified by the ASCE 7 Standard or other standards, and in a manner that is directly relevant to and usable in the design process.

4.3.1. Interpolation methods for peak wind effects

In view of their dependence on time t, Eqs. (64) and (65) yield the observed or estimated peaks of the functions W_{jfq}^e (refer to Section 2.4). These peak maximum or minimum values are of direct interest in design, and reflect rigorously the superposition of wind effects in the x and y directions and in torsion. As noted in Section 2.2.2, wind effects for flexible buildings are not proportional to the square of the wind speed. Using site specific wind speeds from the climatological databases described in Section 2.3 would require the performance of the dynamic analysis for every wind speed and wind direction. An interpolation procedure is therefore used to facilitate evaluation of peak wind effects for flexible buildings.

The analysis is performed for the building using a number of wind speeds evenly incremented for each wind direction for which wind tunnel pressure data are available. The range of wind speeds should be broad enough to properly span the wind speeds in the climatological

database, i.e., the maximum wind speed in the range should be larger than the largest value in the database and the minimum wind speed in the range should be small enough to include the speeds that influence the return period of the wind effect (Section 2.4). This minimum value is specified as V_{th} on p. 5 of the software described in Section 4.5. The wind speeds in the database are used explicitly, but the wind effects they induce are obtained by interpolation from the polar grid created as explained in Section 2.

The software allows two interpolation methods of the wind effects from this polar grid of wind speeds and directions. Method A interpolates linearly between wind speeds and wind directions. Method B interpolates linearly between wind speeds, but considers only the larger of the two values corresponding to the two bounding wind directions. Method B is slightly more conservative.

4.4.   THE HIGH-FREQUENCY FORCE BALANCE (HFFB) METHOD

The methodology described can also in principle be applied to results obtained by the High Frequency Force Balance (HFFB) approach, which owes its popularity to its simplicity. Currently, HFFB is implemented in the frequency domain, in spite of a certain lack of enthusiasm on the part of some practicing engineers for spectral methods, perceived to be less transparent than time domain methods. However, the HFFB approach may equally well be implemented in the time domain. One potential advantage is that wind-induced effects in the x, y directions and in torsion can be added to each other exactly, whereas in spectral methods the phase information is lost and such exact addition is not possible. We also note that spectral methods were used in the 1960s and 1970s largely because time domain methods were prohibitive computationally. This is no longer true today.

In the HFFB approach the information available consists of base moments measured in the wind tunnel for the x and y directions and in torsion. For the particular case of fundamental mode shapes that are linear in z, the base moments in the x and y directions are proportional to the generalized force in Eqs. (58) and (59). If the fundamental mode shapes are not linear in z, it is possible to adjust the results, but this requires making guesses on the distribution of the pressures over the building height. For buildings in open terrain this is possible to some reasonable extent, but informed guesses are more difficult for buildings in a built environment.

In addition, base torsional moments are proportional to sums of torsional moments applied at each floor, whereas the generalized force in torsion consist of sums of torsional moments applied at each floor, weighted by the respective ordinate of the torsional modal shape. Here too it is possible to make adjustments based on guesses concerning the distribution of the torsional moments with height, but in general such guesses are again difficult to make reliably; the errors can be considerable in structures with significant wind-induced torsion affected by the building's specific built environment.

The non-inertial terms (i.e., the terms involving pressures) in Eqs. (61), (62), and (63) must also rely on guessed-at distributions of the wind pressures. To assess approximately the potential for errors inherent in such guesses, recall that the pressures are responsible for the non-resonant response (i.e., the response not associated with inertial forces), that is, typically, for perhaps half the total dynamic response or more. The effect of unavoidable errors in the guessed-at distribution of the pressures with height is therefore, typically, far from negligible.

Finally, the HFFB approach does not allow accounting for more than one mode of vibration in the x or y direction or in torsion.

The situation with respect to the use of the HFFB approach is similar to the situation that prevailed before the advent of structural analysis software, when approximate methods were widely used for the calculation of internal forces in tall buildings. Such methods worked reasonably well, but were thoroughly displaced once digital computation became firmly established. The HFFB approach has served the profession well, but in our opinion it is unwarranted for the structural design of very tall structures, given the superior accuracy of the DAD procedure.

The HFFB procedure is less expensive, but for tall buildings the difference in cost is likely to pale in comparison with the benefits inherent in the more accurate DAD approach. Also, when cost considerations are involved, it should be remembered that, typically, pressure measurements are needed anyway, and some wind tunnel laboratories perform *both* an HFFB test, and measurements of (non-simultaneous) pressures for the design of glazing. The HFFB method also has the advantage of being fast and versatile, with possible changes in building design being easily accommodated during the design stage. Advances in manufacturing techniques may, however, allow changes in models with pressure taps to be comparably fast.

Procedures similar to DAD have been used on an ad-hoc basis in a variety of wind engineering projects. However, the objective of the DAD approach is the development of a systematic approach that meets optimally the structural designers' needs, and allows designers to scrutinize effectively or, given the requisite recorded aerodynamic database and climatological information, to actually perform the estimates.

4.5.   ACCOMPANYING SOFTWARE

A software program called High-Rise Database-Assisted Design (HR_DAD) has been developed to calculate wind effects corresponding to specified mean recurrence intervals (MRIs) for structural members within a flexible building. Currently, the wind effects covered by the software only include the quantities defined by the interaction formulas in Eqs. (64) and (65) and floor deflections and accelerations. This section contains a general overview of the software and its MATLAB files, an example of the use of interaction formulas for members of a 66-story building, and a simple example that uses the software to calculate a peak wind-induced displacement. The software was developed with a user-friendly graphical interface and is available on the website <http://www.nist.gov/wind>.

4.5.1. General overview of the accompanying software

This subsection is intended as an overview of the MATLAB files, their inter-relation, and the graphical-user-interface. The latter is particularly helpful for the calculation of wind effects other than those associated with Eqs. (64) and (65), for example deflections and accelerations.

The HR_DAD software is comprised of 34 MATLAB files, which are arranged as shown in Figure 20.
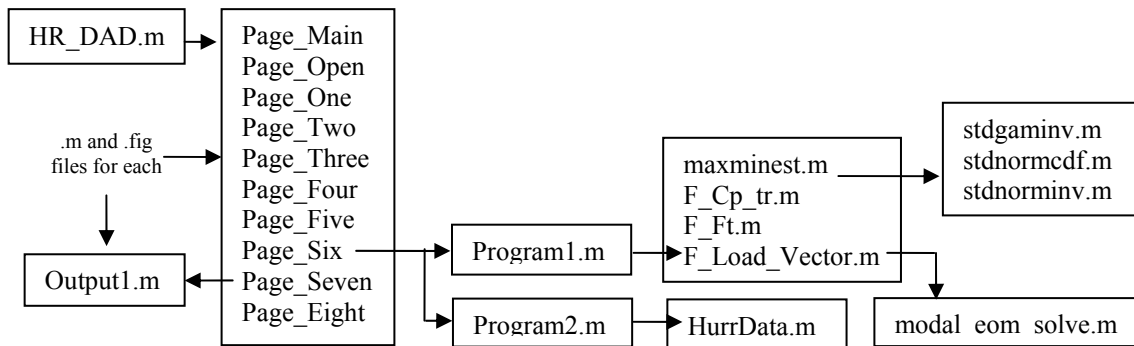
Figure 20. Schematic of the MATLAB file organization for HR_DAD.

The program is started by typing "HR_DAD" at the MATLAB command prompt. This file initializes all the variables and opens up 10 pages: 2 introductory pages (Page_Main and Page_Open) and 8 other pages (Page_One through Page_Eight) that run the program. Each page contains the eight menu tabs located along the left-hand side of the graphical interface. Selection of one of these tabs brings that page to the top of all the opened pages. Pages 1 to 5 contain areas to input values for the variables and open files pertinent to the program. Purple icons within each page that contain the symbol "?" provide additional information for the specific item. For example, the menu labelled "1.Building Info.", which calls the Page_One.m routine, contains an input box for the variable "RNmodes". Clicking on the purple information icon produces a pop-up window that indicates that the variable name within the MATLAB program is RNmodes, that its matrix size is 1 X 1 (i.e., it is a constant), and that the variable specifies the number of vibration modes considered in the analysis. The user defines the necessary variables in pages one through five, which automatically change the values of the (global) variables within the program. The pages and the variables can be selected in any order. The default values specified in the HR_DAD.m file are otherwise used.

The actual calculations are performed in page six by selecting the "Run1" and "Run2" buttons, which run the files called Program1.m and Program2.m, respectively (refer to Figure 1). Program1.m uses all the defined variables to generate the peak (either observed or estimated) wind effect of interest (defined in page five) for the wind directions and wind speeds (WD and WS, respectively, defined in page three) for specified structural members (if the wind effect is member specific). Several defined functions are used, some of which call other defined functions as shown in Figure 20. Comments within the MATLAB script files describe details for these functions. The routine in Program1.m establishes a matrix of peak values that has dimensions length(WS) by length(WD) and saves it under the file location and name specified in page six. The user also has the option of saving the actual wind effect time histories in page six for each combination (WS,WD) bearing in mind that they generate many large files.

The matrix saved in Program1.m is used in Program2.m. The routine in Program2.m cycles through each member, loads the saved table of peak wind effects from Run1 (Program1.m), loads the particular hurricane wind speed database (specified in page five) and calculates the peak wind effect for each MRI (specified in page three). The peak wind effect as a function of MRI is saved for each member under the file location and name specified in page six.

Page seven summarizes key input variables and provides the graphical output for a specified member. When the "Go" button is clicked, the file Output1.m is called, which displays the results from Program2.m. The Output1.m page allows the user to redefine the structural member and the MRI. Page eight, "8. Save/Load Data", allows the user to save the current set of variables to a specified file location or load a previously saved file. Finally, the "Exit" button closes all pages and exits the HR_DAD program. The variables, however, still remain in memory.

The user can change the program to suit their particular needs. The graphical interface is modified through the MATLAB figure files, e.g., Page_Four.fig, by typing "guide" at the MATLAB command prompt. The callback functions for these figure files as well as the program routines and functions are found in the MATLAB m-files.

4.5.2. Example: A 66-Story Building

The procedure was applied to a 66-story, 198 m (650 ft) high symmetric building with a 37 m by 37 m (121 ft by 121 ft) square plan (Figure 21), located in an urban environment. Wind tunnel data, supplied by the Boundary Layer Wind Tunnel at the University of Western Ontario for a 1:400 model of the building, consist of wind pressure coefficient time-histories, $C_{Pl}(t)$, simultaneously measured at 201 pressure taps arranged on the four faces of the building model at 10 levels, for 36 wind directions in 10° increments.
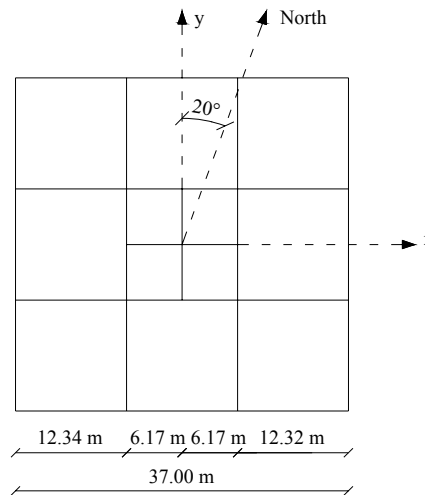
Figure 21. Typical plan view of the 66-story building.

Measurements were made for duration of 59.78 s with a sampling rate of 400 Hz and an hourly mean wind speed at the top of the model of 11.72 m/s (26.2 mi/h). This information is entered into page two of the software. The condition that the reduced frequency nD/V (D and V are the characteristic length and velocity, respectively) be the same for model and prototype must be used for every mean hourly wind speed at the top of the building being used in the calculations (refer to Eqs. (2) and (3)). The data suggest the existence of aerodynamic interference effects due to the presence of neighboring buildings.

A preliminary design of the structural members was based on the along-wind loads approximately equal to those provided in the ASCE 7 Standard for a 42.4 m/s (95 mi/h) mean hourly wind speed at the building's roof height. The structural system consists of steel beams and

columns, and a lateral force resisting system. The 48 periphery columns are spaced evenly at 3.08 m (10.1 ft), and the nine core columns are spaced evenly at 6.17 m (20.2 ft). The base restraints of the perimeter columns are hinges, while the core columns have fixed supports. Floors are spaced evenly at 3 m (9.8 ft) and the column sizes decrease at the 24th and the 44th floors. Perimeter and core columns are connected at each floor by beams extending in both perpendicular directions from the corners of the core area. Wind bracing consists of a system of outrigger and belt trusses between floors 21 and 24, 42 and 45, 63 and 66. Core bracing is provided at all floors. Floor systems, assumed rigid at each floor, are modeled as concrete shells, 0.1 m (.3 ft) thick, located over the entire area of each floor. Gravity loads include the structure self-weight (D), a superimposed dead load (SD) of 0.48 kPa (10 lb/ft^2), and a live load (L) of 2.39 kPa (50 lb/ft^2). The SD and L loads were distributed uniformly over each floor and were applied as vertical point loads to the column joints using appropriate tributary areas.

A modal analysis was performed on the model to evaluate the eigenvalues and eigenfrequencies for the system. The system's displacements were expressed in terms of the first three generalized coordinates corresponding to the three fundamental modes of the structure. These correspond to two purely translational mode shapes (x and y) and one rotational mode shape (φ). The natural periods (T) for these modes are 4.28 s, 4.28 s and 3.99 s, respectively. The fundamental damping ratios (D) are assumed 1.5 % for all three modes. This information is entered in page one of the software.

The software used for the preliminary design and modal analysis is also used to calculate dynamic influence coefficients (page three) and member static load reactions to dead and live loads (page four) for select members. The user must decide the loads for analysis (page one), the interpolation method for direction (page three), load factors for dynamic model (page four) and points considered in time histories (page five). A database of simulated hurricane wind speeds is selected in page five and an appropriate range of wind speeds (WS) and wind directions (WD) is used in page three. The peak wind effect tables are generated in page six as are their mean recurrence intervals.

Selected results are presented for four members whose locations within the structure are described in Table 2.

Table 2. Selected members of the 66-story building example and their locations

Member number	Member type	x coordinate (m) beginning / end	y coordinate (m) beginning / end	z coordinate (m) beginning / end
3838	chord	6.17 / 6.17	0 / 6.17	30 / 30
4093	diagonal	6.17 / 0	6.17 / 6.17	30 / 33
5818	column	18.5 / 18.5	0 / 0	27 / 30
3235	column	18.5 / 18.5	18.5 / 18.5	0 / 3

The hurricane database selected corresponds to New York City, NY, for which the estimated hurricane occurrence rate is 0.305 per year. The wind effect in either Eq. (64) or Eq. (65) is calculated for the wind loads from the preliminary design and from the DAD procedure using the load combination in Eq. (67). These results are shown in Table 3.

Table 3. Summary of wind effects using wind loads from the preliminary design and from the DAD procedure (load combination: 1.2D+L+1.6W)

Member Number	Wind effect, $W_{jf\theta}^e$	
	Preliminary design	DAD procedure
3838	0.22	0.41
4093	0.07	0.15
5818	0.15	0.31
3235	0.34	0.42

As expected, the wind effects calculated by using DAD are greater than those used in the ASCE 7-based preliminary design.

DAD offers the engineer the capability to refine the member designs so that the performance of the members is efficient – and that risk-consistency among members be achieved. For the example of the interaction equation used above, the sizes of members with wind effect ($W_{jf\theta}^e$) values greater than unity need to increase, whereas – to the extent allowed by serviceability constraints – members with $W_{jf\theta}^e$ values much less than unity can be decreased. Resizing individual members within the structure, although possible, may be impractical, but groups of structural members (e.g., large quantities of columns with similar properties) may be changed from the preliminary design to achieve better structural efficiency and risk consistency.

4.5.3. Single-degree-of-freedom (SDOF) oscillator

A simpler application designed to provide a simple check of the software considers a SDOF oscillator excited by a sinusoidal force. The wind effect of interest here is the maximum displacement in the lateral direction. Figure 22 depicts the SDOF model and the requisite parameter values.

$\omega = 10$ rad/s
$\omega_n = \sqrt{k/m} = 10$ rad/s
Period, $T_n = 2\pi/\omega_n = 0.628$ s
$f_n = 1/T_n = 1.592$ Hz

$F(t)=\cos\omega t= \cos(10t)$ $m = 1\ kg$

$L = 1\ m$
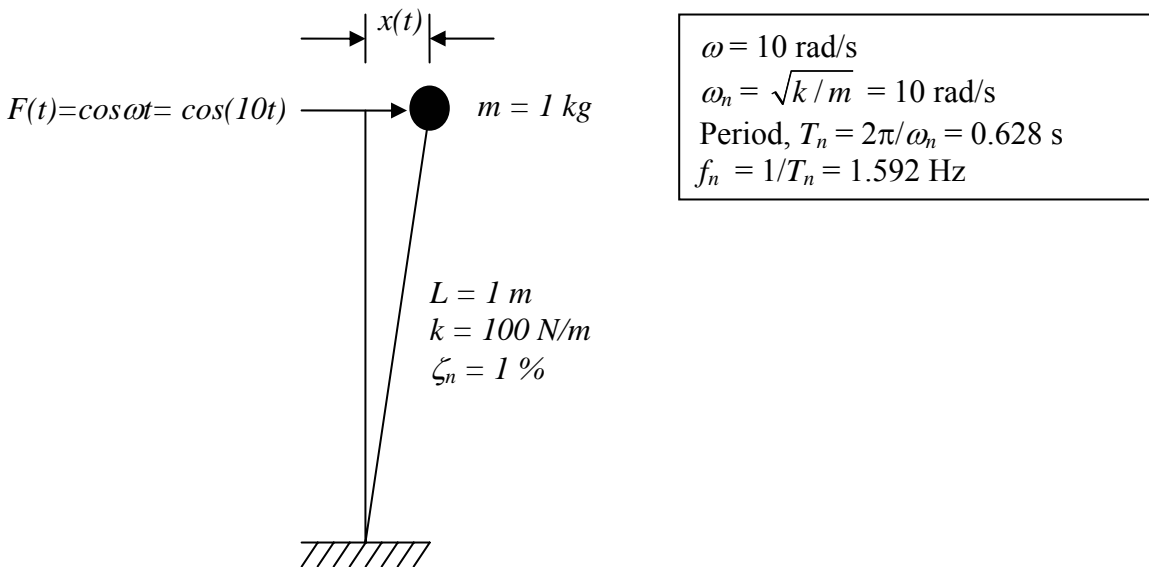$k = 100\ N/m$
$\zeta_n = 1\ \%$

Figure 22. SDOF oscillator example and assumed variable values.

The input variables for this problem are summarized in Table 4. The variables are organized by their respective pages within the program. The definition of the variables can be found within the pages of the software and variables not applicable to this particular wind effect of interest are omitted.

Table 4. Summary of input variables for SDOF oscillator example

Page 1	Page 2	Page 3	Page 4
Nfloors = 1	Ntaps = 1	mem_list[a] = 1	mass[a] = 1 kg
H_bldg = 1 m	taps[a] = [0 0 1 1 1]	dif[a] = [1 1 1 1 1 1 1 1 1 1 1]	frames_DL[a] = [1 0 0 0]
Fdofs = 1	Cp_tr[a,b] = cos(10*t)	props[a] = [1 0 0 0 0]	frames_SDL[a] = [1 0 0 0]
RNmodes = 1	Vm = 1	WS = 1 m/s	frames_LL[a] = [1 0 0 0]
T = 0.628 s	freq = 50	WD = 0°	
D = 1 %	ms = 1	MRI = 1 yr	
evectors[a] = 1	Npoints = 9421		

[a] Saved within a separate file (e.g., evectors is within a file specified in flnMode_shape)
[b] t = [0:dt:188.4] where dt = (1/freq)*(Vm/WS)*ms = 0.02 s.

Variable assignments are made either directly through direct entry in their respective page or through uploaded files specified by file location and name. The analysis is performed by clicking the "RUN 1" button on Page 6, which executes the MATLAB file "Program1.m". The generalized displacements (local variable gen_d), velocities and accelerations are obtained through the "F_Load_Vector" function called within Program1.m. The actual displacement values are obtained thereafter through multiplication by the eigenvector (local variable faix). MATLAB code for the maximum value from this time history can be added to that line; it cannot be typed at the MATLAB command prompt since these variables (e.g., disp_x) are not global. All code beyond these lines is irrelevant for this particular wind effect, so any variables used or errors encountered after these lines are meaningless. Following the above procedure, a maximum displacement of 0.4972 m is obtained. The units result from units used in the input variables.

We are interested in steady-state response, which for an excitation force $F(t) = F_o \cos \omega t$ is:

$$x(t) = F_o H(f) \cos(\omega t - \phi).$$

The mechanical admittance function, $H(f)$, is

$$H(f) = \frac{1}{4\pi^2 f_n^2 m \sqrt{\left[1 - \left(f/f_n\right)^2\right]^2 + 4\varsigma_n^2 \left(f/f_n\right)^2}}$$

Since $\omega/\omega_n = f/f_n = 1$, we have

$$H(f) = \frac{1}{4\pi^2 f_n^2 m 2\varsigma_n} = \frac{1}{4\pi^2 (1.592)^2 (1)(2)(0.01)} = 0.50$$

Therefore,

$$x(t)\big|_{max} = 0.5 \ m$$

which is very close to the value yielded by the HR_DAD software. Although this particular wind effect is not explicitly programmed into HR_DAD, it is easily determined through simple modifications to the program files.

4.6. SUMMARY

This chapter describes the application of DAD to flexible buildings and the calculation of structural response by accounting for the applied loads due to wind and the inertial forces they induce. The procedure presented in this chapter: (1) is capable of accounting for nonlinear fundamental modal shapes, including the fundamental modal shape in torsion, and for higher modes of vibration; (2) automatically adds up in a correct manner time histories of wind effects associated with motions in the x and y directions and torsional motions; (3) readily accommodates load combination requirements specified by standards; (4) accounts for the actual distribution of the wind pressures over the building height; (5) yields for direct design purposes wind effects on all individual members of the structure; and (6) integrates in a simple, transparent, and physically correct manner wind directionality effects associated with the extreme wind climate and the building aerodynamics. Most of these features are not present in procedures based on the measurement of base moments and shears, such as the High Frequency Force Balance (HFFB) method. Like the HFFB method, our procedure is applicable to tall buildings without significant aeroelastic effects. The procedure is applicable for any wind effects, including deflections, accelerations, and internal forces or linear combinations thereof.

This procedure achieves improved accuracy and conformity with the physics underlying dynamic tall building response, as well as clarity, transparency, effectiveness, and user-friendliness from the point of view of the structural designer. To apply the procedure it is necessary that the wind tunnel operator supply the time histories of the pressure data, the wind speeds (unless they are available in the public domain), and the relation between airport speeds at 10 m above ground in open terrain and mean hourly speeds at the top of the building. The procedure then allows the analysis to be conducted by the structural engineer. This restores full control of the design process to the engineer in charge of the project.

References

American Society of Civil Engineers (ASCE). (2003). *Minimum Design Loads for Buildings and Other Structures, SEI/ASCE 7-02, 2nd Edition*, Reston, VA.

Batts, M.E., Russell, L.R., and Simiu, E. (1980), "Hurricane wind speeds in the United States." *J. Struct. Div.*, ASCE, 100(ST10), 2001-2015.

Chen, Y., Kopp, G.A., and Surry, D. (2003a), "Prediction of pressure coefficients on roofs of low buildings using artificial neural networks." *J. Wind Eng. Ind. Aerodyn.*, 91, 423-441.

Chen, Y., Kopp, G.A., and Surry, D. (2003b), "Interpolation of pressure time series in an aerodynamic database for low buildings." *J. Wind Eng. Ind. Aerodyn.*, 91, 737-765.

Fritz, W., Iancovici, M., and Simiu, E. (2004), "Applicability of database-assisted design to tall buildings." *Proceedings of 8th International Conference on Flow-Induced Vibrations, Paris, France, 6-9 July 2004,* (CD-ROM).

Ho, T.C.E., Surry, D., Morrish, D. and Kopp, G.A. (2005), "The UWO contribution to the NIST aerodynamic database for wind loads on low buildings: Part 1. Archiving format and basic aerodynamic data." *J. Wind Eng. Ind. Aerodyn.* 93, 1-30.

Jang, S., Lu, L., Sadek, F., and Simiu, E. (2005), "Database-assisted wind load capacity estimates for low-rise steel frames." *J. Struct. Eng.*, 128(12), 1594-1603.

Main, J.A. (2005), "Combining wind pressure databases with structural analysis to predict peak responses for rigid buildings." *Proceedings, 6th Asia-Pacific Conference on Wind Engineering, Seoul, Korea, 12-14 September 2005,* (CD-ROM).

Main, J.A. (2005), "Interpolation issues in the estimation of peak internal forces using wind pressure databases." *Proceedings, 6th Asia-Pacific Conference on Wind Engineering, Seoul, Korea, 12-14 September 2005,* (CD-ROM).

The MathWorks, Inc. (2005). *MATLAB and Simulink for Technical Computing.* <http://www.mathworks.com> (accessed Oct. 27, 2005).

Rigato, A., Chang, P. and Simiu, E. (2001). "Database-assisted design, standardization, and wind direction effects." *J. Struct. Eng.*, 127(8), 855-860.

Sadek, F. and Simiu, E. (2002). "Peak non-Gaussian wind effects for database-assisted low-rise building design." *J. Eng. Mech.* 128(5), 530-539.

Sack, R.L. (1984). *Structural Analysis*, McGraw Hill, Inc., N.Y.

Simiu, E., Sadek, F., Whalen, T.M., Jang, S., Lu, L.-W., Diniz, S., Grazini, A., and Riley, M.A. (2003). "Achieving safer and more economical buildings through database-assisted, reliability-based design for wind." *J. Wind Eng. Ind. Aerodyn.*, 91, 1587-1611.

Simiu, E. and Scanlan, R.H. (1996). *Wind Effects on Structures*, 3rd Ed., Wiley-Interscience, N.Y.

Venanzi, I., Fritz, W.P., and Simiu, E. (2005). "Effect of distance between the elastic center and the mass center on the wind-induced dynamics of tall buildings." *Proceedings, 6th Asia-Pacific Conference on Wind Engineering, Seoul, Korea, 12-14 September 2005,* (CD-ROM).

Whalen, T.M., Sadek, F. and Simiu, E. (2002), "Database-assisted design for wind: basic concepts and software development." *J. Wind Eng. Ind. Aerodyn.* 90, 1349-1368.

Whalen, T.M., Shah, V., and Yang, J.S. (2000), "A pilot project for computer-based design of low-rise buildings for wind loads – The WiLDE-LRS user's manual." *NIST GCR 00-802*, National Institute of Standards and Technology, Gaithersburg, MD, USA.

Whalen, T.M., Simiu, E., Harris, G., Lin, J. and Surry, D. (1998), "The use of aerodynamic databases for the effective estimation of wind effects in main wind-force resisting systems: application to low buildings." *J. Wind Eng. Ind. Aerodyn.* 77&78, 685-693.

Appendix A:

User's Manual for windPRESSURE, Database-Assisted Design Software for Rigid, Gable-Roofed Buildings

Joseph A. Main

PEAK RESPONSE ESTIMATION for STATIC STRUCTURES USING RECORDED EXPERIMENTS

wind **PRESSURE**
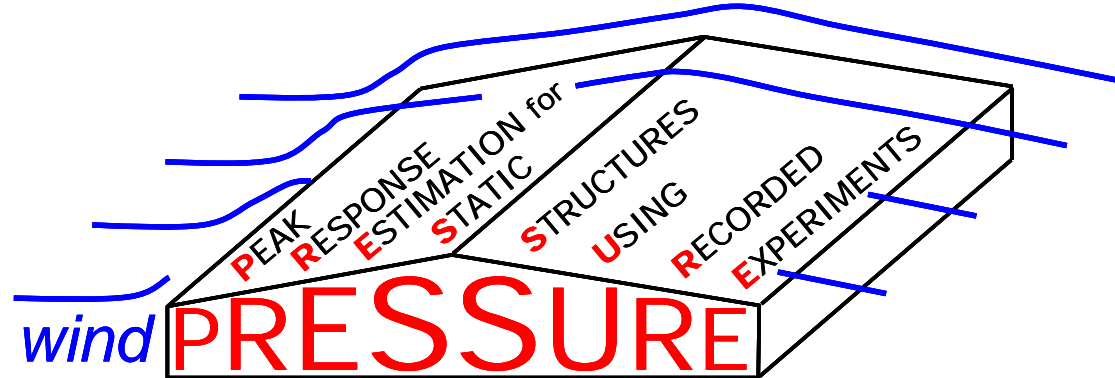
Database-**A**ssisted **D**esign Software
for Rigid, Gable-Roofed Buildings

User's Manual

developed by Joseph A. Main
Building and Fire Research Laboratory
National Institute of Standards and Technology

Updated February 10, 2006
Current version available at www.nist.gov/wind

Disclaimer: Certain trade names or company products are specified in this document to specify adequately the procedure used. Such identification does not imply recommendation or endorsement by NIST, nor does it imply that the product is the best available for the purpose. The "stand-alone" version of this software requires installation of the MATLAB[1] Component Runtime (MCR) Libraries provided by The MathWorks, Inc. The author's limited rights to the deployment of this program are limited by a license agreement between NIST and The MathWorks. The license agreement can be found at www.mathworks.com/license/. The author, NIST, and The MathWorks and its licensors are excluded from all liability for damages or any obligation to provide remedial actions.

---

[1] MATLAB®. © 1984 – 2005 The Mathworks, Inc.

Installation and Setup

The following files are required for use of the **windPRESSURE** software, and are being made available at www.nist.gov/wind. The files can also be obtained on CD by request.

- **windPRESSURE** program files: provided in the following alternative forms:
  - MATLAB m-files (requires version 7 of MATLAB)
  - Stand-alone executable (for Windows 2000/XP; requires installation of MCRInstaller.exe, which is also provided)

- Building input files: two sample files are provided:
  - BLD_W=120,L=187.5,H=18,R=5,Open_Country.csv
  - BLD_W=120,L=187.5,H=18,R=5,Directional.csv

- HDF pressure databases: Results are provided from four tests conducted at the University of Western Ontario, and results from three different wind directions are provided from each test. All models have the same roof slope of 1:12, length scaling of 1:100, width of W = 36.6 m (120 ft), and length of L = 57.2 m (187.5 ft), but the eave height and terrain conditions are different, as follows:
  - eave height of H = 3.7 m (12 ft), "Open_Country" terrain
  - eave height of H = 5.5 m (18 ft), "Open_Country" terrain
  - eave height of H = 5.5 m (18 ft), "Suburban" terrain
  - eave height of H = 7.3 m (24 ft), "Open_Country" terrain

- Simulated directional hurricane wind speed data: data files are provided from 55 different locations (mileposts) along the Gulf of Mexico and North Atlantic coasts.
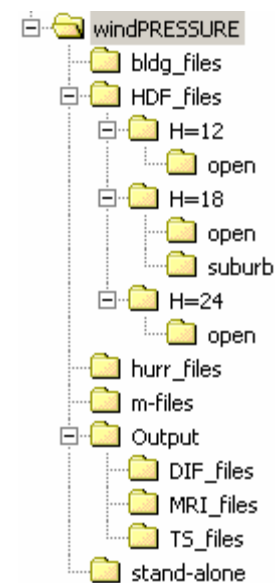
Figure 1. Recommended windPRESSURE directory structure.

It is recommended that users create a single folder named "windPRESSURE" on their local hard drive, in which to save all downloaded files and folders, and a recommended directory structure is shown in Figure 1. The "m-files" folder contains all MATLAB m-files (required only for execution within MATLAB), and the "stand-alone" folder contains the stand-alone executable and related files (required only for stand-alone execution). The "bldg_files" folder contains the building input files, the "HDF_files" folder contains HDF pressure database files (separate subfolders must be created within this folder for each of the four tests listed above), and the "hurr_files" folder contains simulated directional hurricane wind speed files. As shown in Figure 1, it is also

recommended that separate folders be created for the following three types of output files: <u>Directional Influence Factor (DIF) output files</u>, <u>Time Series output files</u>, and <u>Mean Recurrence Interval output files</u>.

For execution within MATLAB, add the "m-files" folder to the MATLAB search path, and save changes:
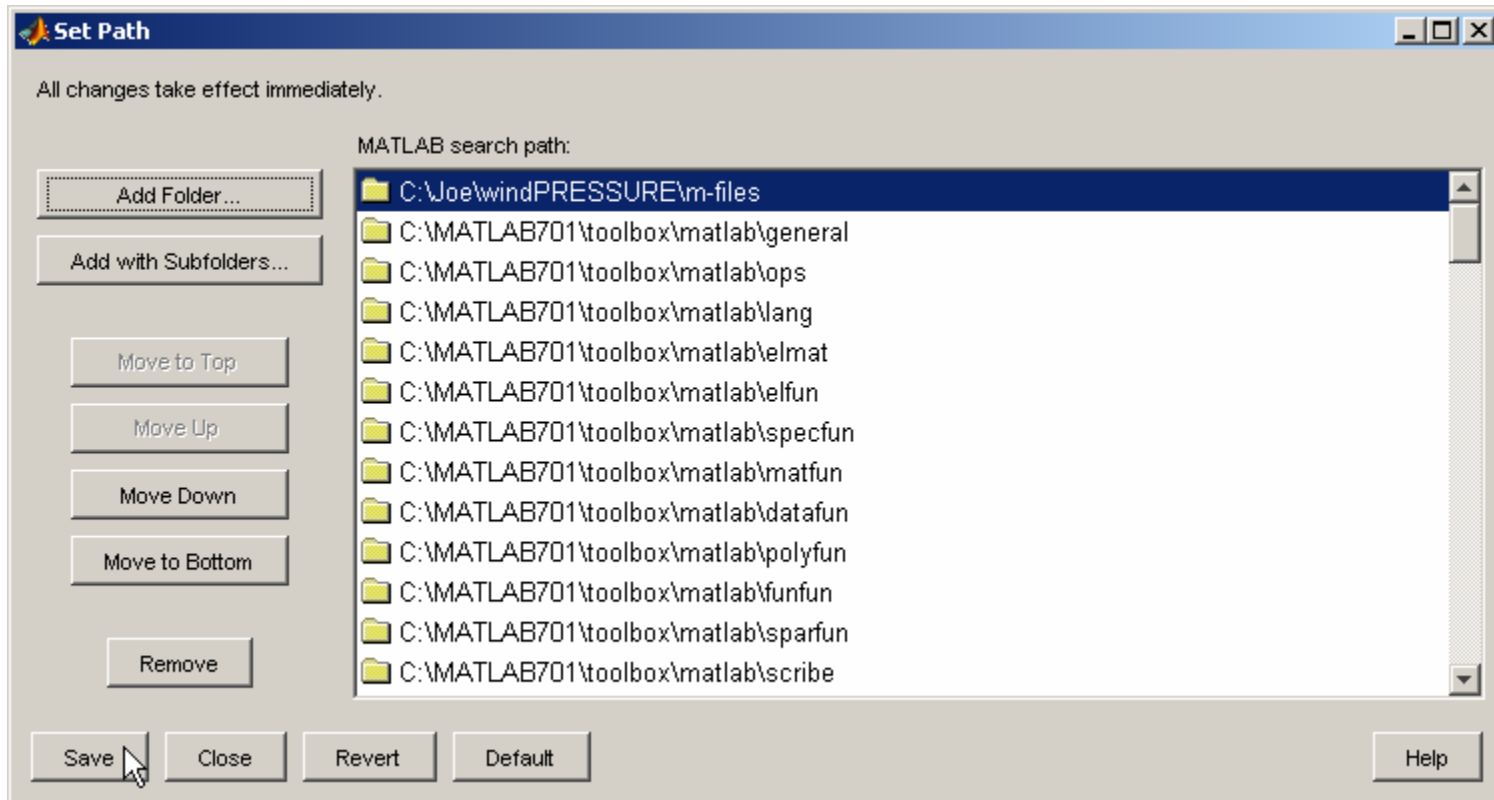
Figure 2. Adding "windPRESSURE\m-files" to the MATLAB search path.

The **windPRESSURE** software can then be executed by typing "windpressure" at the MATLAB command prompt.

For stand-alone execution, the MCRInstaller must first be installed by executing the application "MRCInstaller.exe". The **windPRESSURE** software can then be launched by double-clicking the file "windpressure.exe" within the "stand-alone" folder. The stand-alone version of **windPRESSURE** may take up to a minute to initialize upon execution, so please be patient.

Graphical User Interface

Launching the windPRESSURE software opens the graphical user interface shown in Figure 3. Within this interface, a building input file can be selected and its contents displayed graphically, and the folder containing HDF pressure databases can also be selected, upon which all subfolders will be searched for HDF files and the

Figure 3. Graphical interface for calculation, interpolation, and display of Directional Influence Factors.

available results listed. The folder in which <u>DIF output files</u> should be stored and retrieved can also be selected through this interface, and the results to be stored the output file can be selected by pressing the "Output options…" button, which opens the dialog box shown in <u>Figure 4</u>. Directional Influence Factors can then be computed by selecting an available set of H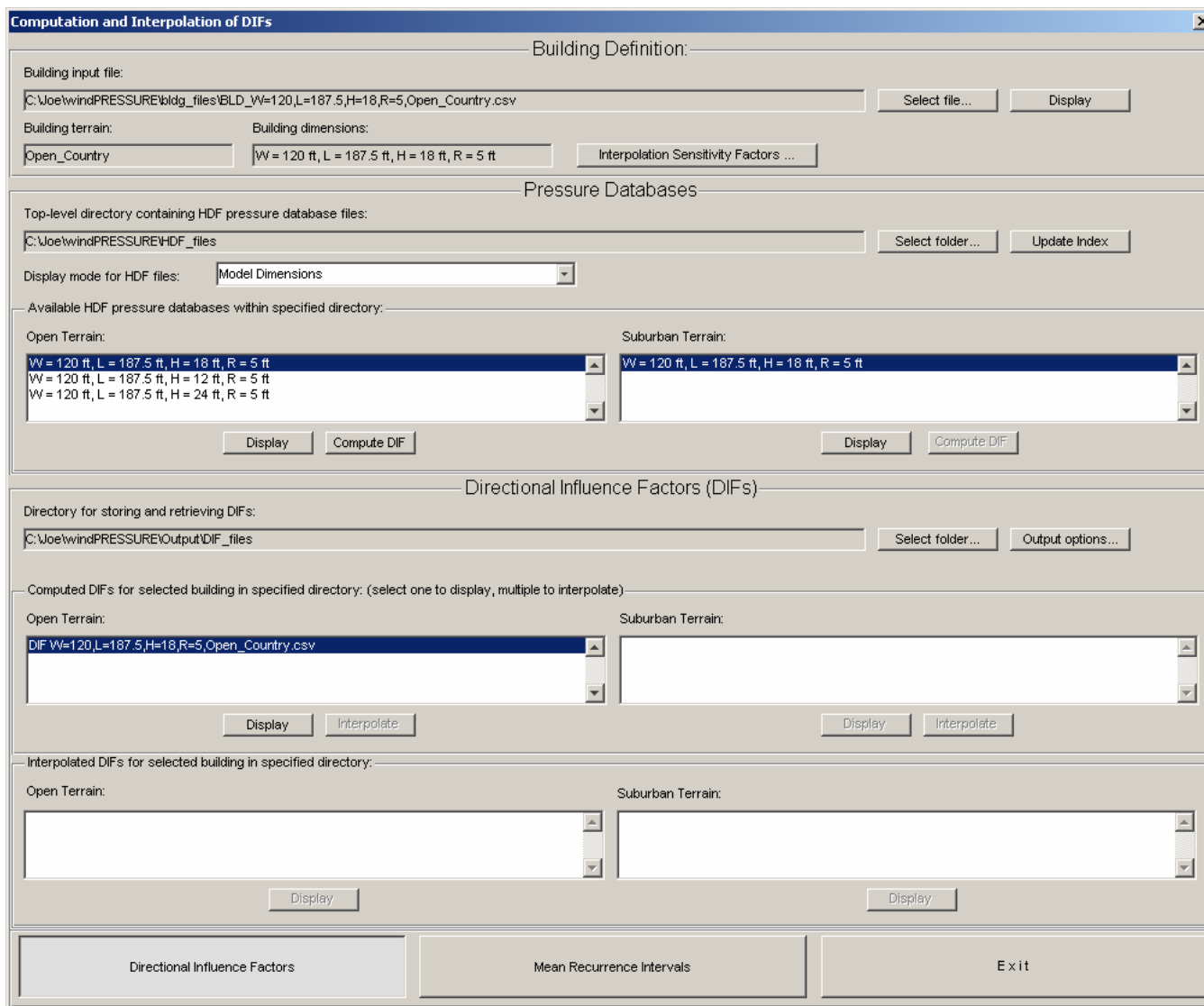DF pressure databases and pressing the "Compute DIF" button. If the dimensions of the wind tunnel model do not match the dimensions of the structure of interest, the pressure tap coordinates will be automatically scaled to match the structure of interest.
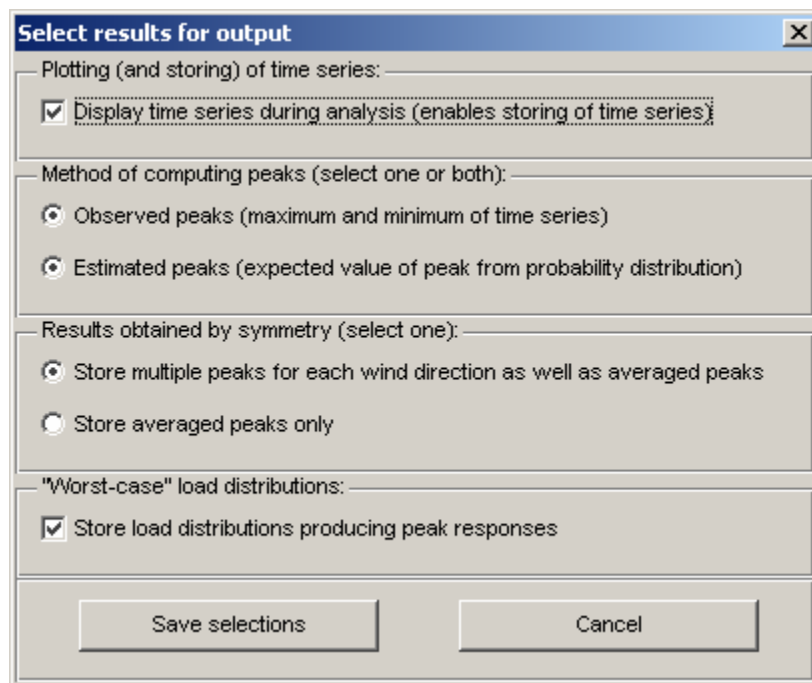
Figure 4. Output options for computation of Directional Influence Factors.

If the option "Display time series during analysis" is selected in the dialog box shown in <u>Figure 4</u>, then time series of computed responses will be plotted during the analysis, as shown in <u>Figure 5</u>, with the option of saving these results to a <u>Time Series output file</u>. Once DIFs have been computed, the user will be prompted to confirm the name with which to save the file, and the listing of available DIF files within the interface of <u>Figure 3</u> will be updated. The results in the DIF files can then be displayed graphically by selecting a DIF file and pressing "Display", which opens the graphical interface shown in <u>Figure 6</u>, in which the quantities to display can be selected.
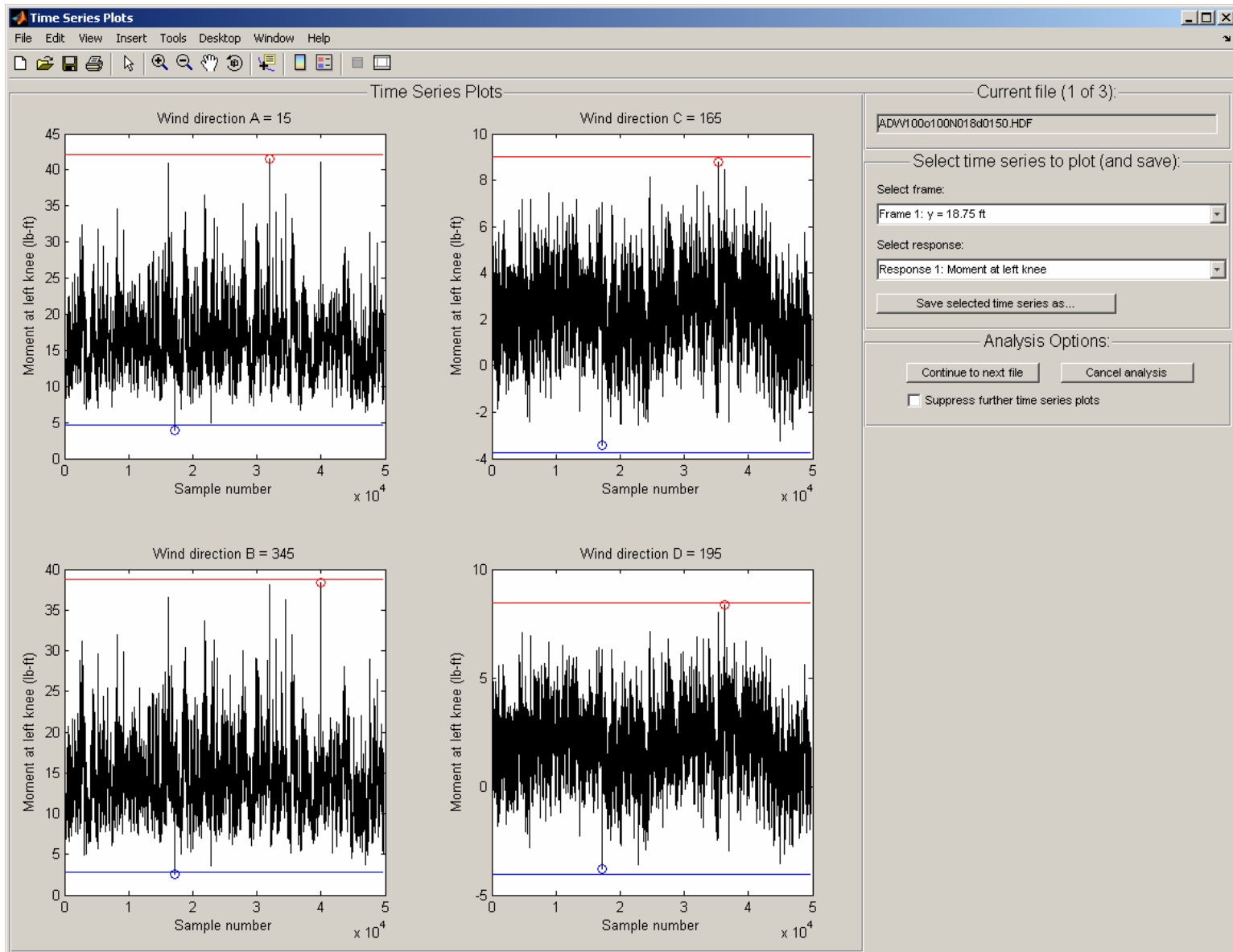
**Figure 5. Graphical interface for plotting and saving of response time series
(Observed peaks circled, estimated peaks shown as horizontal lines).**
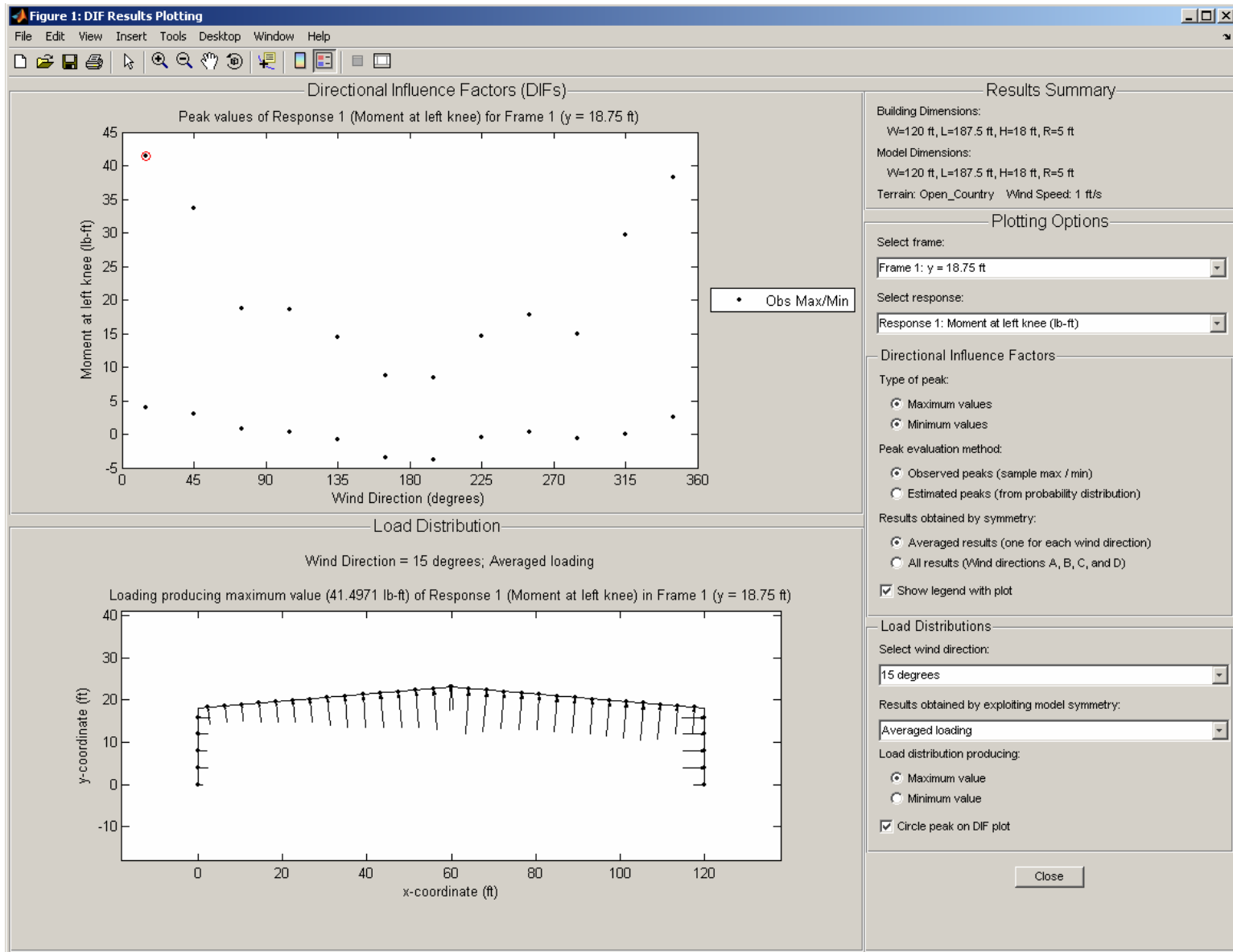
Figure 6. Graphical interface for displaying DIF file contents.

The windPRESSURE software incorporates an interpolation scheme to allow estimation of DIFs for the structure of interest from DIFs computed from several different wind tunnel models with dimensions that do not match the dimensions of the structure of interest. Interpolation can be performed within the interface of Figure 3

simply by selecting several DIF files computed from different HDF files (with the same terrain conditions) and pressing the "Interpolate" button. The interpolated results will then be saved and displayed in one of the lower panels shown in Figure 3. The interpolation scheme performs a weighted average of the selected DIFs based on the "closeness" of the model dimensions to the dimensions of the structure of interest, and the sensitivity to different dimensions used in assessing this "closeness" can be adjusted by pressing the "Interpolation Sensitivity Factors" button in the interface of Figure 3, which opens the dialog box shown in Figure 7, in which the sensitivity factors can be adjusted and saved.

Figure 7. Dialog box for adjusting sensitivity factors used in interpolation of DIFs.

By pressing the "Mean Recurrence Intervals" button at the bottom center of the graphical interface shown in [Figure 3](#) , another graphical interface is opened, which is shown in [Figure 8](#). This interface handles the second major stage of the analysis, in which DIF results files are combined with simulated directional hurricane wind speeds to compute peak responses with specified Mean Recurrence Intervals. The folder containing the simulated hurricane wind speed data files can be selected through the interface, and the building location can
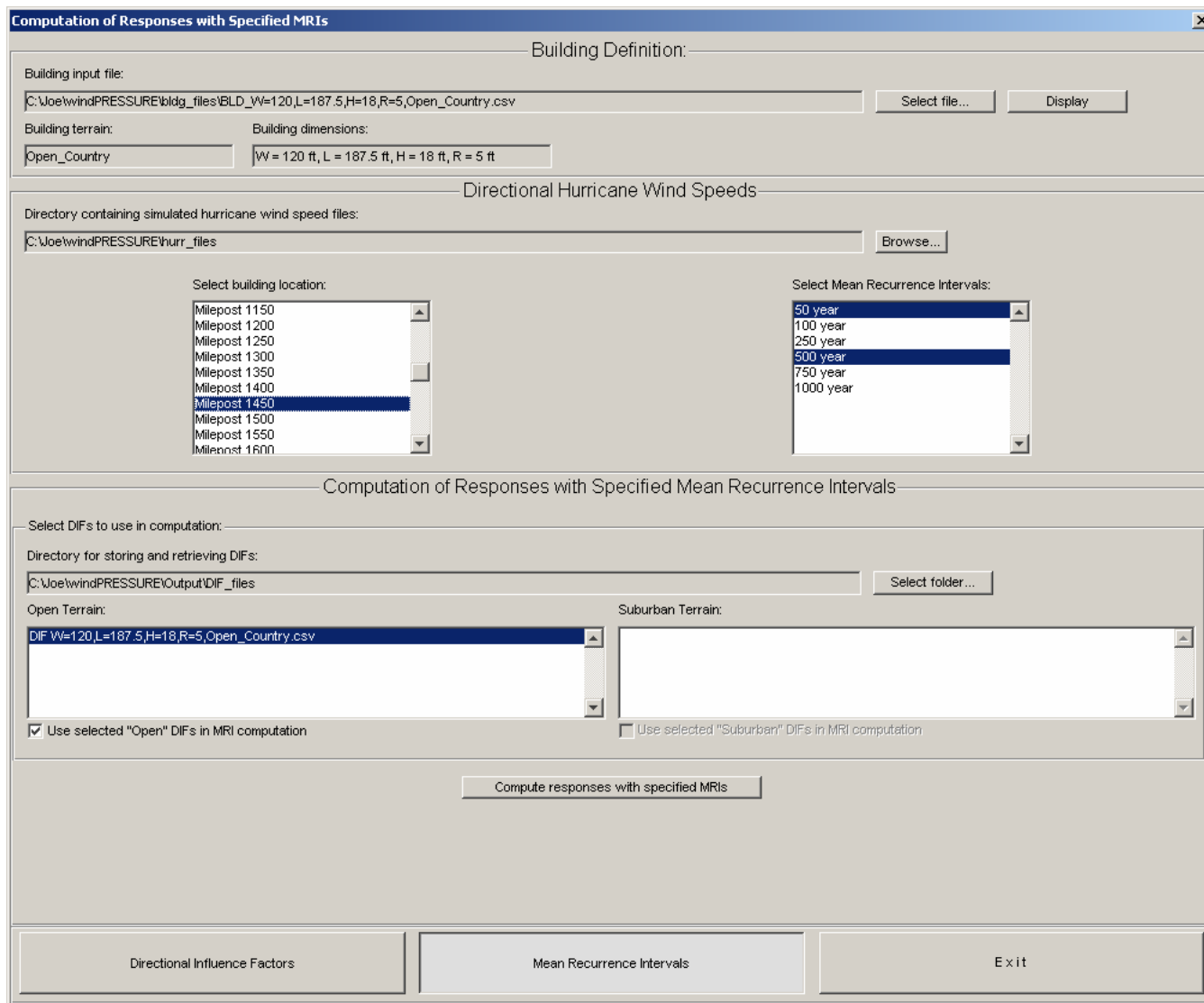
Figure 8. Graphical interface for computing responses with specified Mean Recurrence Interval.

then be selected from the list of available mileposts. The MRIs for which responses are desired can also be selected through the interface, along with the DIF results file(s) to be used, and results can then be computed by pressing the "Compute responses with specified MRIs" button. The results are displayed graphically as shown in Figure 9 and Figure 10, and they can then be saved to an MRI output file, if desired.
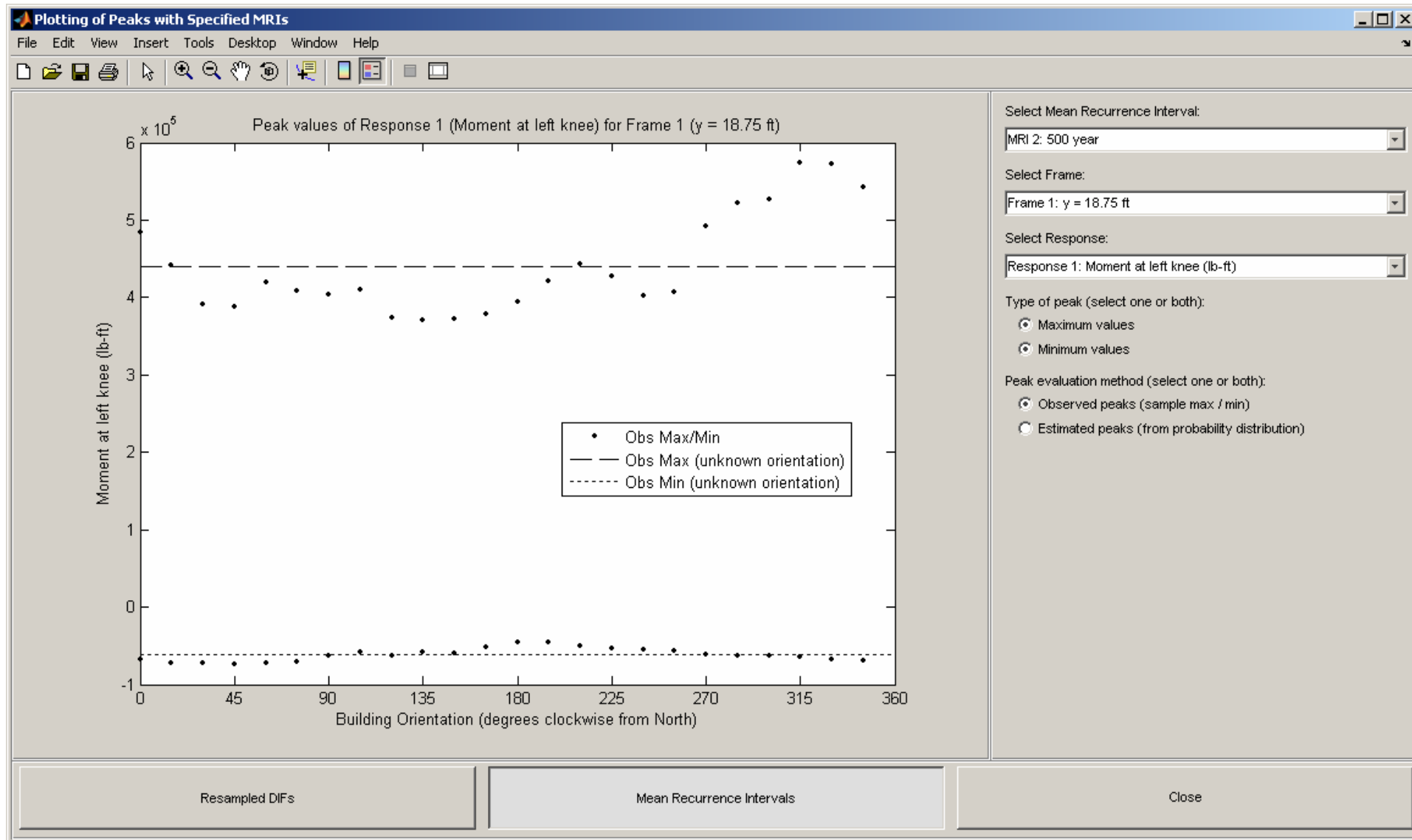
Figure 9. Graphical interface for displaying responses with specified Mean Recurrence Intervals.
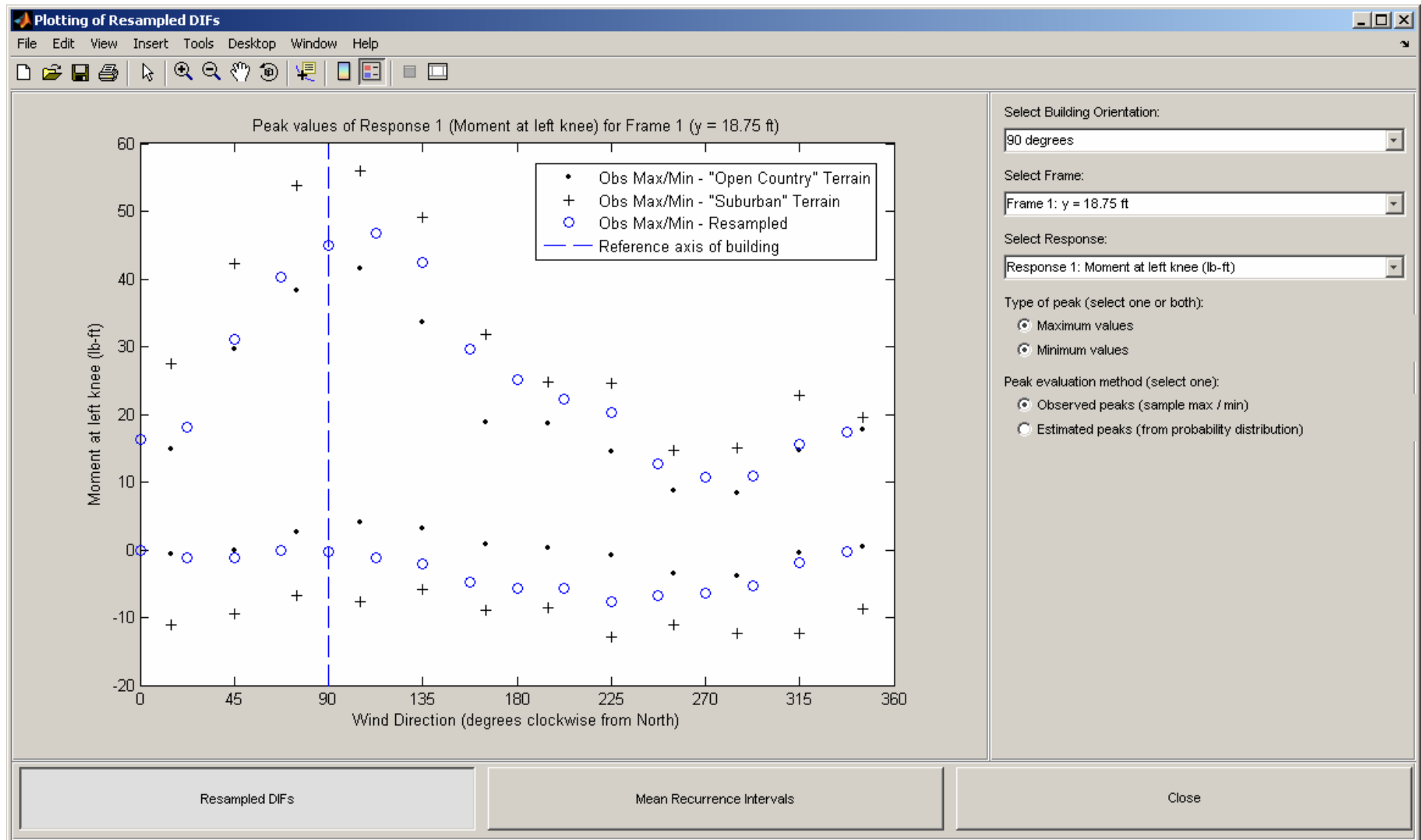
Figure 10. Graphical interface for displaying resampled DIFs used in computing responses with specified MRIs.

Building Input File

This section describes the contents and format of the building input file, a comma-delimited text file that defines the characteristics of the building to be analyzed. The building input file can be created and edited using standard spreadsheet software and must be saved in the comma-separated values (CSV) file format in order to be properly interpreted by the windPRESSURE software. This CSV file can then be selected for analysis through the graphical user interface. A sample building input file is shown in Figure 11.

The building input file consists of keywords followed by tabular input data. Keywords begin with an asterisk[2], and the following keywords are required in each building input file (underscores are used in the keywords rather than spaces):

      *UNITS
      *BUILDING_DIMENSIONS
      *TERRAIN
      *FRAME_LOCATIONS
      *ATTACHMENT_LOCATIONS
      *RESPONSE_NAMES
      *INFLUENCE_COEFFICIENTS

Input data begins on the row immediately following each keyword, and the purpose and format of the input data corresponding to each keyword are described in the following sections. The keywords and corresponding input data can be entered in the input file in any order, but no extraneous rows are permitted. Errors will result if the input data does not match the expected format for the specified keyword. Header rows are included with the input data for most keywords, so that columns can be labeled, making the input file easier to read. These header rows must not be omitted, or the input data will not be properly read and errors will result. Suggested column labels for the header rows are indicated in the following sections. However, the entries in the header rows are not actually read by the software, and alternative column labels can be used, or these rows can simply be left blank. Additional annotation can be added to the input file by using the % symbol: lines beginning with % are treated as comments and are ignored in reading the building input file.

---

[2] Any line that begins with an asterisk will be interpreted as a keyword, and an error will result if the text following the asterisk is not a recognized keyword.

	A	B	C	D	E
1	*UNITS				
2	Length	Force	Wind Speed		
3	ft	lb	ft/s		
4	*BUILDING_DIMENSIONS				
5	Width	Length	Height	Roof Rise	
6	120	187.5	18	5	
7	*TERRAIN				
8	Open_Country				
9	*FRAME_LOCATIONS				
10	Number	Previous y	Current y	Next y	
11	1	0	18.75	37.5	
12	2	18.75	37.5	56.25	
13	*ATTACHMENT_LOCATIONS				
14	Index	Face	s-coordinate		
15	1	1	0		
16	2	1	3.9628		
17	3	1	7.9255		
18	4	1	11.8883		
19	5	1	15.851		
20	6	2	2.4459489		
21	7	2	6.47024981		
22	8	2	10.4945507		
23	9	2	14.518952		
24	10	2	18.5432529		
25	11	2	22.5675538		
26	12	2	26.5918547		
27	13	2	30.7938695		
28	14	2	34.9958842		
29	15	2	39.197899		
30	16	2	43.3999138		
31	17	2	47.6019286		
32	18	2	51.8039433		
33	19	2	56.0059581		
34	20	2	60.2079729		
35	21	3	2.4459489		
36	22	3	6.47024981		
37	23	3	10.4945507		
38	24	3	14.5188516		
39	25	3	18.5432529		
40	26	3	22.5675538		
41	27	3	26.5918547		
42	28	3	30.7938695		
43	29	3	34.9958842		
44	30	3	39.197899		
45	31	3	43.3999138		
46	32	3	47.6019286		
47	33	3	51.8039433		
48	34	3	56.0059581		
49	35	3	60.2079729		
50	36	4	0		
51	37	4	3.9627		
52	38	4	7.9255		
53	39	4	11.8883		
54	40	4	15.851		
55	*RESPONSE_NAMES				

	A	B	C	D	E
54	40	4	15.851		
55	*RESPONSE_NAMES				
56	Number	Name	Units		
57	1	Moment at left knee	lb-ft		
58	2	Moment at left pinch	lb-ft		
59	3	Moment at ridge	lb-ft		
60	*INFLUENCE_COEFFICIENTS				
61	Index	Response 1	Response 2	Response 3	
62	1	0	0	0	
63	2	2.329420753	1.21937469	-0.1936405	
64	3	4.671338512	2.45359782	-0.3701987	
65	4	7.025427709	3.70228257	-0.5301197	
66	5	9.389759981	4.96313775	-0.6760393	
67	6	1.889956502	0.99903698	-0.1359321	
68	7	0.27035551	2.29715756	-0.2705476	
69	8	-1.337309219	3.60888028	-0.3892217	
70	9	-2.929570639	4.94016138	-0.4860298	
71	10	-4.498361784	6.29836218	-0.55138	
72	11	-6.032809156	7.69736889	-0.5697854	
73	12	-7.865522007	8.96619818	-0.4857403	
74	13	-9.277245595	6.43755353	-0.2531691	
75	14	-10.51706029	4.11316423	0.21438615	
76	15	-11.58179296	1.99680046	0.92126281	
77	16	-12.46827048	0.09223242	1.87179825	
78	17	-13.17331971	-1.5967697	3.07032988	
79	18	-13.69376754	-3.0664358	4.52119506	
80	19	-14.02644084	-4.3129955	6.22873119	
81	20	-14.16816646	-5.3326788	8.19727564	
82	21	-1.232504702	-0.8181609	-0.1359321	
83	22	-2.766216957	-1.8218584	-0.2705476	
84	23	-4.288008409	-2.8115395	-0.3892217	
85	24	-5.794363054	-3.78256	-0.4860298	
86	25	-7.277273191	-4.7259702	-0.55138	
87	26	-8.725839557	-5.6285745	-0.5697854	
88	27	-9.87711152	-6.3047615	-0.4857403	
89	28	-11.19951629	-7.0247001	-0.2531691	
90	29	-12.35001216	-7.5403832	0.21438615	
91	30	-13.32542601	-7.8480409	0.92126281	
92	31	-14.12258471	-7.9439028	1.87179825	
93	32	-14.73831512	-7.8241988	3.07032988	
94	33	-15.16944413	-7.4851588	4.52119506	
95	34	-15.4127986	-6.9230124	6.22873119	
96	35	-15.46520541	-6.1339896	8.19727564	
97	36	0	0	0	
98	37	-1.549064236	-1.0378109	-0.1936405	
99	38	-3.085631467	-2.0607734	-0.3701987	
100	39	-4.61002726	-3.0692743	-0.5301197	
101	40	-6.124179976	-4.0656047	-0.6760393	
102					

Figure 11. Sample building input file (BLD_W=120,L=187.5,H=18,R=5,Open_Country.csv).

*UNITS

Purpose: Define units used in the building input file and in the output of results.

Format of Input Data:

Length	Force	Wind Speed	
length_units	**force_units**	**ws_units**	← text entries

← header row (aligned with first row)

Currently, only the units shown in the following table are supported, and the units must be typed in the input file exactly as shown in the second column of the table.

Quantity	Units
Length	ft
Force	lb
Wind Speed	ft/s

The length units specified here apply to the building dimensions specified in the *BUILDING_DIMENSIONS section, the roughness lengths specified in the *TERRAIN section, the *y*-coordinates specified in the *FRAME_LOCATIONS section, and the *s*-coordinates specified in the *ATTACHMENT_LOCATIONS section. The force units specified here apply to the unit force used in evaluating the influence coefficients specified in the *INFLUENCE_COEFFICIENTS section. The units of the influence coefficients themselves are specified in the *RESPONSE_NAMES section and do not need to match the units specified here, as long as the influence coefficients result from a unit force with the force units specified here. The wind speed units apply to the Directional Influence Factors (DIFs) that are output by the software: these DIFs give the peak values of each response quantity of interest corresponding to unit wind speeds with the units specified here, from different directions.

*BUILDING_DIMENSIONS

Purpose: Define the dimensions of the building to be analyzed. The building dimensions are defined using four length dimensions: the width W_0, length L_0, eave height H_0, and roof rise R_0, as shown in Figure 12. The length units specified in the *UNITS section must be used to define these dimensions.

Format of Input Data:

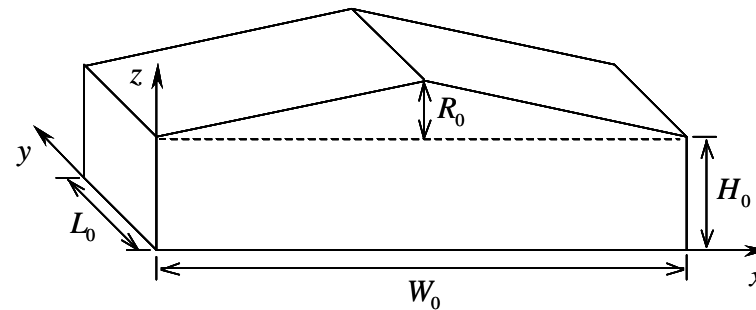| Width	Length	Height	Roof Rise	
W0	L0	H0	R0	← numerical values

← header row

Figure 12. Definition of building dimensions

*TERRAIN

<u>Purpose:</u> Define roughness of the terrain surrounding the building to be analyzed, which may vary with wind direction.

<u>Format of Input Data:</u>

terrain	← text entry							

N	NE	E	SE	S	SW	W	NW
z0(1)	z0(2)	z0(3)	z0(4)	z0(5)	z0(6)	z0(7)	z0(8)

← header row — included only in
← numerical values — "Directional" case

The **terrain** entry in the first row specifies the type of terrain, and must be one of the following:

Open_Country	Suburban	Directional

The second and third rows of input data should be included only if "Directional" terrain is specified in the first row. "Open_Country" terrain corresponds to a roughness length of z_0 = 0.03 m (0.1 ft) for winds from all directions. "Suburban" terrain corresponds to a roughness length of z_0 = 0.3 m (1 ft) for winds from all directions. Specifying "Directional" terrain requires that roughness lengths be defined for winds from each of eight different wind directions. These directions begin with the north and increase by 45° increments in the clockwise direction, as indicated by the column labels in the header row above (the second row of input data). The roughness lengths corresponding to each of these directions are specified in the third row of input data, and the length units specified in the *UNITS section must be used to define these roughness lengths.

*FRAME_LOCATIONS

<u>Purpose:</u> Define the location of each structural frame to be analyzed, along with the locations of its neighboring frames, and assign an identifying number to each frame to be analyzed, for use in the output of results.

<u>Format of Input Data:</u>

Number	Previous y	Current y	Next y	
1	frame_coords(1,1)	frame_coords(1,2)	frame_coords(1,3)	← header row
2	frame_coords(2,1)	frame_coords(2,2)	frame_coords(2,3)	← numerical values
...	...	...	...	← numerical values
f	frame_coords(f,1)	frame_coords(f,2)	frame_coords(f,3)	← numerical values

The first labels above: ← header row, ← numerical values, ← numerical values, ← numerical values
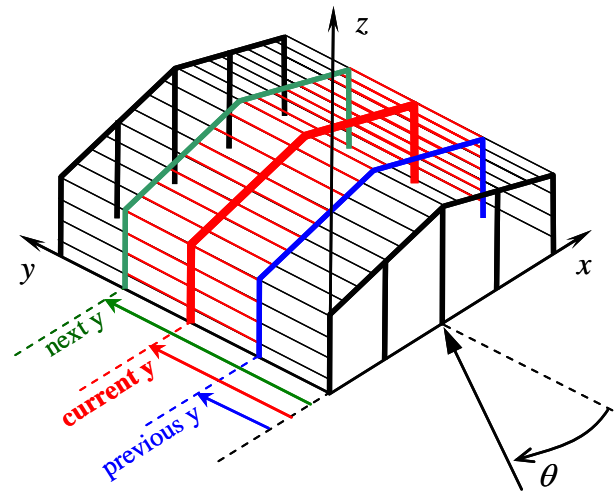
Figure 13. Definition of frame locations

The input data consists of f rows (preceded by one header row), where f is the number of frames to be analyzed, which can be as few as one. Each of these f frames must be identical. If more than one type of structural frame is to be used in the building (e.g., if some frames have interior columns or if the section properties of the frames differ), then separate building input files must be created for each distinct type of structural frame, and separate analyses must be performed for each type of frame, using these different building input files. The frames to be analyzed do not need to be adjacent. Each frame to be analyzed is assigned a number in the first column of the input data. These frame numbers, which are used in the output of results, must start at 1 and increment by 1, ending with f. For each frame to be analyzed, it is necessary to define the y-coordinates of three frames: the previous frame, the current frame, and the next frame, as

illustrated in <u>Figure 13</u> (the frames span in the x-direction). These coordinates are defined in the second, third, and fourth columns of the input data, respectively. The "current" frame is the frame to be analyzed, which is shown in red in <u>Figure 13</u>. The "previous" frame and the "next" frame are the neighboring frames, which shown are blue and green in <u>Figure 13</u>. The positions of these neighboring frames are required in order to determine the lengths of the girts and purlins that span between the current frame and the neighboring frames. The girts and purlins spanning between the current frame and the neighboring frames are highlighted in red in <u>Figure 13</u>, spanning in the y-direction. If there is no "previous frame" (i.e., if the current frame is at the end of the building near $y = 0$) then the y-coordinate of the current frame should be specified for both the "Current y" and the "Previous y" (i.e., in both the second and third columns of the input data). Similarly, if there is no "next frame" (i.e., if the current frame is at the end of the building near $y = L_0$), then the y-coordinate of the current frame should be specified for both the "Current y" and the "Next y" (i.e., in both the third and fourth columns of the input data). As shown in <u>Figure 13</u>, $y = 0$ corresponds to the windward face of the building for a wind direction of $\theta = 0°$. It is noted that the origin of the coordinate system shown in <u>Figure 13</u> is at the opposite corner of the building from the origin used in defining the pressure tap coordinates in the standard HDF pressure database file.

*ATTACHMENT_LOCATIONS

<u>Purpose:</u> Define the locations at which girts and purlins are attached to the structural frames.

<u>Format of Input Data:</u>

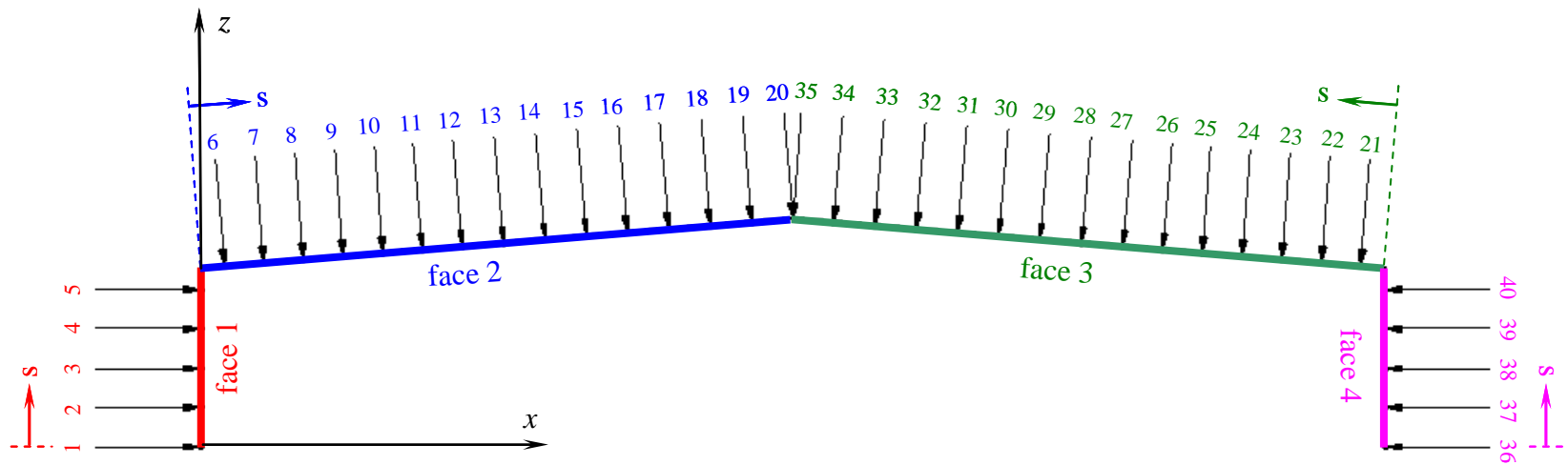| Index	Face	s-coordinate	
1	attach_pts(1,1)	attach_pts(1,2)	← header row
2	attach_pts(2,1)	attach_pts(2,2)	← numerical values
...	...	...	← numerical values
m	attach_pts(m,1)	attach_pts(m,2)	← numerical values

Figure 14. Definition of girt and purlin attachment locations

The input data consists of m rows (preceded by one header row), where m is the number of locations at which girts and purlins are attached. Each attachment location is assigned an index in the first column of the input data, and these indices must start at 1 and increment by 1, ending with m. These indices are used in the *INFLUENCE_COEFFICIENTS section to define the influence coefficients corresponding to a unit force at each attachment location. The location of each attachment point is defined by specifying the face number (in the second column of the input data) and a local "s-coordinate" in the plane of that face (in the third column of the input data). The face numbers and s-coordinates are defined as shown in Figure 14, in which the attachment locations are indicated by arrows normal to each face. The x- and y-coordinates in Figure 14 correspond to the global coordinate system shown in Figure 13, and it is noted that face 1 corresponds to $x = 0$. The indices of the

attachment locations must be assigned in order of increasing face number and then – for each face – in order of increasing values of the *s*-coordinate. This ordering is illustrated in Figure 14, in which the arrows indicating the attachment locations are labeled with the index number, using the same color as the corresponding face. If an attachment location coincides with the boundary between two faces, then separate indices must be defined for the attachment location on each of the adjoining faces. This is illustrated at the ridge of the building in Figure 14, where index 20 is used to denote the ridge location on face 2, and index 35 is used to denote the ridge location on face 3. It is noted that if the attachment locations are symmetric about the ridge, then the *s*-coordinates of the attachment locations on faces 1 and 2 are equivalent to the *s*-coordinates of the attachment locations on faces 4 and 3, respectively.

*RESPONSE_NAMES

<u>Purpose:</u> Assign numbers to the response quantities to be computed, which must coincide with the response numbers used in the *INFLUENCE_COEFFICIENTS section, and provide descriptive names (e.g., "Moment at left knee", "Vertical displacement at ridge") and units (e.g., "lb-ft", "in") for these response quantities, for use in labeling of results.

<u>Format of Input Data:</u>

Number	Name	Units
1	resp_names{1}	resp_units{1}
2	resp_names{2}	resp_units{2}
...	...	...
r	resp_names{r}	resp_units{r}

← header row

- numerical
- text entries
- text entries

The input data consists of *r* rows (preceded by one header row), where *r* is the number of response quantities to be computed, which can be as few as one. Each response to be computed is assigned a number in the first column of the input data, for use in the output of results. These response numbers must start at 1 and increment by 1, ending with *r*. For each of these response quantities, a descriptive name must be provided in the second column of the input data, and the corresponding units must be provided in the third column. Influence coefficients for each of these response quantities must also be provided in the *INFLUENCE_COEFFICIENTS section, and the units of the influence coefficients must be consistent with the units provided in this section. Apart from this requirement of consistency, there are no restrictions on the units that can be used, as the units provided here are not actually interpreted by the software. The response names and units are used only for labeling of the results, as a convenience to the user.

*INFLUENCE_COEFFICIENTS

<u>Purpose:</u> Define influence coefficients for each of the responses to be computed, for which descriptive names and units are provided in the *RESPONSE_NAMES section. The influence coefficients define the value of each response quantity resulting from a unit force at each of the girt and purlin attachment locations, defined in the *ATTACHMENT_LOCATIONS section. The unit forces used to evaluate these influence coefficients must have the force units specified in the *UNITS section.

<u>Format of Input Data:</u>

Index	Response 1	Response 2	...	Response r	
1	N(1,1)	N(1,2)	...	N(1,r)	← numerical values
2	N(2,1)	N(2,2)	...	N(2,r)	← numerical values
...	...	...	...	...	
m	N(m,1)	N(m,2)	...	N(m,r)	← numerical values

(header row: ← header row)
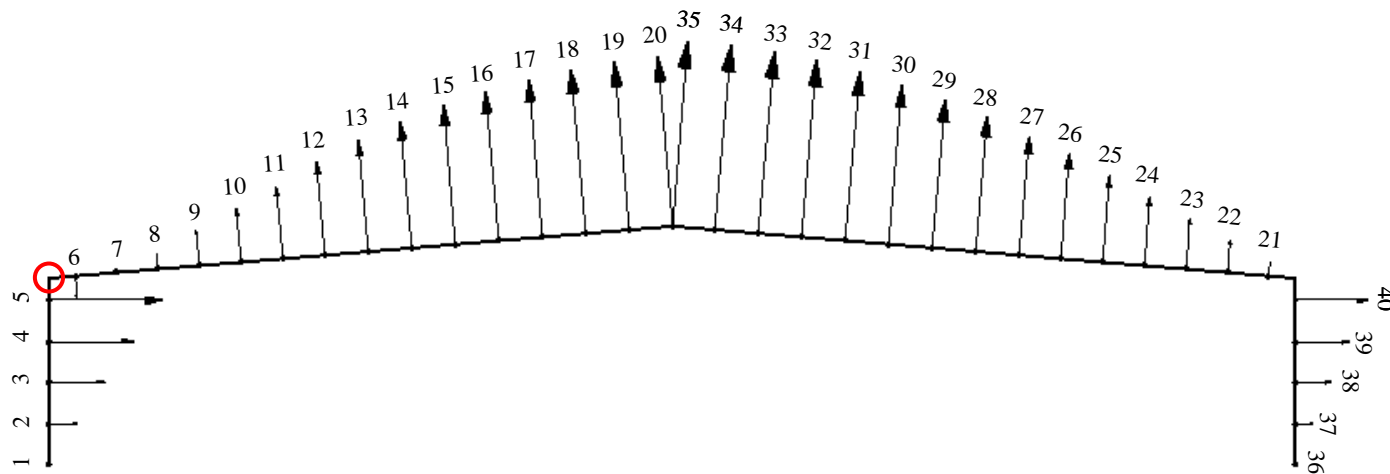
Figure 15. Influence coefficients associated with bending moment at left knee (Response 1). Attachment indices, as defined in Figure 14, are labeled.

The input data consists of *m* rows (preceded by one header row), where *m* is the number of attachment locations. The first column of the input data specifies the attachment index, as defined previously in the *ATTACHMENT_LOCATIONS section, and the attachment indices must start at 1 and increment by 1, ending with *m*. The next *r* columns, where *r* is the number of responses to be computed, define the value of each

response quantity resulting from a unit force at each attachment location. These unit forces act normal to the corresponding face in the direction of positive pressure (i.e., towards the center of the building) as illustrated by the arrows at each attachment point shown in Figure 14. The unit forces used to evaluate these influence coefficients must have the force units specified in the *UNITS section. There are no restrictions on the units of the resulting influence coefficients, but the units must be consistent with those indicated in the *RESPONSE_NAMES section.

Directional Influence Factor (DIF) Output File

This section describes the contents and format of DIF output files, which are comma-delimited text files in which computed Directional Influence Factors are saved. DIF output filenames must begin with "DIF" to be recognized by the windPRESSURE software. DIF output files contain the following sections.

*UNITS
*BUILDING_DIMENSIONS
*MODEL_DIMENSIONS
*WEIGHTING_FACTORS (included only the results were obtained by interpolation)
*MODEL_TERRAIN
*FRAME_LOCATIONS
*ATTACHMENT_LOCATIONS
*RESPONSE_NAMES

If "Observed peaks" are selected in the output options (Figure 4), then the following sections will be included:

*DIF_OBS_MAX   *DIF_OBS_MIN

If both "Observed peaks" and "Store multiple peaks for each wind direction" are selected in the output options (Figure 4), then the following sections will be included:

*DIF_OBS_MAX_ALL   *DIF_OBS_MIN_ALL

If the DIFs were obtained by interpolation and "observed peaks" were contained in the original DIF files used in interpolation, then "bounding" results from each original DIF file will be included in the following sections:

*DIF_OBS_MAX_BND   *DIF_OBS_MIN_BND

If "Estimated peaks" are selected in the output options (Figure 4), then the following sections will be included:

*DIF_EST_MAX   *DIF_EST_MIN

If both "Estimated peaks" and "Store multiple peaks for each wind direction" are selected in the output options (Figure 4), then the following sections will be included:

*DIF_EST_MAX_ALL   *DIF_EST_MIN_ALL

If the DIFs were obtained by interpolation and "estimated peaks" were contained in the original DIF files used in interpolation, then "bounding" results from each original DIF file will be included in the following sections:

*DIF_EST_MAX_BND   *DIF_EST_MIN_BND

If "Store load distributions producing peak responses" is selected in the output options ([Figure 4](#)), then the following sections will be included:

    *LOAD_DISTRIBUTION_MAX   *LOAD_DISTRIBUTION_MIN

If both "Store load distributions producing peak responses" and "Store multiple peaks for each wind direction" are selected in the output options ([Figure 4](#)), then the following sections will be included:

    *LOAD_DISTRIBUTION_MAX_ALL   *LOAD_DISTRIBUTION_MIN_ALL

If the DIFs were obtained by interpolation and load distributions were contained in the original DIF files used in interpolation, then "bounding" results from each original DIF file will be included in the following sections:

    *LOAD_DISTRIBUTION_MAX_BND   *LOAD_DISTRIBUTION_MIN_BND

The purpose and format of each of the preceding sections are described in the following.

*UNITS

Format and Purpose are the same as in the [building input file](#).

*BUILDING_DIMENSIONS

Format and Purpose are the same as in the [building input file](#).

*MODEL_DIMENSIONS

<u>Purpose:</u> Provide the dimensions of the wind tunnel models used in computing the DIFs.

<u>Format:</u> 4 columns; 1 header line, b lines of data, where b is the number of building models. $b=1$ unless the results were obtained by interpolation:

Width	Length	Height	Roof Rise
W1	L1	H1	R1
W2	L2	H2	R2
...	...		...
Wb	Lb	Hb	Rb

(header)

*WEIGHTING_FACTORS

This section is included only if the DIF results were obtained by interpolation.

<u>Purpose:</u> Report the weighting factors for each model used in computing DIFs by interpolation.

<u>Format:</u>

Model 1	Model 2	...	Model b
WF1	**WF2**	**...**	**WFb**

(header)

The output data consists of 1 row with m columns, where m is the number of models used in interpolation.

*MODEL_TERRAIN

<u>Purpose:</u> Report the terrain of pressure database files used to compute the DIFs.

<u>Format:</u> The output data consists of one entry (1 row, 1 column), which specifies type of terrain and may be either "Open_Country" or "Suburban".

*FRAME_LOCATIONS

Format and Purpose are the same as in the [building input file](#).

*ATTACHMENT_LOCATIONS

Format and Purpose are the same as in the [building input file](#).

*RESPONSE_NAMES

Format and Purpose are the same as in the [building input file](#).

*DIF_OBS_MAX

Observed maximum values of each response for a unit wind speed from each direction. If multiple results are obtained for some wind directions (by symmetry), then only the averaged results are reported here.

*DIF_OBS_MIN

Observed minimum values of each response for a unit wind speed from each direction. If multiple results are obtained for some wind directions (by symmetry), then only the averaged results are reported here.

*DIF_OBS_MAX_ALL

Observed maximum values of each response for a unit wind speed from each direction. All results obtained by symmetry are reported, with each tested wind direction resulting in results for four different wind directions, denoted Wind Direction A, B, C, and D.

*DIF_OBS_MIN_ALL

Observed minimum values of each response for a unit wind speed from each direction. All results obtained by symmetry are reported, with each tested wind direction resulting in results for four different wind directions, denoted Wind Direction A, B, C, and D.

*DIF_OBS_MAX_BND

This section is included only if the DIF results were obtained by interpolation, and it reports the *DIF_OBS_MAX values from each model used in interpolation, if "observed" peaks were available.

*DIF_OBS_MIN_BND

This section is included only if the DIF results were obtained by interpolation, and it reports the *DIF_OBS_MIN values from each model used in interpolation, if "observed" peaks were available.

*DIF_EST_MAX

Estimated maximum values of each response for a unit wind speed from each direction. If multiple results are obtained for some wind directions (by symmetry), then only the averaged results are reported here.

*DIF_EST_MIN

Estimated minimum values of each response for a unit wind speed from each direction. If multiple results are obtained for some wind directions (by symmetry), then only the averaged results are reported here.

*DIF_EST_MAX_ALL

Estimated maximum values of each response for a unit wind speed from each direction. All results obtained by symmetry are reported, with each tested wind direction resulting in results for four different wind directions, denoted Wind Direction A, B, C, and D.

*DIF_EST_MIN_ALL

Estimated minimum values of each response for a unit wind speed from each direction. All results obtained by symmetry are reported, with each tested wind direction resulting in results for four different wind directions, denoted Wind Direction A, B, C, and D.

*DIF_EST_MAX_BND

This section is included only if the DIF results were obtained by interpolation, and it reports the *DIF_EST_MAX values from each model used in interpolation, if "estimated" peaks were available.

*DIF_EST_MIN_BND

This section is included only if the DIF results were obtained by interpolation, and it reports the *DIF_EST_MIN values from each model used in interpolation, if "estimated" peaks were available.

*LOAD_DISTRIBUTION_MAX

This section reports the load distribution producing the maximum observed value of each response quantity for each wind direction. Load values are given for each index defined in the *ATTACHMENT_LOCATIONS section, and the units of these load values are given by the force units in the *UNITS section. If multiple results are obtained for some wind directions (by symmetry), then averaged peak load distributions are reported here.

*LOAD_DISTRIBUTION_MIN

This section reports the load distribution producing the minimum observed value of each response quantity for each wind direction. Load values are given for each index defined in the *ATTACHMENT_LOCATIONS section, and the units of these load values are given by the force units in the *UNITS section. If multiple results are obtained for some wind directions (by symmetry), then averaged peak load distributions are reported here.

*LOAD_DISTRIBUTION_MAX_ALL

This section reports the load distribution producing the maximum observed value of each response quantity for each wind direction. All results obtained by symmetry are reported, with each tested wind direction resulting in results for four different wind directions, denoted Wind Direction A, B, C, and D. Load values are given for each index defined in the *ATTACHMENT_LOCATIONS section, and the units of these load values are given by the force units in the *UNITS section.

*LOAD_DISTRIBUTION_MIN_ALL

This section reports the load distribution producing the minimum observed value of each response quantity for each wind direction. All results obtained by symmetry are reported, with each tested wind direction resulting in results for four different wind directions, denoted Wind Direction A, B, C, and D. Load values are given for each index defined in the *ATTACHMENT_LOCATIONS section, and the units of these load values are given by the force units in the *UNITS section.

*LOAD_DISTRIBUTION_MAX_BND

This section is included only if the DIF results were obtained by interpolation, and it reports the *LOAD_DISTRIBUTION_MAX values from each model used in interpolation, if load distributions were available.

*LOAD_DISTRIBUTION_MIN_BND

This section is included only if the DIF results were obtained by interpolation, and it reports the *LOAD_DISTRIBUTION_MIN values from each model used in interpolation, if load distributions were available.

Time Series Output Files

If "Display time series during analysis" is selected in the output options Figure 4, then response time series can be saved through the graphical interface shown in Figure 5. Time series can only be saved for one frame and one response at a time (each response can be saved in turn, if desired), and responses are automatically saved for the four different wind directions obtained by symmetry (Wind Directions A, B, C, and D). As shown in the dialog of Figure 16, the time series can be saved in one of two formats: in comma-delimited text format (*.csv) or in MATLAB format (*.mat).

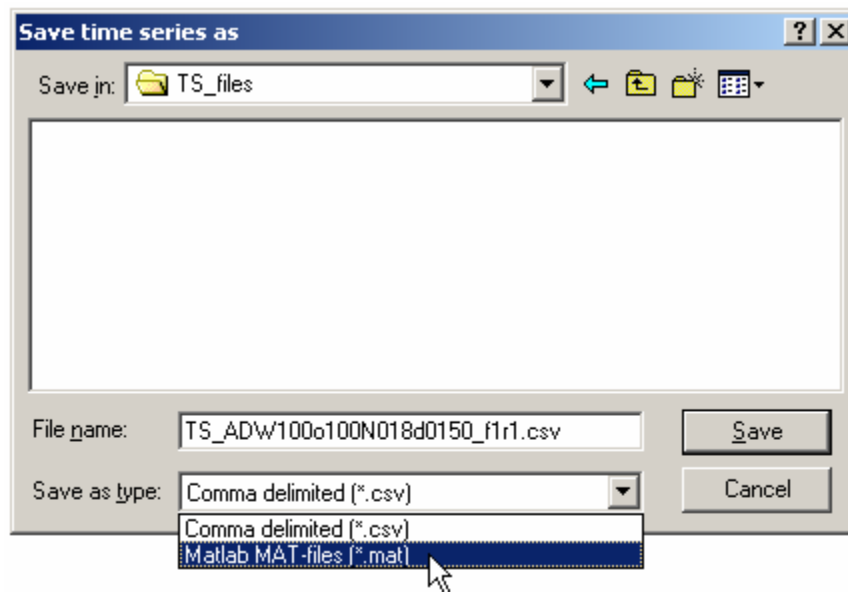**Figure 16. Dialog box for saving of time series.**

A portion of a time series output file in CSV format is shown in Figure 17. As shown, identifying information is written in header rows at the top of the CSV file.

If the time series is saved in MATLAB format (*.mat), then the time series and identifying information are stored in a structure array named "TS_structure" in a MATLAB file with the specified name. The file can be loaded within MATLAB using the syntax shown in the following example:

load 'TS_ADW100o100N018d0150_f1r1.mat'

	A	B	C	D
1	HDF pressure file: ADW100o100N018d0150.HDF			
2	Frame 1: y = 18.75 ft			
3	Response 1: Moment at left knee (lb-ft)			
4	Number of samples: 49792			
5	Wind Dir A	Wind Dir B	Wind Dir C	Wind Dir D
6	15	345	165	195
7	Time Series A	Time Series B	Time Series C	Time Series D
8	10.401	9.40555	1.41843	1.05829
9	10.5932	9.59051	1.63415	1.13809
10	10.1893	9.15111	1.2277	0.777493
11	9.70398	8.59027	1.02474	0.708408
12	9.19046	8.13591	0.470464	0.025218
13	9.56308	8.54659	0.776976	0.45033
14	10.4377	9.27259	1.58364	1.0993
15	10.7204	9.66025	2.00571	1.35543
16	10.0225	8.88006	1.62351	1.14902
17	9.04601	7.82999	0.406228	0.00721043
18	8.60808	7.49577	-0.078962	-0.477685
19	9.0158	7.81092	0.541478	0.113351

Figure 17. Portion of sample time series output file.

The times series and identifying information given in the headers of the CSV file shown in Figure 17 are stored in fields with the following names:

TS_structure.HDF_filename	'ADW100o100N018d0150.HDF'	(HDF pressure file)
TS_structure.frame_label	'Frame 1: y = 18.75 ft'	
TS_structure.resp_label	'Response 1: Moment at left knee (lb-ft)'	
TS_structure.n_s	49792	(Number of samples)
TS_structure.theta_a	15	(Wind Dir A)
TS_structure.theta_b	345	(Wind Dir B)
TS_structure.theta_c	165	(Wind Dir C)
TS_structure.theta_d	195	(Wind Dir D)
TS_structure.ts_a	[1x49792 double]	(Time Series A)
TS_structure.ts_b	[1x49792 double]	(Time Series B)
TS_structure.ts_c	[1x49792 double]	(Time Series C)
TS_structure.ts_d	[1x49792 double]	(Time Series D)

Mean Recurrence Interval (MRI) Output File

The MRI output files contain the following sections.

*UNITS

Format and Purpose are the same as in the building input file.

*BUILDING_DIMENSIONS

Format and Purpose are the same as in the building input file.

*MODEL_DIMENSIONS

Format and Purpose are the same as in the DIF output files.

*FRAME_LOCATIONS

Format and Purpose are the same as in the building input file.

*MODEL_TERRAIN

Format and Purpose are the same as in the DIF output files.

*RESPONSE_NAMES

Format and Purpose are the same as in the building input file.

*MRI_LIST

Purpose: Define the Mean Recurrence Intervals for which peak responses where

Format: One row with values in one or more columns giving the Mean Recurrence Intervals for which responses were requested.

*MRI_MAX_OBS

This section is included if "observed" peaks were available in the selected DIF file(s), and it gives the maximum values of each response quantity corresponding to the specified return periods, computed using "observed" peaks.

*MRI_MIN_OBS

This section is included if "observed" peaks were available in the selected DIF file(s), and it gives the minimum values of each response quantity corresponding to the specified return periods, computed using "observed" peaks.

*MRI_MAX_EST

This section is included if "estimated" peaks were available in the selected DIF file(s), and it gives the maximum values of each response quantity corresponding to the specified return periods, computed using "estimated" peaks.

*MRI_MIN_EST

This section is included if "estimated" peaks were available in the selected DIF file(s), and it gives the minimum values of each response quantity corresponding to the specified return periods, computed using "estimated" peaks.

Appendix B:

Notes for Installation and Use of HR_DAD, Database-Assisted Design Software for Flexible Buildings

William P. Fritz

High-Rise Database-Assisted Design (HR_DAD)

DAD Software for Flexible Buildings

How to download and install the software:

The HR_DAD software has been developed using the MATLAB language and is available through the internet at <http://www.nist.gov/wind>. All 34 MATLAB files required to run the software are zipped into one file, HR_DAD.zip, for a single download. Simply download this zip file and copy the 34 files into a directory whose path is accessible by MATLAB. To run the software, simply type "HR_DAD" at the MATLAB command prompt, which runs the script file of similar name and opens ten figure files.

Basics of using the HR_DAD_software:

The ten opened figure files (i.e., pages) are used to input the values for the required variables used by the HR_DAD software. All variables are initially assigned an empty set in the HR_DAD.m script file. Variable values can be assigned in any order in pages one through five. The variable names within the software are typically shown in parentheses before the input box on the page. In several instances, a saved MATLAB file is opened within a page to load variables that contain vectors or matrices. Purple help icons with a "?" sign provide the required variable name, the variable size, a description of the variable and the specific organization of the variable's contents.

Once the variables are assigned values by the user, the first portion of the HR_DAD program is run on page six. The results of this first run are saved at the location specified with the "Save As" button. Tables of peak wind effects must be saved and are used for the second portion of the program that calculates mean recurrence intervals of the wind effects. The results of run two are also saved at a specified location. Graphical output is displayed through page seven, which uses the Output figure file. Page eight allows the user to save the current variable set at any point in the assignment process or load a previously saved set of variables into the software.

A wind speed database is required to estimate the mean recurrence intervals of the wind effect. The simulated hurricane wind speeds are available on the website. Simply save a file to the same location as the software and then specify its milepost in page five as the variable "Hmp". These data are used in conjunction with the tables of peak wind effects in the second portion of the program.

Examples for the HR_DAD software

Two examples are provided with the HR_DAD software: 1) a 66-story building with accompanying directional wind tunnel measurements and 2) a single-degree-of-freedom (SDOF) oscillator with a sinusoidal force.

The first example illustrates the full use of the software. The example is downloaded in two stages. The first stage involves downloading the complete set of variables, which are contained

in the zip file named "66-story Example.zip". Once the files are copied to a location that is accessible by MATLAB, run HR_DAD and load the file called "Bldg66_122905" through page eight of the software (see Basics above). This updates all variable values and the displayed values within the pages. The second stage involves downloading the 36 files that contain directional wind tunnel measurements in 5° increments. These files are large and time-consuming to download, but are necessary to estimate the mean recurrence intervals of peak wind effects. Note that the downloaded zip file contains results that do not need these large files; the wind tunnel measurements are only needed if the analyses are rerun. A subset of the 36 pressure files can be used bearing in mind that the tables of peak wind effects are calculated for each wind direction (specified through the variable "WD" in page three) and that the directional extreme wind speeds (e.g., simulated hurricane wind speeds mentioned above) are interpolated among these tables of peak wind effects. Thus, the fewer wind directions used, the coarser the mesh of available peak wind effects and the greater the variability in the estimates of mean recurrence intervals. Further details are provided in Section 4.3.1 of this report.

The second example illustrates the ability to easily manipulate the software and obtain a peak wind effect other than the interaction equation for individual members. This example is downloaded through the single zip file named "SDOF example.zip". Once the files are copied to a location that is accessible by MATLAB, run HR_DAD and load the file called "sdof" through page eight of the software (see Basics above). This updates all variable values and the displayed values within the pages. As described in Section 4.3.1 of this report, the wind effect of interest is the maximum deflection of the single mass. This requires slight modification to the script file Program1.m: the maximum deflection should be calculated right after the equations of motion are integrated.